THE UNIVERSITY OF MICHIGAN
RADIO ASTRONOMY OBSERVATORY

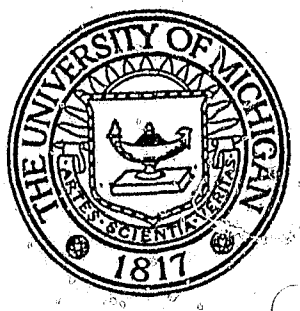

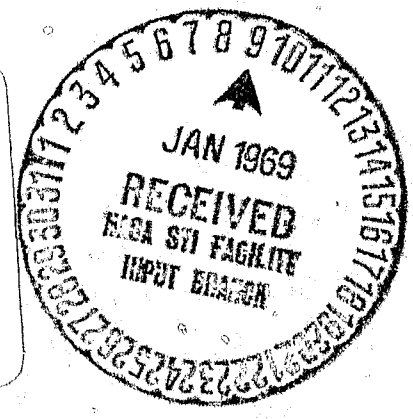

DEPARTMENT OF ASTRONOMY

INSTRUMENTATION FOR RADIO ASTRONOMY MEASUREMENTS ABOARD THE OGO-V SPACECRAFT

Technical Report
NASA Contract NAS5-9099

Submitted By:

Fred T. Haddock
Project Director

September 20, 1968

Written By:

B. D. MacRae

Approved By:

R. G. Peltzer

THE UNIVERSITY OF MICHIGAN
RADIO ASTRONOMY OBSERVATORY

ABSTRACT

This report describes the design considerations and performance characteristics of a satellite-borne instrumentation system designed and constructed at the University of Michigan Radio Astronomy Observatory. The system is designed to make radio astronomy measurements at eight discrete frequencies from 50 kHz to 3.5 MHz. These measurements are to detect Solar and Jovian radio frequency bursts and to determine the relative average level of cosmic background radiation down to 50 kHz.

Procedures used for preflight and in-flight noise calibrations are discussed. A description of the ground support equipment used for preflight testing is given.

The instrument was successfully launched aboard the OGO-V(E) spacecraft on 4 March 1968 into an elliptical orbit having the following approximate parameters: perigee, 292 kilometers; apogee, 147,000 kilometers; inclination to the equator, 31°; period, 63 hours, 25 minutes.

The initial data from the instrument looks excellent and the instrument should successfully fulfill its mission.

The scientific aspects and results of this program will be published separately.

PREFACE

This is the final technical report concerning the instrumentation designed and constructed at the University of Michigan Radio Astronomy Observatory Laboratory for making radio astronomy measurements at eight discrete frequencies from 50 kHz to 3.5 MHz. The radiometer was designed for satellite-borne observations. The purpose of the measurements is twofold: to measure the relative average level of cosmic background radiation and to detect Solar and Jovian radio bursts at these eight frequencies. The instrument was flown aboard the OGO-V spacecraft launched 4 March 1968 from the Eastern Test Range at Cape Kennedy, Florida.

The scientific results and aspects of this program will be published separately.

TABLE OF CONTENTS

LIST OF TABLES

LIST OF FIGURES

INSTRUMENTATION FOR RADIO ASTRONOMY MEASUREMENTS ABOARD THE OGO-V SPACECRAFT

I. INTRODUCTION

This report describes the design considerations and performance characteristics of an instrumentation system designed and constructed at the University of Michigan Radio Astronomy Observatory Laboratory for satellite-borne radio astronomy observations. These observations are carried out at eight discrete frequencies from 50 kHz to 3.5 MHz (50, 100, 200, 350, 600, 900, 1800, and 3500 kHz) and their purpose is to detect Solar and Jovian radio frequency bursts and to measure the relative average level of cosmic background radiation down to 50 kHz. Due to the wide frequency range covered by the radiometer, it not only provides correlation with the data obtained from our earlier radiometers flown on OGO spacecrafts I-IV; but also extends our observations down to much lower frequencies. These lower frequencies may provide areas for more detailed observations for future radiometers.

The radiometer system, as shown in Figure 1, consists of a 30 foot monopole antenna, a stepping superheterodyne receiver, a noise calibrator, and a power supply. The inboard 10 feet of the monopole antenna is coated with Dupont Kapton to insulate the boom from the plasma sheath surrounding the spacecraft. This requirement was necessary since the antenna is shared with an electric field experiment (Aggson, GSFC; E-26). The antenna assembly was, in fact, supplied by GSFC.

The antenna is self-extending, requiring only momentary ordnance power to release it. There is also provision for ejecting the antenna element from the spacecraft if this becomes desirable due to spacecraft operational considerations. There are telemetry outputs which indicate the deployment status and whether the element ejection circuit is armed.

The first stage in the receiver is a low noise preamplifier having an unbalanced input. There is also incorporated in this preamplifier stage filtering elements to reduce the susceptibility of the radiometer to signals outside the signal passband.

Following the preamplifier is a balanced diode mixer which is fed from a complex of eight crystal-controlled oscillators. The selection of the active oscillator is controlled by internal logic, the input of which is a timing pulse derived from the spacecraft clock. A telemetry output is provided to identify the operating center frequency of the radiometer. The DC voltage on the mixer and crystal filter stages is also monitored through the telemetry system. The output of the mixer feeds a 10.7 MHz crystal filter which determines the IF bandwidth.

After suitable buffering, the output of the crystal filter is fed to a four stage gain-controlled IF amplifier. Following the IF amplifier is an envelope detector the bias of which is temperature stabilized. This bias voltage is fed to the telemetry system for monitoring purposes. The output of the detector feeds an emitter follower stage which provides the AGC voltage for the IF amplifier and isolates the detector from the final signal conditioning circuitry.

The final conditioning of the radiometer data consists of establishing a post detection time constant of approximately 0.21 seconds and constraining the DC output voltage to a range of 0 to 5.1 volts. This last conditioning is to achieve compliance with the telemetry system requirements. This final stage also provides a low output impedance.

A solid-state noise diode and an associated amplifier is incorporated in the radiometer to provide inflight calibration. The noise calibrator provides a white noise source over the operating frequency of the radiometer. Four levels of calibration are provided through the use of a logic-controlled attenuator. The radiometer is calibrated approximately every 10 minutes. The calibration sequence is also controlled by the radiometer's internal logic. A telemetry output is provided which defines the calibration levels during the calibration sequence. There are two telemetry outputs associated with the noise calibrator which indicate the current through the noise diode and the temperature of the noise diode.

A voltage regulator circuit was included in the system to provide isolation from the noise associated with the spacecraft power supply and to insure stable voltages for the critical circuits in the radiometer. Current limiting was included to protect the series regulating element from accidental or transient shorts. Extensive filtering is provided to reduce conduction of RFI from the regulator circuitry to critical RF circuits. A telemetry output is provided to monitor the regulator output voltage.

The radiometer has two normal modes of operation: a frequency sequencing mode and a single frequency operation mode. The frequency stepping mode is controlled, as mentioned earlier, by internal logic triggered by a timing signal from the spacecraft.

The change from this mode to the single frequency mode is controlled by a ground command. The desired operating frequency may be selected by ground command once the radiometer has been placed in the single frequency mode. A third ground command returns the radiometer to the frequency stepping mode.

An internal free-running multivibrator, normally synchronized with the spacecraft timing signal, provides the radiometer timing in the event the spacecraft timing signal is lost. The frequency of this multivibrator is adjusted such that useful radiometer data may be obtained even though the frequency stepping is no longer synchronized with the telemetry system.

A brief description of the ground commands used by the radiometer is given below:

1. Power ON/OFF - Self explanatory
2. Antenna Deploy - Used in conjunction with the spacecraft ordnance supply to deploy the antenna.
3. Enable Frequency Stepping/Arm Ejection Circuit - This command provides the dual function of placing the radiometer in the frequency stepping mode as described above and arming the ejection circuitry in the antenna assembly. This ejection circuitry is automatically disarmed by ordnance buss turn-on.

4. Antenna Eject - Used in conjunction with the spacecraft ordnance supply and the preceeding command to eject the antenna element from the spacecraft. The decision to use this command will be based on spacecraft operational considerations.
5. Disable Frequency Stepping - This command places the radiometer in the single frequency mode of operation.
6. Single Frequency Step - The operating frequency of the radiometer will be changed by one step (eg. 50 to 100 kHz) each time this command is sent.

The instrument described was successfully launched aboard the OGO-V spacecraft on 4 March 1968. Prior to launch this spacecraft was officially designated as the OGO-E spacecraft and under this designation, our assigned experiment number is E-20. The experiment is mounted in Solar-Oriented Experiment Package 1 (SOEP-1) with the antenna extending out from the spacecraft in the -X direction (spacecraft coordinate system).

II. DETAILED DESCRIPTION OF INSTRUMENT

A. ANTENNA ASSEMBLY

1. General Operation

The antenna unit consists of a 30 foot roll of beryllium copper element wound on a spool with the associated support structure. A plating of silver on top of gold is deposited on the element to improve its thermal properties. The inboard 10 feet of the element is coated with Dupont Kapton to insulate the boom from the plasma sheath surrounding the spacecraft. The copper element is heat treated in such a way that in the relaxed state it forms a cylindrical tube approximately 0.50 inches in diameter. This material is backwound on the spool with the free end of the element secured to a cylindrical aluminum post. This post is the outboard section of a two-section structure which can be separated using an internal ordnance device. This allows the extended element to be ejected from the spacecraft leaving only the support structure on board if this is deemed desirable. The element spool is held in place by a restraining strap which may be released through the use of a second ordnance device. Microswitches sense the position of the spool so that there is a positive indication of antenna deployment.

The antenna is self-erecting. The electrically energized deployment squib pulls a pin which releases the restraining strap and allows the element to unwind. The spool, by virtue of the stored energy in the element, moves outward and the antenna erects as a cylindrical boom behind the spool. The spool is released automatically at the end of the erection process.

The ejection process is initiated by firing an ordnance device inside the element support post structure. This device allows the outboard section of the post to separate and this section along with the element is ejected, leaving only the antenna support structure onboard.

The control of the antenna deployment and ejection as well as circuitry for monitoring the status of the antenna is housed in a box between the antenna structure and the SOEP mounting surface.

A detailed description of the antenna assembly will not be given in this report as this unit was furnished by the Fields and Plasma Branch, GSFC (E-26) who shared the antenna with us.

2. Antenna Equivalent Circuit

The equivalent circuit for the monopole antenna is shown in Figure 2. The approximate free space values of R_A and C_A may be calculated from:[1,2]

$$R_A = 60\pi^2 (h/\lambda)^2 \qquad (1)$$

and

$$C_A = 2\pi\epsilon_o h/\ln(h/a) - 1 \qquad (2)$$

where:

R_A = Antenna radiation resistance

C_A = Antenna capacitance

h = Monopole length (30 feet)

λ = Free space wavelength

ϵ_o = Free space permittivity (8.85×10^{-12} farads/meter)

a = Antenna wire radius (0.25 inches)

Using equation (1) to calculate radiation resistance, it is possible to predict values ranging from 1.37×10^{-3} ohms at 50 kHz to 6.75 ohms at 3.5 MHz.

Using equation (2), the predicted free space value of antenna capacitance is approximately 72.6 picofarads.

C_B in the antenna equivalent circuit is stray capacitance. This stray capacitance is due to the proximity of grounded surfaces to the antenna and the signal leads. During a final qualification test on the antenna, careful measurements were made on the unit mounted on a flight SOEP.[3] These measurements showed the base capacitance of the antenna unit itself to be approximately 7.5 picofarads. There is approximately 6 inches of coax between the antenna unit and the radiometer input. The shunt capacitance of this coax contributes an additional 7.5 picofarads. Thus the total C_B is approximately 15 picofarads.

It should be noted that C_B forms a capacitive voltage divider with C_A which decreases the available signal voltage level at the input to the radiometer. For this reason, every effort in design and component placement was made to minimize the value of C_B.

B. RADIOMETER ELECTRONICS

1. General Operation

The system block diagram is shown in Figure 1. This diagram illustrates the interrelationships between various portions of the radiometer electronics. The antenna assembly was discussed in section A.

The receiving system consists of a stepping superheterodyne receiver with a center frequency tunable from 50 kHz to 3.5 MHz in eight steps, a noise calibrator, associated power supply, and an antenna.

Antenna signals are amplified first by a low-noise broadband preamplifier. The preamplifier input is filtered to prevent telemetry signals from entering the radiometer. A low pass filter in the preamplifier rejects undesired frequencies above 3.5 MHz. The antenna and input circuits are untuned. However, the input circuitry is designed to obtain the maximum sensitivity for the untuned case.

The preamplifier output is mixed with a crystal-controlled, stepped-frequency local oscillator signal to achieve the tuning in 8 steps across the frequency band with center frequencies from 50 kHz

to 3.5 MHz. The IF bandwidth is 10 kHz (6 db) and is determined by a crystal filter in the mixer output. Frequency stepping is done in synchronism with the data system.

The IF amplifier is gain controlled (AGC) with a response that is logarithmic and has a useful dynamic range of 55 db. The output of the second detector is filtered with a time constant of 0.21 seconds.

An analog voltage is generated in the oscillator circuitry which identifies the operating center frequency.

A solid-state noise calibrator is switched to the preamplifier input with the antenna disconnected for calibration. The antenna relay and the calibration level-controlling relays are driven from internal logic. An analog voltage corresponding to the levels of noise used for calibration is generated and fed to the main commutator. Approximately 37 seconds is required for calibration, after which the antenna is restored to the radiometer input. Calibration occurs approximately every 10 minutes.

Figure 3 shows the voltages or signals required or expected at the radiometer's interfacing connectors.

The package dissipates approximately 2.1 watts over a base plate area of 49.1 square inches. This gives a power density of approximately 0.04 watts per square inch. There are no local hot spots that are likely to cause difficulty. The outside of the blivet is painted black (to aid in the SOEP's thermal design) with the exception of the baseplate which is gold plated for good electrical and thermal conductivity. See Figures 5 and 7.

The blivet and covers are magnesium with selective gold plating to improve the electrical conductivity.

The mechanical layout of the radiometer package is shown in Figures 4 and 6. The outside dimensions of the electronics package

are 7.25" x 7.0" x 4.8". The package mounts to the SOEP by four (4) 10-32 bolts.

The radiometer operates on a continuous duty cycle, being turned on and off only by ground commands. The average power consumption of the experiment after antenna erection is 2.1 watts. A peak power of 4.5 watts is required during the calibration cycle. The power profile for the experiment at the extremes of spacecraft buss voltage is illustrated in Figure 8.

2. Timing

The sequency of events in the radiometer is illustrated in Figure 9. Line A shows the train of timing pulses furnished by the spacecraft and recurring at 1.152 second intervals. This is the repetition rate of the data system main frame at the 1 Kilobit/second rate and the pulse occurs 31.2 μsec before the first bit of the following complete telemetry frame. Each pulse causes the radiometer frequency to change as shown in line B The eight frequency steps, F1 through F8, constitute a subcycle of approximately 9.2 seconds.

During each frequency step the three main commutator data samples are taken, the first being the frequency identification voltage and the last two being the radiometer output samples. This is illustrated in line C.

The subcycle repeats continuously except in the event of a ground command to disable the frequency stepping.

The calibration cycle consists of four subcycles of eight frequency steps each as shown in line B' (same as line B but drawn to a smaller time scale). The calibrator level, as shown in line D', is held constant during the first subcycle. Thus all eight frequencies are calibrated at the same level. This is repeated for the remaining three subcycles at successively increased calibrator output levels. At the end of the 36.9 second calibrate cycle, the calibrator is disconnected and the antenna is reconnected to the radiometer input.

The calibration occurs only once during a main cycle. A main cycle consists of 64 subcycles (580.8 sec or 9.83 min), of which four are devoted to calibration. This is shown in line D". The antenna is connected to the radiometer for the remaining 60 subcycles (approximately 94% of the time). Action of the antenna relay is illustrated in line E".

3. Preamplifier

3.1 System Sensitivity

The system sensitivity of the radiometer was optimized for use with a 60 monopole[1] and a broadband untuned input circuit.[1,4,5]

The outline below summarizes the steps followed in the development of this system:

(a) Selection of a low noise transistor for the input stage. The 2N930 was found to be satisfactory for this application.

(b) Selection of the best circuit configuration consistent with the lowest noise figure and other system requirements. The common collector configuration was chosen for the input stage.

(c) Determination of the four noise parameters F_o, R_N, G_o, and B_o;[6] and their variations with operating point.[4,7,8]

(d) Adjustment of the operating point for the minimum $R_N G_o^2$ product, which is the condition for lowest noise figure in the untuned case.[4]

(e) Computation of the $R_R T_R$ product with the specified values of series antenna capacitance C_A = 110 picofarads and base shunt capacitance C_B = 20 picofarads. The following equation was used:[4]

$$R_R T_R = R_R T_o (F_o - 1) + R_R R_N T_o X/G_s \qquad (1)$$

where:

$X = (G_s - G_o)^2 + (B_s + B_B - B_o)^2$

R_R = Antenna radiation resistance

---

[1] The length of the antenna was later shortened to 30 feet due to spacecraft considerations. The effect of shortening the antenna on the system operation is indicated on the applicable plots.

T_o = 290°K reference temperature

T_R = Effective receiver input noise temperature

G_s = Equivalent shunt conductance of the source

B_s = Equivalent shunt susceptance of the source

B_B = Shunt susceptance due to C_B

F_o, R_N, B_o, and G_o are the noise parameters of the system.

(f) Laboratory measurements of $R_R T_R$ using an optimized preamplifier circuit. Data was taken at several frequencies and at several values of C_A.[4] Sensitivity data on this unit using C_B= 20 picofarads was compared with that obtained using equation (1) and the correlation was good.

(g) Using the values of $R_R T_R$ found experimentally for C_A= 160 picofarads and C_B= 20 picofarads, the values of T_R were then computed by dividing by the calculated values of R_R found for a monopole using:[1]

$$R_R = 60\pi^2 (h/\lambda)^2 \qquad (2)$$

where (h/λ) is the length of the monopole in wavelengths. This equation is accurate within a few percent for $(h/\lambda) < 0.1$ and is an approximation for a monopole using the spacecraft as a counterpoise.

(h) The tangential temperature T_T, was then found from the equation:

$$T_T = \frac{5T_R}{\sqrt{B\tau}}$$

---

[2]A value of 60 picofarads was used for C_A for the values of T_T corresponding to the 30 foot monopole. This corresponds quite closely with experimentally determined values.

where

B = Receiver bandwidth in Hertz (10^4 for this radiometer)

τ = Post detection filter time constant in seconds (0.21 seconds)

The fact 5 is an arbitrary factor arising from the ratio of frequent peak to rms value of the output, and is base.. on observational experience.

The system tangential temperature T_T, is shown plotted for both a 60 foot and a 30 foot monopole[2] on an anticipated cosmic brightness background model in Figure 10. The data points are those observed in UM/RAO 1962 and 1965 rocket experiments.[9,10]

Further increases in system sensitivity can be realized by appropriate averaging in the data reduction program, provided the phenomena being studied are either stationary or varying considerably slower than the data rate. If N independent samples are averaged, the sensitivity can be increased by a factor of $\sqrt{N}$.

3.2 Preamplifier Circuit

The low noise preamplifier is shown in Figures 11 and 12. Q_{101} is a common collector input stage adjusted for low noise as discussed above. This is followed by a common emitter stage, Q_{102}, and an emitter follower output stage, Q_{103}. All stages are biased for low dc drift and degenerated for stabilized gain. The voltage gain of the preamplifier is approximately 14 db.

A Chebyshev low-pass filter is incorporated in the preamplifier between the second and third stages. This filter has an in-band ripple of 0.1 db, is 3 db down at 4.1 MHz, and is 75 db down at 10.7 MHz.

The filter serves three purposes:

(a) Rejection of spurious responses, notably at the IF and image frequencies.

---

[2] A value of 60 picofarads was used for C_A for the values of T_T corresponding to the 30 foot monopole. This corresponds quite closely with experimentally determined values.

(b) Rejection of the self-noise produced at spurious frequencies, thus improving the overall noise figure of the system.

(c) Suppression of radiation at the local oscillator frequencies (10.75 to 14.20 MHz) from the receiving antenna.

Q_{103} provides a low output impedance which is suitable for driving the mixer stage.

The two LC filters on the input of the preamplifier are traps set at the two telemetry transmitter frequencies. These prevent antenna pickup from the spacecraft transmitters from interfering with the radiometer.

The series input resistor and series output inductor are additional filtering elements which were added as a result of radio frequency interference (RFI) tests conducted on the radiometer. These elements markedly reduced the susceptibility of the radiometer to both radiated and conducted interference outside the frequencies of interest.

4. Mixer and Crystal Filter

The mixer, crystal filter, and drivers are shown in Figures 13 and 14.

The mixer is a balanced diode mixer which feeds directly into a driver stage. The collector load of the driver stage is a crystal filter having a center frequency of 10.7 MHz. This stage, and the stage following the filter, provide the proper termination for the filter so that maximum flatness is achieved in the pass band.

The crystal filter is the element which determines the IF bandwidth. The specifications for the crystal filter are as follows:

Center Frequency	10.700 MHz ± 0.005 MHz
Bandwidth	
6 db attenuation	10 kHz ± 0.5 kHz
60 db attenuation	24 kHz ± 1.5 kHz

Passband Ripple	1.0 db	Maximum
Insertion Loss	2.0 db	Maximum
Spurious Response Rejection	80 db	Minimum

(From 1.0 MHz to the lower 80 db point, and from the upper 80 db point to 40 MHz)

The crystal filter stage has an emitter follower output, providing a low output impedance for driving the IF amplifier. This eliminates the problem of driving the variable input impedance of the IF amplifier, reduces pickup in the IF amplifier input cable, and simplifies adjustment of the matching termination for the crystal filter.

5. Logic

5.1 General Operation

The basic logic used to generate the timing sequence is illustrated in Figures 15, 16, and 17. A timing pulse from the spacecraft (see section 2) enters the pulse drive redundancy circuit (PDR) every 1.152 seconds in normal operation. A pulse suitable for driving the flip-flop chain is produced at the output of the PDR at this rate. This drives two count-down chains of flip-flops. The Main Logic chain (FF1 to FF9) has a scale of $2^9 = 512$ and drives the calibration sequence. FF4 - FF9 are shown in Figures 20 and 21. The Oscillator Switching chain has a scale of $2^3 = 8$ and applies dc power to the local oscillators in the proper sequence through suitable selector gates and drivers.

The flip-flops are ac coupled and were designed to have good temperature stability and good noise immunity.

On occasion it may be desired to operate the radiometer at a fixed frequency for an extended period of time. For this reason a stepping disable relay was introduced into the system. This single frequency step circuitry is illustrated graphically in Figure 15 and schematically in Figure 11.

The stepping disable relay is a latching type which requires only a 50 millisecond pulse to change state. A ground command energizes relay coil L2 (Figure 15) which moves the relay contacts to the right and disables the normal frequency stepping when fixed frequency operation is desired. This places the radiometer in a fixed tuned mode of operation without disrupting the normal calibration sequence.

The appropriate frequency of operation can now be obtained through the use of another ground command which provides a pulse input to the Oscillator Switching Logic, bypassing the PDR circuitry. A single pulse is produced for each ground command sent so that individual frequencies are easily selected.

Another ground command is sent which energizes relay coil L1 (Figure 15) and returns the input of the Oscillator Switching Logic to the output of the PDR circuit when it is desired to return to the normal stepping mode of operation. Energizing L1 latches the relay in this position and it will remain there until another disabling command is sent.

5.2 Pulse Drive Redundancy Circuit (PDR)

The Pulse Drive Redundancy (PDR) circuit is shown in Figures 16 and 17. Its purpose is to maintain sequential operation of the radiometer in the event the spacecraft timing pulse falls below specifications, becomes intermittent, or fails completely. The characteristics of the timing pulse were discussed in section 2, and will not be repeated here.

The first stage of the PDR circuit is an emitter follower which isolates the Schmitt trigger (Q_{402} and Q_{403}) from the spacecraft timing signal. This is necessary to keep the input impedance at a high level independent of the state of the Schmitt trigger.

The Schmitt trigger produces an output pulse when the pulse level from the emitter follower exceeds a predetermined margin. This output

feeds both a free-running multivibrator (Q_{404} and Q_{405}) and one input of a two-input OR gate (D_{401} and D_{402}).

The free-running multivibrator is synchronized by the Schmitt trigger output pulse in such a way that its output pulse is in phase with the Schmitt trigger pulse. This multivibrator output pulse forms the other input to the two-input OR gate. The output of the OR gate is fed to both the Main Logic and Oscillator Switching Logic timing chains.

The PDR circuit will produce pulses at the free-running multivibrator rate in the event of a failure of the spacecraft timing signal. This rate has been set at approximately 0.434 pps. This rate, which is half the normal timing rate, was chosen so that of the four data samples taken during a frequency step at least half would be usable for data reduction. What this means is that at least half the data samples would have been taken a sufficient number of radiometer time constants after frequency switching to be useful.

5.3 Oscillator Switching Logic

The logic that determines which of the eight oscillators is operating at any given time is illustrated in Figures 18 and 19. The logic consists of a three-stage counter, a diode matrix, and eight power switches such that only one oscillator is in operation at a time.

5.4 Calibration Control

A description of a calibration cycle follows:

(a) When the outputs of FF6 - FF9 are "true" (~15.0 volts) the antenna relay RY_{101} (Figure 11) is energized and switches the radiometer from the antenna to the internal dummy antenna. At this time the attenuator relays are still deenergized and no noise is injected into the dummy antenna.

(b) When the output of FF4 becomes "true", RY_{702} (Figure 27) is energized and pulls the contacts to the left injecting a noise

level approximately 20 db above the mean value of T_R. RY_{702} remains energized for a complete frequency stepping sequence since FF1 - FF3 must count 8 subcycles ($2^3 = 8$) before the state of FF4 will change.

(c) When the output of FF4 goes "false", (~0 volts) the output of FF5 will go "true" and energize RY_{701} (Figure 27). Thus the contacts of RY_{701} will move to the left and a noise level of approximately 40 db above the mean value of T_R is injected into the dummy antenna.

(d) When the output of FF4 again becomes "true", both RY_{701} and RY_{702} will be energized and the contacts of RY_{702} will move to the left. In this position, a noise level of approximately 65 db above the mean value of T_R is injected into the dummy antenna. This is the highest level of calibration.

(e) When the output of FF4 goes "false", the output of FF6 will also go "false" since it will have counted the four cycles of FF4. When the output of FF6 goes "false", the antenna relay RY_{101} is de-energized and the radiometer input is returned to the antenna. The output of FF6 going "false" also means that the two-input AND gates for the attenuator relay drivers are no longer satisfied and will not be satisfied again for 60 subcycles (beginning of the next calibration cycle). Thus the attenuator relays will not be operated during the normal counting of the Main Logic chain until the outputs of FF6 - FF9 are again all "true".

The input to the counter is the output signal from the Pulse Drive Redundancy (PDR) circuitry under normal frequency stepping operation. Thus the frequency of operation of the radiometer is changed every 1.152 seconds and is in synchronism with the telemetry system. The PDR circuit produces an output pulse approximately every 2.3 seconds to step the radiometer frequency in the event of failure of the spacecraft timing signal.

The input to the Oscillator Switching Logic is a pulse produced by ground command during single frequency operation.

6. Local Oscillators

Eight crystal controlled oscillators are used in the radiometer with frequencies ranging from 10.75 MHz to 14.20 MHz (Figures 22 and 23). The circuits for four of the eight oscillators are illustrated in Figure 25. The other four circuits are identical with the exceptions noted on the drawing. This circuit was developed to require neither inductive elements nor critical adjustments. This allows a single circuit to be used with all eight crystals with little or no individual adjustment. This also allows the operating frequencies of the radiometer to be changed at any time within the 50 KHz to 3.5 MHz spectrum by simply changing a crystal.

The circuit, which was designed for high stability of both the output frequency and amplitude, consists of a slightly degenerated common emitter feedback amplifier with the crystal element in the feedback path. This circuit provides both low drive voltage to the crystal and a low output impedance with a good waveform at the emitter. This point is coupled through a switching diode to a common output buss.

The oscillator which is selected by the logic has +11.2 volts applied to its input while all the other oscillators' power inputs are grounded. This causes the selected oscillator to operate while the others are deenergized.

Diode switching is used between the oscillator circuits and the common output buss so that the inactive oscillator circuits will not load the active oscillator output. Current through the selected diode lowers its dynamic impedance to a low value (nominally 25-30 ohms) and raises the dc level on the common output buss to a value of from 1.5 to 4.0 volts depending on the circuit selected. This will be discussed later under frequency identification. Since all the power inputs to the other oscillator circuits are grounded, the diodes in these circuits are back-biased by the dc level of the output buss. In this condition, the

capacity of each diode is approximately 1.5 pf, giving a total capacitance loading of approximately 10.5 pf on the common output buss. This impedance does not represent an appreciable loading of the buss at the highest oscillator frequency (14.2 MHz).

The power is switched from the previously selected circuit to the new circuit when a new frequency is selected by the logic. The rf buildup time to produce a fully stable output is 3 to 8 milliseconds after power is applied to an oscillator circuit. The oscillator output decays to zero in less than 1 millisecond when power is removed from a circuit. This rf buildup time is insignificant since even at a 64 kilobit/second sample rate, 18 milliseconds elapses after switching and before the first data sample is taken.

An analog voltage staircase is generated and fed to the telemetry system on a main commutator word (M/C 13) so that the frequency of operation of the radiometer is identified. The means of generating this staircase is a resistor in the oscillator circuit which is in series with the output switching diode. The value of the resistor determines the current through the diode and thus the dc level on the common output buss (see above). This dc level is fed to the telemetry and uniquely determines the frequency of operation.

7. IF Amplifier and Detector

The specifications for the OGO-V radiometer IF amplifier were defined as follows:

(a) The amplifier should be gain-controlled (AGC) with a logarithmic response $\pm$ 1 db over a 40 db range of input signal and should have a 55 db useful range.
(b) Maximum small signal voltage gain from amplifier input to envelope detector input of 70 db (approximately).
(c) DC output range of from 0.05 volts (no signal) to 4.9 volts (maximum signal).

(d) DC output impedance < 1000 ohms.

(e) Center frequency = 10.70 MHz.

(f) Bandwidth = 400 to 600 kHz between 3 db points.

(g) No-signal output variation < 0.06 volts for a temperature range from -10°C to +50°C.

(h) Dynamic temperature stability of < 3 db variation in input signal for the same dc output over a range of =10°C to +50°C.

(i) The center frequency shift with both temperature and signal level should be small enough so that the gain at 10.70 MHz is no less than .95 maximum gain.

Extensive research was conducted to design an amplifier which met all of these requirements. The result is illustrated in Figures 24 and 26.

Of all the AGC principles investigated, the most successful was the use of a variable impedance element in the emitter circuit of a common emitter amplifier. This allows the gain variation of the stage to be controlled by the emitter current.

Certain types of germanium diodes show a wide variation in forward resistance with diode current while displaying a very low temperature coefficient of resistance with varying current. Typical values of forward resistance for the 1N498 diode are as follows:

Diode Current	Forward Resistance
microamps	ohms
50	805
100	450
250	198
500	108
1000	59

As the AGC voltage is varied, a varying emitter current will flow through the diode, modulating its forward resistance according to the table above. Gain variations of over 30 db per stage can be obtained using this method with well controlled logarithmic response of over 20 db per stage.

A four stage AGC amplifier having two variable gain stages, one of which is a cascode stage, was designed and built for the OGO-V radiometer. In addition to being gain-controlled it is temperature compensated at two critical points with sensistors. This amplifier fulfills all the requirements set forth above as being necessary for proper overall system operation.

Following the four stage IF amplifier is an envelope detector, the dc bias of which is stabilized by a thermistor-sensistor combination. The output is fed to an emitter follower amplifier. The AGC voltage for the IF amplifier is developed in the emitter circuit and is fed back to the first two stages of the amplifier for gain control.

The drive for the final output driver is developed in the same emitter circuit. The elements which determine the post detection time constant (τ) of 0.21 secs are located between this emitter follower and the final driver.

The radiometer output voltage which is fed to the telemetry system is developed in the emitter circuit of the final driver. The output voltage is constrained to be between 0 and 5.1 volts by the combination of D_{207} and D_{208} which determine the emitter bias and collector voltage respectively. This constraint satisfies the requirement of the telemetry system on the OGO spacecraft.

The ordnance circuitry shown in Figures 24 and 26 was used for the original antenna assembly. This circuitry was not used for the antenna assembly flown on the OGO-V spacecraft. (see section A)

8. In-flight Calibrator

A solid state noise generator is used so that the radiometer can be calibrated in flight during the previously discussed timing sequence. This circuitry is illustrated in Figure 27 and 29.

Solid state noise diodes with well known noise properties were investigated for use and life test data was collected on 10 units for more than two years. In all cases it was found that the noise properties of these diodes (noise spectrum, absolute output level, and temperature coefficient of noise output) remained constant provided that they were supplied from a constant current source. In only one case did the noise properties of a diode change during the life test, and this was accompanied by a current change very early in the life test.

The circuit incorporating the solid state noise diode and the associated video amplifier was designed to produce a maximum RT product of approximately $2.5 \times 10^{8} \Omega^{\circ}K$. The response of the video amplifier is flat from 20 kHz to 1.2 MHz and is 3 db down at approximately 4.0 MHz. The overall gain of the amplifier is approximately 12 db. The amplifier is temperature compensated at critical points and uses degenerate feedback to achieve a high degree of gain stability.

The noise spectrum of the diode is essentially white to well beyond the cutoff frequency of the video amplifier and thus does not influence the overall noise spectrum presented to the radiometer input during calibration.

To monitor the current through the noise diode during flight, since this is the critical parameter in determining the noise output of the diode, a series resistor provides a voltage drop which is fed to the telemetry system. This level is put out on a subcommutator word and provides continuing information on the diode current during flight.

A temperature-sensitive network consisting of a thermistor-resistor combination is incorporated into the noise amplifier circuitry

to provide in-flight information about the noise diode temperature. The output of the thermistor bridge is put on a subcommutator word. The calibration for this bridge is shown in Figure 28.

It should be noted that the solid state noise diode is not the primary standard for calibration of the radiometer. The primary standard is a thermionic diode noise source which was used during the laboratory calibration of the radiometer. This will be covered under the section on preflight calibration. The only purpose of the in-flight calibrator is to determine the magnitude of any gain changes which may occur in the radiometer during flight.

A four-level calibration is used to achieve adequate calibration of the entire useful dynamic range of the radiometer at all frequencies. The calibration cycle consists of four frequency subcycles (see section 2 and 5.4) each having a 9.2 second duration. During the first subcycle the noise calibration signal is zero but the radiometer input is switched from the antenna to an internal dummy antenna. During the second, a low noise level is applied to the dummy antenna. During the third and fourth subcycles, successively higher noise levels are applied to the radiometer input through the dummy antenna. At the end of the fourth subcycle, the antenna relay restores the antenna to the radiometer input and the noise attenuator relays are restored to their original states.

The noise attenuator relays along with their associated drivers and the antenna relay driver are shown in Figure 27. The contacts of the two attenuator relays are shown in their normal positions. Since the attenuator relays are non-latching types, the contacts will be moved to the left only during the time the relay coils (RY_{701} and RY_{702}) are energized. Tke relay drivers are driven from a two-input AND gate so that the attenuator relays will not be operated except during the four subcycles of interest. The inputs for the relay drivers are the outputs of FF4 - FF9 (Figure 20).

Relay contacts which move in synchronism with the contacts carrying the calibration noise levels carry dc voltages whose stepped values, fed to the telemetry system, identify the contact positions of RY_{701} and RY_{702} and thus the calibration level at any time during the calibration cycle. Due to relay limitations, the dc level on this telemetry word is the same for the first two calibration levels but changes for the remaining two. The telemetry word is used for radiometer frequency identification (see Figure 11) during normal radiometer operation (not during calibration).

9. Voltage Regulator

One of the most important considerations in the design of a highly sensitive radio frequency radiometer is the avoidance of radio frequency interference (RFI) generating circuitry. While filtering can be used to adequately reduce external RFI, internally-generated RFI is much more difficult to eliminate. It was for this reason that a series regulator circuit was chosen over a converter circuit for supplying power to the radiometer from the spacecraft.

A converter power supply has three main advantages:

(a) It provides good input/output isolation.

(b) It is efficient.

(c) It can provide a dual polarity output voltage higher than the input voltage.

On the other hand, a converter has two major disadvantages for a satellite-borne radio astronomy receiver:

(a) The circuitry is more complex, calling for more components, which means a lower reliability figure.

(b) The circuit lends itself to generation of large amounts of RFI.

Since the radiometer uses single polarity low voltage circuits exclusively, and careful design can provide adequate input/output isolation from a series regulator, as well as approximately the same efficiency as a converter; we chose the regulator circuit, primarily for RFI reduction.

The specifications for the series regulator are as follows:

Input Voltage Range	
Continuously	+23.5 to +33.5 volts
Intermittently (up to 10 minutes)	0 to +42 volts
Transient Tolerance (10 ms maximum)	+50 volts
Line Regulation (23.5 to 33.5 volts)	<0.1%
Load Regulation (0 to 125 ma)	<0.1%
Temperature Coefficient (-20°C to +60°C)	<0.01%/°C

It should be pointed out that these regulation figures are not the actual figures for voltage regulation at the circuits since all critical circuits have temperature-compensated zener diodes on the circuit boards to provide additional regulation. Thus a realistic figure for the regulation at the critical circuits is 0.01% for all line and load conditions over a temperature range from -10°C to +30°C.

The regulator circuit is illustrated in Figures 30 and 31. C_{323} forms a low impedance path for noise on the spacecraft supply. It also filters out noise generated in the regulator and keeps it from being reflected unto the spacecraft buss.

Q_{301} and Q_{302} form a Darlington pair amplifier with Q_{301} being the series control element in the regulator circuit. The control voltage to the base of Q_{302} comes from the output of the sensor amplifier, Q_{305} - Q_{304}. The input to this sensor amplifier is the output voltage sensing network consisting of R_{309}, R_{310}, R_{311}, and R_{313}. R_{309} is a sensistor which improves the temperature coefficient of the regulator. There is also a sensistor in the emitter circuit of Q_{305} which, in combination with D_{302}, sets the operating point for the first stage of the sensor amplifier. Again, this sensistor at the critical first stage of the amplifier, increases the temperature stability of the

regulator circuit. D_{303}, in the emitter circuit of Q_{304}, sets the operating point for the second stage of the sensor amplifier.

R_{312} and R_{314} form a voltage divider which senses the regulator output voltage and feeds this level to a subcommutator word for monitoring purposes during flight.

Current limiting circuitry was incorporated to protect the series pass transistor from transient or accidental shorts. The circuit consists of R_{304}, D_{301}, and Q_{303}. When the voltage drop across R_{304} exceeds the threshold voltage of D_{301} in series with the base-emitter junction of Q_{303}, Q_{303} conducts, lowering the base drive to Q_{302}. This increases the collector-emitter voltage drop across Q_{301} and rapidly drives the regulator output voltage to zero.

Special precautions were taken to reduce the conduction of RF noise from the regulator to the RF circuits and also between the RF circuits. D_{302} was bypassed so that any noise generated in this zener would not be introduced into the buss voltage.

A high degree of decoupling between critical boards was accomplished by using LC filter networks in addition to the low ac impedance presented by the zeners. This effectively isolates the circuits from each other and reduces the interchange of RFI.

Also illustrated in Figure 31 are the LC line filters. These serve the dual purpose of reducing external RFI conducted into the experiment and reducing the level of internally-generated RFI conducted out of the experiment onto the spacecraft wiring.

A temperature sensing network consisting of R_{302}, R_{303}, and R_{305} was incorporated into the regulator circuitry so that the temperature of the series pass transistor may be monitored. This monitor would give an indication of abnormal power dissipation in the series transistor and allow shutting off of the radiometer before serious damage was done to the regulator. The calibration for this network is shown

in Figure 28. The output of the bridge is fed to the Test Interface Connector (J-102) for preflight monitoring. There is no provision for in-flight monitoring of this temperature.

C. GROUND SUPPORT EQUIPMENT

1. General Operation

The Ground Support Equipment (GSE) was designed to operate and checkout the radiometer before, during, and after various qualification tests. The GSE consists of three suitcase-mounted units.[1] The units are designated as follows:

(a) Test Monitoring Unit (Suitcase A)
(b) Spacecraft Simulator Unit (Suitcase B)
(c) Stimulus Unit (Suitcase C)

The three units, mounted in the suitcases, are shown in Figure 32.

Four test modes are possible with the GSE. The first test mode monitors the output from the package when the radiometer is separated from the spacecraft and no connection is made to the Spacecraft Interface Connector. In this mode the radiometer would be changing frequency at its internal free-run rate (~1 step/2.3 sec). The monitoring mode requires only Suitcase A.

The second test mode consists of dynamically stimulating and monitoring the experiment when it is completely separated from the spacecraft. This mode requires the use of all three suitcases.

The third test mode consists of stimulating and monitoring the experiment when it is integrated into the spacecraft. This mode requires the use of Suitcases A and C.

The fourth test mode is used to test the antenna ordnance devices and requires only the use of Suitcase B.

2. Test Monitoring Unit (Suitcase A)

The Test Interface Connector on the radiometer provides access

[1]The descriptions which follow are only general descriptions of the Suitcase Units. For detailed descriptions, along with discussions of their use, refer to Reference 11.

to thirteen test points which are used to ascertain the proper operation of the radiometer. The test points were selected so that proper circuit operation can be completely determined by monitoring DC levels only. Suitcase A contains a digital voltmeter (DVM) and the necessary switching to select and display any one of the test signals from the radiometer. It also contains a calibration control to disable the radiometer's internal calibration cycle and an auxiliary + 28 volt supply.

Figure 33 is a block diagram of the Test Monitoring Unit. The Test Point selector switch selects the test point voltage to be applied to the self-contained digital voltmeter. Any one of thirteen (13) test points may be selected.

A key-lock switch activates an auxiliary +28 volt power supply to power the experiment.

A calibration control switch disables the experiment's calibration cycle.

The DVM switch selects the input to the DVM. In the Test Point position it is connected to the Test Point selector switch. In the External position it is connected to the binding posts on the front panel. In the S/C Voltage position it is connected to the 28 volt S/C bus and reads the voltage applied to the experiment from either Suitcase A, Suitcase B, or the spacecraft.

The circuit diagram for Suitcase A is shown in Figure 34.

3. Spacecraft Simulator Unit (Suitcase B)

The Spacecraft Simulator Unit supplies all signals and power normally supplied to the radiometer by the spacecraft.

Figure 35 is a block diagram of the Spacecraft Simulator Unit. This unit furnishes the +28 volt power for the radiometer electronics, the +28 volt power for the ordnance circuit and the 50 millisecond impulse commands.

Operating the AC key lock switch applies power to the adjustable power supply and to the power supplies (+6V, -6V, +18V, and +28V) which are required for the suitcase electronics. The Electronics On switch simulates the radiometer electronics on-off command.

The 50 millisecond commands are sent by grounding the command lead selected by the Impulse Command Select switch for 50 milliseconds. The grounding operation is accomplished by the Impulse Command relay in the following manner. The Reset pushbutton resets the two flip-flops arming the Command pushbutton. Two lamp drivers operate from the flip-flops and indicate this condition by turning the Reset light on and the Command light off. Pressing the Command push-button causes Flip-Flop 2 to go to the set state which starts the 50 millisecond One Shot and turns the Reset light off. The One Shot pulse output causes the Relay Driver to pull in the Impulse Command relay for 50 milliseconds which grounds the appropriate command line. The Impulse Command relay in reutrning to the deenergized state sets Flip-Flop 1 which in turn causes the Command light to come on. When this light comes on, the operator is certain that the Impulse Command relay has operated properly. Flip-Flop 2 acts as a circuit lock-out and assures the operator that only one command will be sent each time he completes the Reset-Command sequence.

The pulse Generator has two repetition rates (.868 pps and 8.68 pps), an adjustable pulse width of 10 - 30 microseconds, and an adjustable output of 0 - 18 volts. The pulse simulates the spacecraft timing signal.

The Ordnance Power key lock switch actuates the Squib Power relay, the Ordnance Power relay and completes the +28V Interlock Circuit for the Impulse Command relay. The Squib Power relay places a fixed one ampere load on the power supply and shorts out the internal charging resistor. The Ordnance Power relay simulates the Ordnance Power On command and makes ordnance power available at the radiometer package. The +28V Interlock circuit inhibits the Impulse Command relay in the

Squib Test and Antenna Deploy command posltions until the Ordnance Power key lock switch is actuated.

The Squib Fire relay is actuated for 50 milliseconds when the Squib Test command is sent. This relay applies the ordnance power to the Squib Test jack for 50 milliseconds only.

The circuit diagram for the Suitcase B unit is shown in Figure 36.

4. Stimulus Unit (Suitcase C)

Suitcase C contains the temperature limited diode, the video amplifier, and the associated power supplies which comprise a noise source for simulating the cosmic noise input to the radiometer. The suitcase also contains a H-P 651A Test Oscillator for measuring the gain of the video amplifier.

Figure 37 is a block diagram of the Stimulus Unit. The noise source consists of a temperature limited diode followed by a four stage video amplifier. A voltage which is proportional to the noise diode emission current is available at a front panel jack. A connection may be made between this jack and the External Input to the DVM in Suitcase A to allow the diode current to be adjusted with greater accuracy than possible using the panel meter in Suitcase C. The value of diode current is set by adjusting the diode filament voltage furnished by the regulated filament supply.

The noise diode B+ supply furnishes power to the diode plate circuit and to the operational amplifier in the filament voltage regulator.

The video amplifier power supply furnishes +18 volts for operation of the video amplifier.

The isolation transformer and filters provide 115 VAC, 0.7 amperes, 60 Hz power for external use.

The H-P 651A Test Oscillator is externally connected for calibration purposes.

The circuit diagram for the Suitcase C unit is shown in Figure 38. The circuit diagram for the video amplifier in the noise calibration source is shown in Figure 39.

III. PREFLIGHT CALIBRATION

A. GENERAL

The preflight calibration of the OGO-V(E) radiometer can be divided into three categories:[12]

(a) Determination of the input impedance of the radiometer at the eight operating frequencies.

(b) Determination of the parameters which define the noise figure of the radiometer at the eight operating frequencies.

(c) Measurement of the overall system response over the anticipated temperature and input signal operating ranges.

The first two series of measurements were conducted at room temperature with the data recorded by hand. The last series of measurements were made using the UM/RAO Data Logger facility. This facility not only allowed automatic control of the radiometer but also produced a computer-compatible digital magnetic tape.

The tape was processed on the UM/RAO Scientific Data Systems (SDS) 930 Computer and produced both digital printout and Calcomp plots of the system response curve.

The first calibration of the flight unit radiometer was conducted 15 August 1966. The final calibration prior to launch was conducted 25 September 1967.

B. INPUT IMPEDANCE MEASUREMENTS

The equipment setup for the determination of the radiometer's input impedance is shown in Figure 40. The generator was adjusted for an input signal of approximately 10 millivolts rms at the radiometer. The bridge was then adjusted for a null as indicated on the Keithley meter and the impedance indicated on the bridge noted. This measurement was repeated for each of the eight operating frequencies of the radiometer.

The components of the input impedance of the radiometer at the eight frequencies are shown in Table 1.

C. DETERMINATION OF NOISE PARAMETERS

The four noise parameters, F_o, R_N, B_o, and G_o, were determined at each of the eight operating frequencies of the radiometer.[4,6]

D. OVERALL SYSTEM RESPONSE CALIBRATION

1. General

It was known from our experience with earlier radiometers that a large effort was involved in obtaining adequate preflight calibration. Therefore, we approached the calibration program through a study to determine the feasibility of using the UM/RAO Data Logger facility for the system response calibration. We used the prototype radiometer to resolve the interfacing problems and to prove the feasibility and desirability of using the facility for this program.

It became immediately evident from the preliminary tests that the man-hours of effort required for the calibration program would be drastically reduced. In addition, three major advantages are offered using the Data Logger over recording the data by hand:

(a) A large amount of human error is removed. This is because human operators are not required to make many tedious measurements and record large volumes of data.

(b) A much larger volume of data can be taken, allowing averaging of the samples. This allows more accuracy in the data recorded in a noisy environment.

(c) The fact that the output of the facility is a digital tape allows the data to be processed immediately using computer programs to produce plots of the system response. This type of presentation allows rapid evaluation of the adequacy of the calibration procedure.

The total time required to record eleven parameters, at 100 different noise and supply voltage conditions for each of seventeen temperatures was approximately 25 hours. This did not include the time for the temperature chamber to stabilize. The stabilization time was approximately one hour for each temperature. The calibration program was completed in 40 man-hours. This is less than 25% of the normal time required to do a similar task by hand, based on our experience with earlier radiometers. This, in addition to the other advantages listed above, represented a significant improvement over similar programs on other radiometers.

2. Test Setup

A block diagram of the setup is shown in Figure 41.

The Data Logger facility consists of a SDS Model MU31-1 Multiplexer, a SDS Model AD20-14 Analog-to-Digital Converter, an Ampex Model TM4113-D Digital Tape Handling System and special sequence and control circuitry constructed in the UM/RAO Laboratory from Computer Control Company 1 MHz logic modules.

The multiplexer has 16 input channels with an input impedance of approximately 100 kΩ. The maximum switching rate for this model is 15 kHz. The acceptable input voltage range is between ± 10 volts.

The A-D converter converts each sample to a thirteen bit plus sign bit digital representation. Thirteen bits provide a resolution of better than one part in eight thousand. The conversion rate for this model is 13,300 samples per second. The Converter also includes sample and hold circuitry which provides a sample aperature of less than 1 microsecond.

The TM4113-D Tape Handling System is designed to read and write tapes that are compatible with the UM/RAO SDS 930 Computer. It can be operated at tape densities of either 200 or 556 characters per inch and tape speeds of either 30 or 60 inches per second. It

uses 2400 foot reels of 1/2 inch magnetic tape.

In addition to the sequencing and control circuitry provided for control of the Data Logger facility, control circuitry was built to automatically sequence the radiometer through its eight frequency steps. This circuitry stepped the radiometer and then provided a delay of approximately one second before the radiometer data was recorded. This delay allowed the radiometer output to fully stabilize before it was sampled.

The Data Logger facility is shown in Figure 42.

The temperature chamber used for the calibration was an Associated Testing Laboratories Model SLHU-1-LC-1. This chamber is capable of providing any temperature between -75 and +220°C with a temperature control of ± 1.1°C after stabilization.

The external noise source used for the calibration was a broadband noise source designed and constructed at the UM/RAO Laboratory.[11] This generator is similar in design to the Suitcase C Unit.

The output of the noise generator was fed through a Weinschel Model 64A precision attenuator which allowed the attenuation of the noise signal to be set to 1 db with a precision of ± .03 db.

The ground support equipment (GSE) used was a Suitcase B Unit which provided power and the necessary impulse commands to exercise the radiometer. A complete description of this unit and its operation can be found in reference 9.

The junction box was built to provide an interface between the cable to the Test Interface Connector on the radiometer and the input cables to the Data Logger Facility. This box contains scaling resistor strings and the necessary interfacing connectors. The junction box also contained a means of defeating the normal calibration sequence in the radiometer so that the radiometer did not go into the calibration cycle during the test. This allowed

the calibration as well as the frequency stepping to be controlled externally.

3. Radiometer Configuration

For all of the calibration runs, the radiometer was kept in the manual frequency stepping mode with the internal calibration sequencing disabled. The stepping of the radiometer circuitry was controlled by a switch closure whose timing was determined in the control logic circuitry of the Data Logger. This circuitry changed the radiometer frequency, provided a delay of approximately one second and then initiated the sequence to write the data samples on the magnetic tape.

The control of the radiometer's internal calibration cycle was accomplished with a switch on the junction box which grounded the output of FF1 of the Main Logic chain. This was done through the Test Interface Connector on the radiometer. Only when the switch was "open" could timing pulses from Suitcase B cause the Main Logic chain to count. Therefore, it was possible to stop at any level of the internal calibration for an extended period of time. It was also possible to keep the radiometer from going through its internal calibration by use of the same switch. This allowed use of the external calibration source for noise injection.

The radiometer input conditions for which data was recorded are listed in Table 2.

4. Calibration Results

As mentioned earlier, the output of the Data Logger facility is a digital tape. This tape was processed after each temperature run as a check on the calibration procedure. The average time from the end of the temperature run to digital printout for the complete run was approximately 30 minutes. An example of the digital printout is shown in Figure 43.

The plotting of the data was normally not done until a sufficient number of temperatures had been run to show temperature variations in the system response. If it were desired to plot the data immediately, a turn-around time comparable with the time for digital printout was possible.

The data plotting was done on a California Computer Products (Calcomp) plotter. This device was driven by a controller designed and constructed at the UM/RAO which interfaced with the SDS 930 computer.

An example of a Calcomp plot of the radiometer calibration data is shown in Figure 44.

IV. RELIABILITY ASSURANCE PROGRAM

A. COMPONENT SELECTION

In general, all components used in the radiometer were chosen from devices which had been previously qualified for space application. The devices were chosen from the Preferred Parts Lists (PPL) prepared by Goddard Space Flight Center, Marshall Space Flight Center, and the Jet Propulsion Laboratory wherever possible. The only exceptions to the use of these lists were in areas where strict adherence to the lists would have adversely affected the system operation.

An attempt was made to select devices which had been qualified to a Military Specification when it was not possible to use a device from the PPL.

In two areas where it was necessary to use devices which neither appeared on the PPL or had been qualified to a Military Specification, screening specifications were written to which all the devices used were subjected. These specifications were written after many conversations with the people responsible for the preparation of the PPL.

The number of different device types was reduced as much as possible to facilitate procurement and to simplify the reliability screening requirements.

B SCREENING PROCEDURES

1. General

Documented test data is available on practically all electronic components which demonstrates 100% screening is necessary on the devices to assure a highly reliable part. This philosophy of 100% screening was followed throughout our reliability assurance program.

Screening specifications were written for all the semiconductors as well as for the oscillator crystals, crystal filters, and relays

following initial component selection. Trips were then taken to all manufacturers from whom we anticipated or contemplated procuring the devices. We discussed our screening requirements with them and in some cases modified our requirements.

Following these trips, we selected the manufacturers from whom we would purchase the devices and held another series of discussions to finalize our requirements. A final screening specification was prepared in view of the selected manufacturers' in-house specifications. A list of these specifications is given in Appendix A, along with a typical specification, in this case for a silicon transistor.

2. Vendor Screening

A summary of the screening procedures used by the vendors for the various devices is given below:

(a) Silicon Transistor
   1. Visual inspection on a sample basis
   2. High Temperature storage
   3. Temperature cycling
   4. Constant acceleration
   5. Gross leak test
   6. Helium leak test
   7. Burn-in
   8. X-ray inspection

(b) Silicon Computer Diode
   1. High temperature storage
   2. Thermal shock
   3. Visual inspection
   4. Burn-in

(c) Germanium Diode
   1. Thermal Shock
   2. Constant acceleration
   3. Visual inspection
   4. Reverse bias at elevated temperature

(d) Silicon Reference Diodes
    1. Visual inspection
    2. High temperature storage
    3. Thermal shock
    4. Constant acceleration
    5. Gross leak test
    6. Helium leak test
    7. Burn-in
    8. X-ray inspection
(e) Oscillator Crystal
    1. Vibration on a sample basis
    2. Visual inspection
(f) Crystal Filter
    1. Vibration on a sample basis
    2. Electrical measurements
    3. Visual inspection
(g) Relay
    1. High temperature bake
    2. Visual inspection
    3. Electrical measurements
    4. Operating life test on a sample basis
(h) Electrolytic Capacitor
    1. Leak test
    2. Shock and vibration test
    3. Thermal shock
    4. Life test
    5. DC leakage
    6. Capacitance
    7. Dissipation factor
    8. Visual inspection
    9. X-ray inspection
(i) Ceramic Capacitor
    1. Leak test
    2. Flash test

3. Burn-in
4. Visual inspection

(j) Metal Film Resistor

1. Vibration
2. Thermal shock
3. Noise screening

The tests indicated were performed in the sequence shown and on a 100% basis except where noted.

The tests to be performed were selected after conversations with the manufacturers and persons concerned with reliability at Bell Telephone Laboratories, Hughes Aircraft, General Dynamics, GSFC, MSFC, and JPL.

The basis for acceptance or rejection of a device was the incremental change in one or more critical parameters before and after a burn-in or operating life test. The only exceptions to this criteria were the electrolytic capacitor and the metal film resistor. The manufacturers of these devices had developed tests which satisfied other space programs and these tests were used in lieu of operating life test screening.

3. UM/RAO Screening

Incoming inspection was performed on the devices on a 100% basis. This consisted of a verification measurement of the critical parameters in the determination of the reliability of the device for those devices which had been screened by the vendor. These parameters were the same as those specified in the vendor's screening specification.

There were four devices which were not screened by the vendor: a medium-power silicon transistor, a low-current regulator diode, a series of inductors, and a transformer. In-house screening was performed on these devices and consisted of the following tests:

(a) Medium-power silicon transistor
    1. High temperature storage
    2. Burn-in
    3. Electrical measurements
    4. Visual inspection

(b) Low-current silicon reference diode
    1. High temperature storage
    2. Burn-in
    3. Electrical measurements
    4. Visual inspection

(c) Inductor
    1. Thermal Shock
    2. Electrical measurements
    3. Visual inspection

(d) Transformer
    1. Thermal shock
    2. Electrical measurements
    3. Visual inspection

The 100% incoming inspection proved to be the most effective screening procedure of all in that it revealed many possible problem areas with the devices and resulted in the upgrading of a number of devices by the vendors. This effort was aided greatly by the assistance of the Failure Analysis Laboratory at GSFC. They provided us with both the personnel and facilities to perform detailed inspections of some devices. The result of these inspections were improved devices from the vendors.

C. DOCUMENTATION

1. Screening Data

Prior to and subsequent to burn-in or operating life tests, electrical measurements were made on all the semiconductor devices. It was a requirement of the screening specifications that this data

be transmitted as part of the device order to the UM/RAO Laboratory.

Using this data as input to a statistical analysis program developed at the Laboratory, a preferential listing of the individual devices was obtained. These listings were used to select devices to be included in the radiometer and those to be retained as spares. It should be realized that all the devices used in this analysis had already passed our screening specifications.

2. Serialization

During incoming inspection, all components were assigned a UM/RAO part number. This serial number preserved the component number assigned by the vendor so that complete traceability of the individual component was possible.

All test data taken by UM/RAO personnel on a component was recorded in a Component Data Log (CDL). This log contained the movement of all components from the time they were received until their incorporation into the radiometer package. It also contained any subsequent movement of the component in the event it was later removed from the radiometer for any reason whatever.

D. COMPONENT CONTROL

Following incoming inspection, all components were placed in a locked storage area. No component left this area without a notation in the CDL as to its destination and use. If the component were later returned, a notation was made of its history while out of storage.

In the event that the device had been subjected to unusual stresses while out of storage, it was returned to incoming inspection to determine whether its electrical characteristics had been altered. The results of this inspection as well as a description of the stresses which necessitated the inspection were recorded in the CDL.

E. CONSTRUCTION PRACTICES

All construction of the flight radiometers was carried out in the UM/RAO Laboratory clean room by NASA - qualified personnel. The work of these personnel was inspected by qualified inspectors and recorded in construction logs.

Upon completion of an individual board, it was thoroughly tested and conformal coated before being placed in storage to await final construction. The boards were stored in the same locked area as the components and their movement in and out of this area was recorded in a log similar in nature to the CDL.

F. FAILURE ANALYSIS

During preliminary construction, four (4) component failures occurred. The failed components were sent to the Failure Analysis Laboratory at GSFC. The results of their investigations were as follows:

(1) Failure of a silicon computer diode - open
The cause of the failure was mechanical, perhaps caused by a faulty bonding procedure. All of the remaining devices in the lot were examined for similar faults and none were found. The failure was classified as an isolated case, at least as far as our lot is concerned.

(2) Failure of a DC relay - open circuit on NC contact set
The cause of the failure was extreme pitting of the contact set. Pitting was also observed on the other contacts in the same relay. Since our application of this relay is under dry circuit conditions, this failure was not explainable. Six (6) additional relays from the same lot were sent to the GSFC Failure Analysis Laboratory for their investigation. Their testing of the relays revealed that the amount of wiping action on the contacts varies between relays and this may contribute to the failure. However, since our application

is very low current, the relay should not display the failure mode we observed. The failure was attributed to a manufacturing flaw. All the remaining relays from the same lot were operated for approximately 10,000 cycles and their contact characteristics measured again. None displayed any contact resistance degradation.

(3) Failure of two (2) inductors - open

The cause of the failure was determined to be a mechanical failure of the bonding of the lead in the ferrite core. This allowed the lead to rock under normal handling conditions and fractured the lead to the coil wire. It was strongly recommended by the Failure Analysis Laboratory that we not use this type inductor for space applications. We accepted their recommendation and replaced all of our flight inductors with another type which had been qualified to a Military Specification including a lead pull test.

V. INTERFERENCE TESTS

A. INITIAL INTERFERENCE TEST

1. General

In line with the continuing work by the EMC group at TRW Systems to reduce the existing interference levels on the OGO spacecraft, a test was conducted using the UM/RAO E-20 prototype radiometer to ascertain its susceptibility to spurious signals.[14] Spruious signals are defined as being any frequency to which the radiometer is not tuned.

In order that the EMC group could gather as much information as possible on as many experiments as possible within the restrictions of time and budget, they arbitrarily divided the experiments into interference generators and susceptible experiments. The E-20 radiometer was selected as one of the most susceptible experiments and the following tests were performed on it:

(a) Audio Frequency (AF) Conducted - 30 Hz to 50 KHz.

(b) Radio Frequency (RF) Conducted - 50 KHz to 65 MHz, 136± 2 MHz, 400 ± 4 MHz.

(c) Radio Frequency Radiated - 15 KHz to 65 MHz, 136 ± 2 MHz, 400 ± 4 MHz.

(d) Transient Conducted - 50 volt, 2 μsec pulse.

2. Test Setup

Figures 45 through 48 show the test setups for various portions of the tests.

3. Radiometer Configuration

For all tests except the second half of the RF Radiated test, the input of the radiometer was terminated in a dummy antenna as shown in Figure 49.

For the 400 MHz section of the RF Conducted test, the signal was fed directly into the dummy antenna.

4. Test Results

Figures 50 and 51 show the threshold levels for the AF conducted interference test. These voltage levels were superimposed on the 28 volt power line and caused a 40 millivolt increase in the radiometer output above the quiescent level.

Table 3 shows the results of the RF conducted interference test. Again the voltage levels shown give a 40 millivolt increase in the radiometer output above the quiescent level. The voltage was superimposed on the 28 volt power through use of a break-out box/isolation transformer combination in the power line. The lone exception to this configuration is the 40 MHz voltage which was injected through a dummy antenna directly into the radiometer.

The RF radiated interference test data is not reproduced here. The reason for this is that any radiated test conducted in an enclosed shielded room is extremely suspect. One can measure radiated power but meaningful field strength measurements are impossible. The interfering frequencies are essentially the same as those revealed in the RF conducted interference test.

The Transient conducted interference test produced no response in the radiometer.

It was obvious from this test that additional low pass filtering in the radiometer was highly desirable.

B. LABORATORY TEST

1. General

As a result of the Radio Frequency Interference (RFI) tests made at TRW Systems,[14] an investigation was conducted at the RAO Laboratory to determine possible means of reducing the susceptibility of the radiometer to spurious (outside 50 KHz to 3.5 MHz passbands) signals.[15]

From the pattern of the spurious responses seen on the initial measurements made on the unmodified radiometer, it appeared that harmonics of the local oscillator frequencies, generated in the mixer circuit, were being fed back to the preamplifier. There they were mixing with the spurious signals, producing frequency components in the signal passband of the radiometer.

Assuming this to be the interference mechanism, a two-step approach was taken to correct the condition. First, a series impedance element was added to the preamplifier input. When the optimum value for this element was determined, a series impedance element was added to the mixer circuit input. This was to reduce the signal fed back from the mixer to the preamplifier.

When the final filter configuration was chosen, the susceptibility test was rerun with the radiometer in the 3.5 MHz channel. This was to confirm the effectiveness of the filter. The results are shown in Table 4.

Finally, a test was run to determine the degradation in radiometer sensitivity as a result of the series input element. The results are shown in Table 5.

C. COMPARATIVE SUSCEPTIBILITY TESTS

1. General

These tests were run to demonstrate the improvement in RFI rejection of the flight unit radiometer as a result of the filtering incorporated.[16] The unmodified prototype radiometer was used for comparison.

The first series of tests were conducted injecting the signal directly into the radiometer input through a dummy antenna. The frequency range covered was 10.7 MHz to 400 MHz.

The next series of tests were the RF conducted interference tests. They were conducted in the same manner as the original RF conducted interference test.[14] They covered the frequency range of 60 kHz to 400 MHz.

The last series of tests were the AF conducted interference tests. Again, they were conducted similarily to the first test. The frequency range was 50 Hz to 60 kHz.

2. Test Setups

(a) Direct Input RFI Susceptibility Test

The test setup for this series of tests was essentially the same as that used in the UM/RAO Laboratory for the filter investigations [15] and is shown in Figure 52.

(b) RF Conducted Interference Test

The test setup for this series of tests is illustrated in Figure 46.

(c) AF Conducted Interference Test

The test setup for this series of tests is illustrated in Figure 45.

3. Radiometer Configuration

For all the test runs, both the prototype and flight unit radiometers were operated at 3.5 MHz with their inputs terminated in a dummy antenna.

4. Test Results

(a) Direct Input RFI Susceptibility Test

If harmonics of the local oscillator frequency were causing the problem, as theorized, spurious responses should appear approximately every 7 MHz with the radiometers operating at 3.5 MHz.

The results of the test are shown in Table 6.

The improvement on RFI rejection in the flight unit over the prototype ran between 10 and 36 db for all spurious response frequencies. The rejection of both units to 136 MHz was equal (no response for ~1.0 volt rms input) but the

flight unit exhibited no response at 400 MHz with a 1.0 volt rms input. This was an improvement of >4.5 db over the prototype. The actual improvement was unmeasureable as 1.0 volts rms is the maximum output capability of the signal generator used.

The filtering in the flight unit made a significant improvement in the reduction of direct coupled interference. It should be noted that this is the most significant interference mode when the antenna is connected to the radiometer.

(b) RF Conducted Interference Test

The results of the RF conducted interference test are not as conclusive as those for the direct coupled interference. Both results are shown in Table 6.

The difference between the units ran between a 6 db degradation in rejection in the flight unit to a 21.6 db improvement. However, the number of frequencies on which degradation occurred is relatively small (<10%) with the average improvement running ~14 db. The evidence is not conclusive but it appears that the filtering made an improvement in conducted interference rejection.

Neither unit exhibited any response at 136 or 400 MHz with approximately 1.0 volt rms signal imposed on the 28 volt power line.

(c) Audio Frequency Conducted Interference Test

The rejection figures for both units were essentially the same and identical with those illustrated in Figures 50 and 51.

D. INTEGRATED SPACECRAFT INTERFERENCE (MALIBU) TEST

1. General

During the Malibu test, an attempt was made to divide the composite interference signals which we observed on the observatory into three components:

(a) Background Signals

These signals originate from sources outside the spacecraft environment. They may be present in the spacecraft environment through radiation or direct connection (e.g., GSE cables).

(b) Signals generated by the spacecraft subsystems.

(c) Signals generated by other experiments.

From this series of tests, we attempted to evaluate the effect on the radiometer of signals from group (b) and (c) in the presence of the background signals.

Two major restrictions were placed on the tests; one due to the physical restrictions of the test site, and the other due to the terrestrial noise environment.

(a) The solar array paddles were not on the spacecraft. There was not enough room at the Malibu test site to deploy the paddles so dummy stub paddles were used to simulate the actual paddles. Other deviations from the normal observatory configuration were used but the dummy paddles were the most significant from our test standpoint.

(b) We could only use a 5 foot antenna on the radiometer instead of the full length antenna. This was due to the high background noise level which would have saturated the radiometer with a longer antenna.

2. Test Setup

The test setup was basically the fully operational observatory with two notable exceptions:

(a) The solar array paddles were not on the spacecraft as noted above. This meant that no charge current was flowing through the array harness. This current can contribute significantly to the RFI which our radiometer sees.

(b) The Attitude Control System (ACS) could not be exercised. This was due to the high interference levels introduced by the GSE cables to stimulate the ACS.

3. Radiometer Configuration

For the first series of tests, the radiometer was locked in Calibrate Level 1. This connects the preamplifier input to a dummy antenna internal to the radiometer package.

For the second series of tests, a 5 foot antenna was connected to the radiometer output.

For both of these series of tests, the radiometer was stepping in the normal manner.

4. Test Results

(a) Conducted RFI Test

No significant interference was seen during the tests run with the radiometer connected to an internal dummy antenna.

(b) Radiated RFI Test

No definitive tests could be run on the noise contributed by spacecraft subsystems for a number of reasons:

(1) The only method of data retrieval was through the spacecraft data handling system. This meant that this system had to be operational at all times.

(2) As mentioned earlier, the ACS system could not be stimulated. This was due to the high noise level

introduced when the ACS GSE cables were connected. These noise levels masked any noise which may have been generated in the ACS system.

(3) The normal power system configuration was not used due to the absense of the solar array paddles. The batteries were charged through external chargers. Thus normal charge cycling effects could not be evaluated.

(4) In order to disable the 2461 Hz synchronization signal, a long cable was necessary. The pickup on this cable was so high as to mask any changes in the spacecraft environment due to the absense of the 2461 Hz signal.

In the area of experiment-generated interference, the tests were more conclusive. It was possible to isolate three (3) major contributors to the RFI which the radiometer encountered on the observatory. These experimenters were contacted and discussions were held as to possible means of reducing the interference levels. As a result of the Malibu test, changes were made in the configurations of all three of these major offenders, either in the experiment itself or the spacecraft harnessing to the experiment.

After a thorough analysis of the test results, a memo was written to TRW Systems outlining our conclusions as to interference sources and our recommendations for solutions to the problem. We also requested additional RFI testing when the spacecraft was in full flight configuration and all experiments were in final flight configuration.

E. HIGH-BAY TEST

1. General

At our Final Experiment Checks at TRW, we requested a special interference test with the spacecraft in full flight configuration. The spacecraft had the solar arrays installed and all of the modifications to experiments and spacecraft that were a result of the Malibu

test were incorporated. Also at this time, a test matrix was run on all experiments with six (6) experiments chosen as being most susceptible to interference. These six experiments were provided with continuous data while the other experiments were being turned on and off. Our experiment was run continuously and this data, along with the data from our special test, was used to evaluate the improvement in the spacecraft environment since the Malibu test.

2. Test Setup

The test setup was the flight-ready observatory in the folded configuration. This meant that the solar arrays as well as all booms were folded in their launch configuration.

The observatory was set up in the high-bay area of the M1 building at TRW Systems.

3. Radiometer Configuration

The radiometer was placed in the normal frequency stepping mode. A dummy antenna was installed on the external antenna terminal block for the special test. The undeployed external antenna was used during the interference matrix test.

4. Test Results

The results of the special interference test essentially confirmed the results of the conducted interference test at Malibu. However, there was a significantly lower average level on all frequencies over that seen at Malibu. This may be attributable to the final grounding configuration on the spacecraft which was much better than the grounding arrangements at Malibu.

The only other detectable changes in our radiometer output were caused by experiments 24 and 27. The level on our 50 KHz channel decreased approximately 0.4 volts when E-24 was turned on and an additional 0.8 volts when E-27 was turned on. The exact cause for this was not determined but the situation will be examined again

during an orbital interference test.

During the interference matrix test no significant differences from our special test were detected except that the average levels were higher. This is attributable to the fact that the input of the radiometer was connected to the undeployed external antenna.

It would appear from these tests that the overall spacecraft environment is much better than that observed at Malibu and that the spacecraft as a whole is quieter than previous OGOs as determined by our earlier experiments.

VI. CORRECTIVE ACTIONS

A. GENERAL

The radiometer electronics package experienced only one failure during the environmental testing. This failure occurred in the prototype package during qualification level testing.

There were three additional anomalies in the operation of the system but they were later proven to be attributable to cabling between the radiometer electronics and the antenna assembly and/or the antenna assembly itself.

The radiometer electronics failure will be discussed in some detail but the failures associated with the antenna assembly will only be outlined with appropriate references to failure reports and/or applicable memos. The reason for this is that the antenna assembly was furnished by GSFC.

B. PROTOTYPE RADIOMETER FAILURE

On 8 January 1967, the prototype radiometer failed during qualification level vibration testing at TRW Systems.[17] The prototype was mounted in the SOEP container and was being subjected to random vibration when the failure occurred.

The radiometer was returned to the UM/RAO Laboratory where it was discovered that the wire carrying +18 volts to the preamplifier board was broken. It was decided that the probable cause of the failure was inadequate stress relief on this wire.

The remaining wires in the prototype package and the two flight packages were all checked for the problem and some rework was done to provide more stress relief on a few wires. The internal wore bundles in all the packages were secured with RTV to restrict their motion.

The prototype radiometer was returned to TRW Systems and successfully completed qualification level vibration testing on 8 February 1967.

C. ADDITIONAL ACTIONS

1. On 8 December 1967, a failure report was written against the Flight Unit 2 radiometer following the 7 day thermal vacuum IST.[18] The single frequency stepping was observed to be erratic at that time.

The problem was later discovered to exist in the interface cabling between the radiometer electronics package and the antenna assembly. A memo was written on the failure and the problem was corrected.

2. On 18 January 1968, two failure reports[19] were written against the Flight Unit 1 antenna assembly. The problem was corrected by GSFC personnel.

3. On 21 February 1968, an anomaly was observed in the monitor word from the Flight Unit 1 antenna assembly. The problem was traced to a cabling interface problem and GSFC personnel corrected the anomaly. A memo was written on the problem and its solution.[20]

APPENDIX A
COMPONENT SCREENING SPECIFICATIONS

The following is a list of the screening specifications prepared by the University of Michigan Radio Astronomy Observatory Laboratory to govern the selection and test procedures of manufacturers supplying devices for the OGO-E radiometer electronics package.

CR-101A	QUARTZ CRYSTAL UNIT, GLASS ENCLOSED, HI-REL SCREENING, SPECIFICATION FOR
CR-102	CRYSTAL FILTER UNIT, HI-REL SCREENING, SPECIFICATION FOR
D-101A	SILICON COMPONENT DIODE, HI-REL SCREENING, SPECIFICATION FOR
D-102	GERMANIUM COMPONENT DIODE, HI-REL SCREENING, SPECIFICATION FOR
DR-101	SILICON REFERENCE DIODE, HI-REL SCREENING, SPECIFICATION FOR
DR-102	SILICON REFERENCE DIODE, LOW CURRENT, HI-REL SCREENING, SPECIFICATION FOR
RL-101	RELAY, DC, HERMETICALLY SEALED, HI-REL SCREENING, SPECIFICATION FOR
T-101	SILICON TRANSISTOR, HI-REL SCREENING, SPECIFICATION FOR
T-102	SILICON TRANSISTOR, MEDIUM POWER, HI-REL SCREENING, SPECIFICATION FOR

The following is a copy of Specification T-101 for three (3) silicon low power transistors. The format used for this specification was similar to that used on the other specifications.

1.0 SCOPE AND PURPOSE

1.1 Scope - This specification covers specific screening requirements for high reliability silicon transistors to be used by The University of Michigan, Radio Astronomy Observatory for space applications.

1.2 Purpose - The purpose of this specification is to set forth the screening requirements for devices procured to this document.

2.0 APPLICABLE DOCUMENTS

2.1 Specifications

MIL-S-19500C	SEMICONDUCTOR DEVICES, GENERAL SPECIFICATION FOR

The applicable military specification for the device procured (if any). The UM/RAO drawing which applies to the device to be procured.

TI QRAS No. 925	RADIOGRAPHIC INSPECTION OF SEMICONDUCTOR DEVICES

2.2 Standards

MIL-STD-750	TEST METHODS FOR SEMICONDUCTOR DEVICES

3.0 REQUIREMENTS

3.1 General Requirements - Devices procured to this document shall be the product of good engineering practices and rigid process control. Where a military specification exists for the device to be procured, the supplier will select the device from a lot of Mil-type devices and will submit a certificate of compliance stating that the device conforms to all requirements of the applicable military specification with the exception of the marking. Where no military specification exists for the device, the UM/RAO will supply a specification to the supplier and a written certificate of compliance to that specification will be required. In either case, the electrical characteristics of the device must conform to the applicable UM/RAO drawing and where conflict exists, the drawing requirements will govern.

3.2 Detail Requirements

3.2.1 Visual Inspection - Visual inspection on a sample basis in accordance with Test Method 2071 of MIL-STD-750.

3.2.2 Environmental Conditioning

3.2.2.1 High Temperature Stabilization - 100% of the device shall be subjected to a +300 ±10°C stabilization bake for a minimum period of 24 hours.

3.2.2.2 Temperature Cycling - 100% of the devices shall be subjected to temperature cycling under the following conditions.

a. 10 cycles minimum
b. Maximum temperature +200°C, minimum temperature -65°C
c. Minimum time at temperature extremes, 15 minutes

3.2.2.3 Constant Acceleration - 100% of the devices shall be subjected to a minimum constant acceleration in the Y_1 plane only of 25,000 G in accordance with Test Method 2006 of MIL-STD-750.

3.2.2.4 Helium Leak Test - 100% of the devices shall be subjected to a helium leak test in which the maximum allowable leak rate shall be 5×10^{-7} cc/sec. Any devices which fail to meet this requirement shall be removed from the lot.

3.2.2.5 Gross Leak Test - 100% of the devices shall be immersed in a suitable liquid at a temperature of approximately + 150°C and held for a minimum of 15 seconds. Any device exhibiting bubble leaks will be removed from the lot.

3.2.3 Burn-In

3.2.3.1 Procedure - 100% of the devices shall be operated for a minimum period of 168 hours under the following conditions:

a. $T_A = 25°C$

b. Sufficient power applied to the device so that it is operating at maximum dissipation conditions for a 25°C free-air temperature.

3.2.3.2 Data Collection - Prior to burn-in, the individual devices will be identified and initial measurements shall be made and recorded. The parameters to be measured will be specified in Appendix A. Subsequent to burn-in, end point measurements will be made on the same parameters and recorded. Any failures which occur during burn-in will be recorded and the parameter failure mode of devices which fail the Δ criteria stated.

3.2.3.3 Failure Criteria

I_{CES} - Measured under the conditions specified in Appendix A.

Any change exceeding 50% of the initial value or 5 na., whichever is greater or which exceeds the initial limit shall be cause for rejection.

h_{FE} - Measured under the conditions specified in Appendix A.

Any change which exceeds 15% of the initial value or which exceeds the initial limits shall be cause for rejection.

V_{CE}(sat.) - Measured under the conditions specified in

Appendix A. Any change which exceeds 15% of the initial value or 60mv, whichever is greater, or which exceeds the initial limits shall be cause for rejection.

3.2.4 X-Ray Inspection - 100% of the devices shall be examined under two-view x-ray according to Texas Instruments QRAS No. 925.

Devices showing any of the defects outlined in section 6.2 of the above document shall be rejected from the lot.

3.2.5 Sequence of Screening - The screening procedures shall be performed on the devices in the following sequences:

a. Visual Inspection
b. High Temperature Stabilization
c. Temperature Cycling
d. Constant Acceleration
e. Helium Leak Test
f. Gross Leak Test
g. Burn-in
h. X-Ray Inspection

The X-Ray inspection shall be the last screening procedure performed on the devices. However, at the manufacturer's discretion, a quality control sample may be withdrawn from the lot for final electrical testing.

Any of the above screening procedures which are part of the manufacturer's normal process control, and which fulfill the requirements of the appropriate paragraph, may be omitted. A written statement of such omissions shall be included with the order.

3.2.6 Data Transmittal - All data procured under paragraph 3.2.3.2 shall be considered as part of the order and will be transmitted with the shipment of devices. The form in which the data shall be transmitted shall be specified in Appendix B.

4.0 QUALITY ASSURANCE

4.1 Responsibility for Performance of Screening and Inspections Unless otherwise specified, the supplier shall be responsible for performance of all screening and inspection requirements prior to submission for UM/RAO inspection and acceptance. The UM/RAO reserves the right to perform any of the specified inspections where it is deemed necessary to insure that the parts and services conform to the requirements of this document.

4.2 Test Equipment and Inspection Facilities - Test equipment and inspection facilities shall be of sufficient quality, accuracy, and quantity to perform the required inspections. The supplier's construction techniques, inspections, quality control measures, etc., shall be subject to inspection by representatives of the UM/RAO. Written notification of any such inspection shall be given in advance.

4.3 Frequency of Screening and Inspection- Unless otherwise specified, screening and inspection shall be performed on all finished devices on a 100% basis.

4.4 Packaging and Delivery of Finished Devices - The finished devices shall be packaged and shipped in a manner specifically designed to minimize possible damage to the devices.

TEST CONDITIONS AND REQUIREMENTS

Parameter	Test Conditions	Range Min.	Range Max.	Max. Deviation from initial measurement
I_{CES}	2N930: V_{CE}=45v, V_{BE}=0		10 na.	±50% or 5 na. whichever is greater.
	2N2412: V_{CE}=25v, V_{BE}=0		10 na.	
	2N1893: V_{VR}=60v, V_{BE}=0		10 na.	
h_{FE}	2N930: V_{CE}=5v, I_C=500μa	150		±15%
	2N2412: V_{CE}=5v, I_C=1ma	30		
	2N1893: V_{CE}=10v, I_C=10ma	35		
V_{CE}(sat.)	2N930*: I_B=.5ma, I_C=10ma		1.0v	±15% or 60 mv, whichever is greater.
	2N2412*: I_B=1ma, I_C=10ma		0.2v	
	2N1893: I_B=5ma, I_C=50ma		1.2v	

*These parameters must be measured with a pulse duration ≤ 300 microseconds and a duty cycle ≤ 2%.

APPENDIX B

INTERFACE SPECIFICATIONS

The following specifications are excerpts from the OGO-E Experiment Interface Specification D-13356, Revision D and are only those sections which pertain to the UM/RAO experiment.

I. MECHANICAL INTERFACE

A. SIZE

The maximum size for a single SOEP shall be 12.5 by 12.5 by 12.5 inches including all electrical connectors and thermal control provisions.

B. ASSEMBLY DIMENSIONS

Within the above stated limits, the experimenter shall choose the dimensions for each experiment assembly. Unless otherwise specified, external dimensions shall not exceed these limits by more than 0.030 inch.

C. WEIGHT

1. GSFC shall have the responsibility for the control of weight budget for OGO experiments.

2. The weight of each experiment assembly shall be assigned by GSFC to the experimenter subject to the following restrictions:

   a. The total weight attached to each SOEP shall not exceed 15.6 pounds.
   b. The total weight of all experiments contained in the two SOEPs shall not differ by more than 2.0 pounds. If the weight difference exceeds this value, then ballast may be required. The weight of such ballast shall be considered experiment weight.

D. MOUNTING PROVISIONS

1. Mounting flanges will be provided for the mounting of appendage containers. All appendage mounted experiments shall be designed to attach to the proper flange.

2. The experimenter shall provide drill templates for all experiment assemblies to GSFC or TRW.

3. Experiments will be mounted to the observatory by means of 10-32 screws. The attachment hole size in the experiment assembly shall be .201 $\pm$ .010 inch diameter.

E. MOVING PARTS

The total angular momentum of moving parts of all experiments shall not exceed .05 pound-foot-second.

F. LOCATION OF ELECTRICAL CONNECTORS

Electrical connectors on appendage mounted experiment containers shall be located in areas designated on the applicable interface drawings.

G. MAGNETIC MATERIALS

The use of magnetic materials shall be avoided unless required in the operation of the experiment.

H. EJECTED MATERIAL

1. Approval for ejection of any portion of an experiment or gases used to operate or deploy a portion of an experiment must be obtained from GSFC.

2. No material may be ejected or extended from any experiment until all appendages have been fully deployed.

3. The relative velocity of material ejected from any portion of the observatory must be sufficient to avoid either an immediate or delayed striking of any other portion of the observatory.

4. The short term change in the angular momentum about the center of gravity of the observatory induced by an ejected component shall be less than .05 lb-ft-sec.

5. All provisions except for commands for ejection or extension of portions of an experiment shall be provided by the experimenter.

I. EXTENDED PORTIONS OF EXPERIMENTS

1. Protruding parts of experiments shall be approved by GSFC and TRW.

2. The location and size of all protrusions of any portion of an experiment assembly outside the space normally assigned to experiments shall be approved by GSFC and TRW.

3. All portions of experiments which extend beyond the space normally assigned to experiments shall not increase the moment of inertia of the observatory about its center of gravity by more than 1 slug foot^2.

4. Extended portions of experiments shall not contact any portion of the observatory before, during or after deployment.

5. Extended portions of experiments shall not shadow the solar cells, sun sensors or horizon scanners to such an extend as to significantly degrade their performance.

II. ELECTRICAL INTERFACES

A. TOTAL EXPERIMENT POWER

The experiments can utilize an average power of 50 watts and a peak power of 80 watts from the spacecraft power system. This power shall be composed of:

1. 40 watts continuous available power

2. 40 watts available to five high power experiments on a 25 percent duty cycle for sunlit portions of the orbit for periods having a maximum duration of 5 minutes. The programming will not exceed two 5 minute discharges per 30 minute charging period.

During eclipse periods there will be no more than two 5 minute discharge periods.

B. POWER INPUTS

1. The observatory system voltage will be 28 $^{+5.5}_{-4.5}$ volts. Power inputs to the experiments will be unregulated and unfiltered. All experiments shall be capable of operating satisfactorily within their own specifications for any system power supply voltage between +23.5 and +33.5 volts dc.

2. The dc internal impedance of the power supply will be less than 1.8 ohms for experiments mounted on the end of a long boom, and less than 1.5 ohms for all other experiment locations. This impedance will increase to 4.5 and 4.0 ohms respectively at a frequency of 50 kHz.

3. An unshielded twisted pair will be used for the +28 volt dc and return. A shielded cable may be used for these lines upon coordination with GSFC and TRW.

4. All power to each experiment will be through command switches and fuses provided as part of the spacecraft.

5. One shot solid state fuses will be included as part of the spacecraft in all experiment power lines to automatically cut off power permanently to an experiment if it draws a current exceeding 0.5, 1, or 3 amps dc depending upon the specific power requirements of the experiment.

6. The maximum current drawn by an OGO experiment shall not exceed the following values unless using high current relays or experiment ordnance command, in which case the maximum current shall be 10 amps.

Maximum Current Duration (milliseconds)	Current (amperes)
0.5	15
2	12
5	9
200	6
steady state	3

7. Ripple Limits

a. All experiments shall be capable of operating satisfactorily within their own specifications when the input power includes open circuit noise of 450 millivolts peak or less, at any frequency between 10 Hz and 50 kHz.

b. No experiment shall feed back onto the power input line periodic electrical noise with a peak to peak amplitude in excess of 20 millivolts at any frequency greater than 10 Hz for more than one-half second intervals. In addition, no measurable interference shall be generated in the 145 to 155 MHz frequency range.

8. Experiments shall not generate conducted or radiated interference which will cause adverse effects on other experiments or spacecraft subsystems during any operating modes. All experiments shall be designed and fabricated in accordance with Paragraph 3.2 of MIL-I-26600. Compliance with this requirement will be verified during experiment integration and test in the spacecraft. For maximum assurance of noninterference on the spacecraft, experiments should demonstrate compliance with Paragraphs 4.3.1, 4.3.2, and 4.3.4 of MIL-I-26600. Responsiblility for corrective action which may result from this requirement will rest with the organization supplying the non-conforming experiment.

9. Experiments shall not be damaged and their functional performance shall not be permanently impaired or degraded as a result

of applied voltage transients of any peak amplitude up to +50 volts dc for a duration of 10 milliseconds or less.

10. Experiments shall not be damaged (their quantitative performance may be out of tolerance) by application of any supply voltage from 0 to +42 volts dc. Maximum duration for voltages between +33.5 and +42 volts shall be 10 minutes.

C. COMMANDS

1. A total of 146 commands will be provided as part of the spacecraft for use by the experiments. These commands will be available to the experiment as follows:

a. 50 commands - power ON
b. 50 commands - power OFF
c. 46 commands - impulse

2. All power to experiments will be supplied through command relays. The power control will be a magnetic latching relay that can be commanded into either the ON or OFF position by a short duration pulse, and requires no additional power to remain in the command position. The relay contact ratings will be 28 volts dc, 2 amperes resistive, 1 ampere inductive. If relay contacts are closed, peak current pulses of 3.5 amps or less can be accommodated for periods of 1 second or less. The relays have a contact bounce period of approximately 1 millisecond. The relay chatter during the initial 1 millisecond has a somewhat random frequency. Except for this period the impulse is a good square wave. In the ON condition, the experiment will be provided with the spacecraft battery voltage. In the OFF condition the experiment will be provided with an open circuit of 100 Megohms. The relay contacts will be double pole, double throw and will be paralleled for reliability.

3. Forty-six impulse commands will be provided. Relay contacts will be closed for 50 to 65 milliseconds by an impulse command.

Grounding of the command line through the relay contacts will be provided upon activation of an impulse command. Power input for this command will be through the experiment power input relay and fuse. The relay contact ratings will be 28 volts dc, 2 amperes resistive, 1 ampere inductive. The relays will have a maximum contact bounce period of 3 milliseconds.

4. Current pulses of 10 amperes maximum for a duration of 50 milliseconds or less will be available through use of the experiment ordnance circuit. Details of the implementation shall be coordinated with GSFC and TRW.

D. TIMING SIGNALS

1. Timing signals with the following characteristics may be supplied to a maximum of 15 experiments:

a. Frequencies available: 3555.6, 222.22, 13.889, 0.86806, 0.054250, and 0.0033906 pps

b. Accuracy of frequencies:

One part in 10^5 for one year

One part in 10^6 for one hour

c. True amplitude: +7 $\pm$3 volts

d. False amplitude: 0 $\pm$1.5 volts

e. Pulse width at 50 percent amplitude points: 20 $\pm$ 6 microseconds

f. Rise time; 10 to 90 percent amplitude points: 5 microseconds

g. Fall time; 90 to 10 percent amplitude points: 15 microseconds

h. Timing pulses will be synchronous with telemetry in the following manner at the 1 kbps rate:

A 3555.6 pps pulse will occur 78.0 microseconds before the first bit of the following complete telemetry frame.

A 222.22 pps pulse will occur 62.4 microseconds before the first bit of the following complete telemetry frame.

A 13.889 pps pulse will occur 46.8 microseconds before the first bit of the following complete telemetry frame.

A 0.86806 pps pulse will occur 31.2 microseconds before the first bit of the following complete telemetry frame.

A 0.05425 pps pulse will occur 15.6 microseconds before the first bit of the following complete telemetry frame.

A 0.00339 pps pulse will occur 0 microseconds before the first bit of the following complete telemetry frame.

2. With the experiment power ON or OFF, the experiment input resistance for timing signals shall be 20,000 $\pm$ 4,000 ohms returned to ground. The capacitive load of the experiment shall be less than 25 picofarads.

3. The timing signals will be distributed throughout the spacecraft, as necessary, through miniature coaxial cable. The cable shield shall be connected to chassis ground at both the source and load end of the cable. The maximum cable capacity will be less than 625 picofarads. The timing signal return shall be through circuit ground.

4. Noise delivered to the experiment on the timing signal lines will be less than 300 millivolts peak to peak for all frequencies from 10 Hz to 50 kHz measured at the spacecraft/experiment interface connector.

5. The maximum amplitude of noise fed back on a timing signal line from any experiment shall be less than 20 millivolts peak to peak measured at the spacecraft/experiment interface connector.

6. The timing signal circuitry of the spacecraft shall not have a fault voltage imposed upon it by an experiment in excess of the values listed below:

a. 0 without series resistance in the experiment

b. $0 < V_f < +33.5$ volts with 10,000 ohms minimum series resistance in the experiment.

Timing signals to other experiments may be outside specification limits under this condition. Operation will be restored upon

removal of fault. These voltages will be measured at the experiment/ spacecraft interface connector.

E. CONNECTORS

1. The standard connector installed in an experiment assembly which electrically couples an experiment to the spacecraft/observatory shall be a male straight pin connector selected from the CINCH DM series. CINCH DM series connectors with high voltage or coaxial pins may be used provided that GSFC and TRW are notified at least six months prior to spacecraft integration to permit procurement of the proper spacecraft connectors. The use of two identical external connectors on one experiment assembly should be avoided. A connector designation, specified by GSFC or TRW shall be permanently marked near each connector in each experiment assembly in a location which is visible when the assembly is mounted in the observatory.

2. Contact insulation shall be unmilled diallylphthalate with glass fiber filler or with acid-leached asbestos filler.

3. The connector case shall be fabricated of non-magnetic brass.

4. Connector pin assignments may be chosen by the experimenter. Pins should be appropriately selected, however, to allow twisted pairs of wires to be routed on adjacent pins and to allow signals susceptible to noise to be isolated from those which are particularly noisy.

5. Experimenters are requested to include test connectors which provide access for troubleshooting to appropriate circuit points within their experimental devices.

6. Connectors contained in the experiments shall be secured with CANNON screw locking mechanism No. 20418-2, non-magnetic.

7. Cadmium plated connectors shall not be used on any OGO experiment.

III. TELEMETRY INTERFACE

A. GENERAL

The wideband telemetry system will include two identical equipment groups, designated equipment group 1 (EG1) and equipment group 2 (EG2). Each equipment group consists of an analog data handling assembly (ADHA) and a digital data handling assembly (DDHA). Under normal conditions, EG1 will be assigned to the handling of real time telemetry data and EG2 to the handling of recorded data. However, the two systems are identical and their functions may be interchanged by ground command.

B ANALOG EXPERIMENTS

1. The analog output signal shall be positive only and shall lie in the 0 to + 5.1 volt range.

2. The analog experiment output impedance shall be chosen by the experimenter in such a manner that the total error in digitization caused by the input impedance of the ADHA is less than 2 millivolts for 8 bit quantization accuracy, less than 22 millivolts for 7 bit quantization accuracy, or less than 62 millivolts for 6 bit quantization accuracy. The appropriate formulas for determination of this error are in Paragraph 3.3.1.2.2 of D-13356, Revision D but are not repeated here.

3. A single analog data output line to each equipment group shall be used for each analog data output. If the same data can be sampled simultaneously by both equipment groups, the two output lines should be isolated from each other such that when one output is loaded by a current of 6 milliamperes, the other output potential shall not change by more than 2 millivolts.

If a single data output line is connected to both equipment groups, the data may be inaccurate if the output is sampled simultaneously by both equipment groups. Since on OGO-E the equipment groups are synchronized, the probability and predictability of this occurrence

is greater.

4. The analog data will be sampled for a conversion time not to exceed 65 microseconds.

5. The analog experiment shall be able to accommodate a current of at least 10 microamperes at the time of comparison without suffering degradation in calibration or performance.

6. Analog data output signals will be transmitted from the experiment to the ADHA on miniature coaxial cable. The coaxial shield shall not be connected to the experiment. The analog signal return shall be through circuit ground. The maximum cable capacitance will be (550 + 75N) picofarads where N is the number of words to which the output is connected.

7. Maximum permissible dc fault voltage applied to an analog data output line shall be between + 33.5 and - 33.5 volts.

IV. THERMAL INTERFACE

A. EXPECTED TEMPERATURES

1. The responsibility for the thermal control to maintain a SOEP baseplate temperature of approximately + 20 $\pm$ 10°C shall rest with GSFC. The control will be passive.

2. The SOEP experiments shall be capable of operating over a temperature range of - 20 to + 60°C.

3. All experiments shall be capable of storage (non-operating at temperatures of - 37 to + 60°C.

B. EXPERIMENT THERMAL DESIGN REQUIREMENTS

1. The internal construction shall be such that all major heat generating components are coupled to the experiment mounting base and cover through adequate heat conducting paths. The experiment cover shall be coupled to the mounting base through adequate heat conduction paths and be constructed of a material (or materials) that enables the

cover to be at substantially the same temperature as the mounting base.

2. The external mounting surfaces of all experiment assemblies shall be electrically conducting.

3. External surfaces with the exception of the mounting base shall be treated or coated to have an emittance of not less than 0.72 at a temperature of 18°C. A suitable coating of metal surfaces is "Cat-a-Lac" No. 463-1-8, manufactured by the Finch Paint and Varnish Company, Torrance, California.

4. The bottom of the mounting base shall have a surface finish of 64 microinches root-mean-squared or better and shall be flat within 0.008 inch in a 8 inch length (or proportional values for other actual base dimensions).

V. MISCELLANEOUS REQUIREMENTS

A. The experimenter shall design each experiment assembly so as to minimize the escape of gases.

B. Materials selected for use in the observatory shall be sufficiently resistant to the anticipated radiation environment to retain their necessary properties for a period of one year.

C. Magnetic Field:

1. All experiments shall be designed so as to minimize the permanent, induced, and transient magnetic field effects seen by a magnetometer experiment. As a design goal the magnetic field of an experiment assembly shall be less than 100 gamma at a distance of 1 foot.

2. Magnetic shielding materials shall not be included in any experiment in order to reduce the magnetic field.

3. Neither the experiment assembly nor any of its component parts shall be deliberately demagnetized in order to reduce the magnetic field.

APPENDIX C

ENVIRONMENTAL TEST SPECIFICATIONS

The following is a specification for all environmental testing performed on the flight model payload by NASA.

A. TEST FACILITIES

1. General

The apparatus used in conducting tests shall be capable of producing and maintaining the test conditions required, with the experiment under test installed on or in the apparatus and operating or non-operating, as required. Changes in test apparatus conditions from the nominal conditions specified by the appropriate test procedures shall not exceed the applicable test procedure requirements or the requirements of Section 4 of this specification, whichever limits.

2. Standard Conditions for Test Area

(a) Temperature	25 ± 3°C
(b) Relative Humidity	55% or less
(c) Barometric Pressure	Room ambient

(Performance data to be corrected to 760 mm Hg if so specified in the applicable experiment test procedure)

3. Measurements

All measurements shall be made with instruments the accuracy of which conforms to acceptable standards and which are appropriate for the parameters measured and the environmental conditions concerned. The accuracy of these instruments shall be verified prior to conduct of test. Documentation specifying instrument accuracy, calibration periods, calibration facilities, and the procedure used to control instrument certification shall be produced on request.

4. Tolerances

The maximum allowable tolerances for test conditions shall be as follows, unless otherwise specified by the applicable test section in the environmental test specification or test procedure:

(a) Temperature	± 2°C (exclusive of accuracy of instruments)
(b) Vibration Amplitude	± 10%
(c) Vibration Frequency	± 2%
(d) Additional Tolerances	Additional tolerances shall be specified.

5. Vacuum Gages

Absolute pressure shall be indicated by a vacuum gage. The gage shall be located such that the environment being sensed is representative of the chamber test space.

B. TEST SEQUENCE

1. Magnetic

At the start of the environmental exposure sequence, the experiment shall be checked for permanent, induced, and stray effect at a distance of at least three times the maximum linear dimension of the assembly. The inverse cube law shall be applied for extrapolation to a distance of one foot. If the extrapolation for each of these fields is equal to 100 gamma or less, no further testing shall be required until completion of the environmental test sequence. Where this value is exceeded, the test shall be continued by measuring the magnetic field at a distance of approximately six times the aforementioned distance. If the extrapolation for permanent or induced magnetic field again exceeds the 100 gamma value, the experiment shall be exposed to a dc magnetic field representing the maximum field it is likely to experience during its lifetime (25 gauss unless otherwise determined). After this exposure, the experiment permanent magnetic field shall be measured and the experiment de-magnetized to its initial state or less.

2. Weight and Center of Gravity

The weight and center of gravity of each experiment assembly shall be determined correct to the units specified below.

Weight	0.01 pound or 0.5% of the total weight (whichever is greater)
Center of Gravity	0.1 inch

The mass property determinations are included as part of the environmental exposures to effect design control. These measurements shall be repeated if the experiment is modified during the test program.

3. Leak Detection

All experiment assemblies designed to hermetically sealed must have provision for demonstrating kf testing the effectiveness of the seal and shall be subjected to a leak detection test.

This section is not applicable to the UM/RAO E-20 experiment.

4. Vibration

The experiment (or appendage container with experiments) shall be attached to the vibration generator via a rigid fixture. Attachment shall simulate the actual attachment of the experiment to the observatory structure.

The operational condition of the experiment during this test shall be representative of that during the launch phase: normally nonoperative. However, it is recommended that the experiment performance be checked between axes as a minimum and, if operation of the experiment does not change its sensitivity to vibration, the experiment may be operated during the test at the discretion of the experimenter.

Each experiment package shall be subjected to vibration along three orthogonal axes in conformance with the schedule below. The orientation for appendage-mounted experiments shall be with the longitudinal axis perpendicular to the plane of the mounting interface.

4.1 Sinusoidal-swept Frequency

The applied frequency shall be swept from the lowest to the highest frequency once for each range. Time rate of change of frequency shall be proportional to frequency at the rate of 4 octaves/ minute (total test time each axis: 1.9 minutes).

Axis	Frequency Range (Hz)	Input Control (Stated)
Longitudinal (Y)	10 - 22	0.33" constant displ. (D.A.)
	22 - 50	8 (0 to peak)
	50 - 400	2.7 (0 to peak)
	400- 2000	5 (0 to peak)
Laternal (X,Z)	10 - 14	0.33" constant displ. (D.A.)
	14 - 50	3.3 (0 to peak)
	50 - 400	2 (0 to peak)
	400- 2000	5 (0 to peak)

4.2 Random Motion Vibration

Gaussian random vibration shall be applied with the "g-peaks" clipped at three times the root-mean-square acceleration specified in the schedule. With the experiment installed, the control accelerometer response shall be equalized such that the specified power spectral sensity (PSD) values are within $\pm$ 3 db throughout the frequency band. The filter roll-off characteristic above 2000 Hz shall be at a rate of 40 db/octave or greater. The following tests shall be conducted for all experiments in each of the orthogonal axes specified in Section 4.1.

Frequency Range (Hz)	PSD Level (g^2/Hz)	Acceleration (g-rms)
20 - 500	.044	5.3 (for 20 - 2000 Hz frequency range)
500 - 2000	.044 with 12 db/ octave roll-off	

Total test time each axis: 2 minutes.

5. Thermal-Vacuum

For all tests, chamber pressure shall be maintained at 5×10^{-5} mm Hg or less. In general, the experiment shall be operated only after these conditions are reached.

Control temperature for these tests shall be the experiment base plate (mounting base) temperature. If the experiment is not being tested in its orbital container, methods shall be devised for maintaining the surrounding temperature equal to the control test temperature.

Stabilization shall be considered achieved when no reference thermocouple varies by more than 1°C per hour.

All appendage-mounted experiment assemblies shall be operated during the temperature soak conditions listed below:

(a) Experiment baseplate temperature maintained at 0°C for at least 12 hours after stabilization.

(b) Experiment baseplate temperature maintained at + 40°C for at least 12 hours after stabilization.

NOTE: The actual test temperatures for the OGO-V radiometer were - 10°C and + 50°C. This was per our request to give added assurance of the operational capability of the experiment.

REFERENCES

1 UM/RAO POGO Memo No. 174, "Influence of Antenna Length on POGO 2.5 MHz Sensitivity", D. Walsh, 5 October 1965.

2 UM/RAO Report No. 67-2, Instrumentation for Measurement of Cosmic Noise at 750, 1225, and 2000 kHz for a Rocket, W.J. Lindsay, et. al., February 1967.

3 UM/RAO OGO-E Memo No. 133, "OGO-E Antenna Capacitance Measurements at GSFC", R. G. Yorks, 12 February 1968.

4 UM/RAO Instrumentation Memo No. 8, "Preliminary Report on EGO-2 Sensitivity", L. W. Orr and B. G. Finch, 1 March 1963.

5 UM/RAO OGO-E Memo No. 105, "Influence of Antenna Length on the OGO-E System Sensitivity", R. G. Peltzer, 20 September 1967.

6 "IRE Standards on Methods of Measuring Noise in Linear Twoports, 1959" and Representation of Noise in Linear Twoports", Proceedings of IRE, Vol. 48, No. 1, January 1960.

7 UM/RAO Report No. 64-9, A Simplified Representation of the Noise Factor of Junction Transistors, B. G. Finch, July 1964.

8 UM/RAO Instrumentation Memo No. 3, "Measurement of Noise Factor and Noise Temperature of Radio Astronomy Receivers for Space Vehicles", D. Walsh and B. G. Finch, 18 December 1962.

9 "Cosmic Radio Intensities at 1.225 and 2.0 MHz up to an Altitude of 1700 KM", D. Walsh, F. T. Haddock, and H. F. Schulte, Space Research IV, North Holland Publishing Company, Amsterdam, 1964 (Proceedings of the Fourth International Space Symposium held in Warsaw in June, 1963.)

10 UM/RAO Report No. 67-12, Cosmic Noise Intensity Measured from a Rocket, D. Walsh and F. T. Haddock, 7 December 1967.

11 UM/RAO Report No. 66-23, Instrument Report on Radio Astronomy Experiment for OGO-E Satellite, B. G. Finch and B. D. MacRae, 15 March 1966.

12 UM/RAO OGO-E Memo No. 100, "OGO-E Calibration Procedure", B. G. Finch, 1 May 1967.

13 UM/RAO Report No. 67-3, Report on Development of Broadband Noise Generator, B. G. Finch, February 1967.

14 UM/RAO OGO-E Memo No. 53, "RFI Tests on OGO-E Prototype at TRW Systems", B. D. MacRae, 15 June 1966.

15 UM/RAO OGO-E Memo No. 54, "RFI Reduction Investigation", B. D. MacRae, 15 June 1966.

16 UM/RAO OGO-E Memo No. 57, "Comparison RFI Susceptibility Measurements Between OGO-E Prototype and FU-1", B. G. Finch and B. D. MacRae, 11 July 1966.

17 UM/RAO OGO-E Memo No. 80, "Failure of E-20 Prototype During Qualification Level Vibration Testing at TRW", B. G. Finch, 26 January 1967.

18 UM/RAO OGO-E Memo No. 117, "TRW Failure Report No. 27634 and Reply from B. D. MacRae", 8 December 1967.

19 UM/RAO OGO-E Memo No. 130, "TRW Failure Reports No. 27649 and 33441", 26 January 1968.

20 UM/RAO OGO-E Memo No. 135, "OGO-E Launch Support Activities at Cape Kennedy", B. D. MacRae, 21 March 1968.

TABLE 1

RADIOMETER INPUT IMPEDANCE

Frequency	R_s	C_s
50 kHz	105 kΩ	33.8 pf
100	122	27.2
200	88.2	24.4
350	87.7	24.2
600	92.3	24.2
900	102	24.2
1.8 MHz	560	24.2
3.5	1.0 MΩ	25.0

R_s = Resistive component of preamplifier input impedance

C_s = Capacitive component of preamplifier input impedance

TABLE 2

RADIOMETER CALIBRATION INPUT CONDITIONS

Stimulus	Input Level	S/C Voltage
Internal	Cal. 1	23.5
		25.5
		28.0
		31.0
		33.5
	Cal. 2	23.5
		25.5
		28.0
		31.0
		33.5
	Cal. 3	23.5
		25.5
		28.0
		31.0
		33.5
	Cal. 4	23.5
		25.5
		28.0
		31,0
		33.5
External	No Input	28.0
	- n db	28.0
	-(n-1) db	
	-(n-2) db	28.0
	-(n-n) db	28.0

*n is the number of db below a reference noise level. n is approximately 80.

TABLE 3

Radiometer Frequency / Interfering Frequency	INITIAL RF CONDUCTED INTERFERENCE TEST RESULTS							
	50 kHz	100 kHz	200 kHz	350 kHz	600 kHz	900 kHz	1800 kHz	3500 kHz
50 kHz	1.4 mv (rms)	13.4 mv (rms)[1]	25.4 mv (rms)	35.3 mv (rms)	35.3 mv (rms)	53.0 mv (rms)	141 mv (rms)	70.7 mv (rms)
64							49.5	70.7
75	120.0	17.0						
93.5							49.5	42.4
100	424	1.0	53.0	49.5	77.7	42.4	141.0	
175				26.9				
200		141.0	1.0		21.2	106.0	247.0	226.0
225						10.6		
300					9.9	3.5	141.0	
350				0.5				
360							70.7	
400								170.0
450						2.8	38.9	
500		113.0		63.6	113.0	70.7	212.0	
600					0.5		1.4	198.0
875								60.1
900						0.5		
1000	198.0	106.0	127.0	91.9	141.0	70.7	601.0	481.0
1167								17.7
1500	919							
1745								24.7
1800							1.4	
3500				184.0	424.0	269.0		1.8
3550	198.0							
3600			21.2					
10.7 MHz	8.8	8.8	12.7	8.5	11.3	7.1	14.1	10.6
21.1	2.5							
21.5		1.4	1.4	1.4				
22.0					1.4			
22.3						1.4		
23.2							1.8	
24.95								1.4
32.0	6.4							4.9
32.4		1.8	1.4					
32.5				1.4	1.4			
34.0						2.0		63.6
35.8							2.1	
43.3*		10.0						
43.7*		10.0						
54.0*		20.0						
64.9*		30.0						
400	250.0	200.0	180.0	200.0	190.0	190.0	400.0	500.0

* Only measured on 100 kHz radiometer channel

[1] These levels injected into the dummy antenna on the radiometer input cause a 40 millivolt increase in the radiometer output above the quiescent level.

TABLE 4

RFI FILTER EFFECTIVENESS

FREQUENCY	THRESHOLD RESPONSE	
	Original	Filter
10.66 MHz	0.45 $mv(rms)_1$	0.60 $mv(rms)_1$
17.6	0.55	0.90
24.8	0.8	2.0
31.8	0.5	2.7
38.8	1.3	10.5
45.8	1.7	20.0
52.8	1.0	25.0
59.8	1.0	30.0
67.1	5.0	55.0
73.8	3.5	80.0
81.2	6.5	50.0
88.2	7.0	102.0
95.5	8.0	70.0
102.4	6.5	130.0
109.6	12.0	115.0
116.4	10.5	160.0
123.6	3.5	500.0
130.6	3.0	160.0
137.6	4.5	85.0
144.6	4.0	160.0
151.6	1.4	65.0
158.6	1.4	65.0
166.0	10.5	230.0
173.0	7.0	140.0

TABLE 4 continued

180.0 MHz	1.4 mv(rms)	45.0 mv(rms)
186.8	1.4	102.0
194.0	6.5	70.0
201.0	9.0	130.0
208.0	2.2	60.0
215.8	2.7	60.0
223.0	10.5	102.0
230.0	10.0	45.0
237.0_2	4.0	65.0
399.0	90.0	270.0
406.0	100.0	200.0

Notes:

Equipment:

1. HP 608C Signal Generator
2. HP 355A Attenuator
3. HP 355D Attenuator
4. Simpson 260 Multimeter

1. These signal levels injected into the dummy antenna on the radiometer input cause a 40 millivolt increase in radiometer output above the quiescent level.

2. This pattern continues with a gradually decreasing susceptibility to 399.0 MHz.

TABLE 5

RADIOMETER SENSITIVITY WITH FILTER

FREQUENCY	THRESHOLD RESPONSE		DEGRADATION
	Original	Filter	
50 kHz	74.8 db[1,2]	74.1 db	0.7 db
100	77.8	77.1	0.7
200	79.7	78.2	1.5
350	79.2	78.0	1.2
600	79.2	78.2	1.0
900	79.8	79.0	0.8
1800	80.0	79.3	0.7
3500	80.0	79.6	0.4

Notes:

1. Equipment:
   a. UM/RAO Laboratory Standard Noise Generator
   b. Non-Linear Systems 2917 Digital Voltmeter
   c. Weinschel 64A Attenuator
2. This value of attenuation with 15 milliamperes of diode current in the Standard Noise Generator causes a 40 millivolt increase in the radiometer output above the quiescent level.

TABLE 6

COMPARATIVE SUSCEPTIBILITY TEST RESULTS

Interfering Freq. (MHz)	Direct Input mv (rms) Proto	FU-1	Conducted mv (rms) Proto	FU-1
10.7	3.0	65.0	11.0	13.0
12.45	70.0	260.0	>500.0[1]	>500.0
14.15	24.0	17.5	>500.0	>500.0
15.9	65.0	>500.0	>500.0	>500.0
17.7	5.2	60.0	31.0	16.0
24.9	4.1	190.0	2.0	12.0
26.6	80.0	>500.0	>500.0	>500.0
31.9	3.5	80.0	12.0	9.0
39.1	18.0	130.0	16.0	26.0
46.1	40.0	320.0	5.0	46.0
53.3	30.0	140.0	5.0	10.0
60.3	34.0	90.0	14.0	46.0
67.5	7.5	>500.0	160.0	40.0
74.5	8.0	160.0	34.0	24.0
81.7	2.0	54.0	140.0	240.0
88.7	1.7	40.0	60.0	55.0
90.5	14.0	>500.0	>500.0	>500.0
94.0	13.0	>500.0	>500.0	>500.0
95.9	2.5	34.0	26.0	40.0
102.9	3.4	>500.0	26.0	180.0
110.1	2.8	46.0		
116.8	5.8	240.0		
124.0	9.5	62.0		
131.0	6.8	31.0		
138.0	0.7	10.0	16.0	190.0
139.6	18.0	>500.0		
145.0	0.65	18.0		
152.4	0.40	14.0		

TABLE 6 continued

Interfering Freq. (MHz)	Direct Input mv (rms) Proto	FU-1	Conducted mv (rms) Proto	FU-1
159.0	0.52	12.5		
166.4	0.90	22.0		
173.5	1.0	14.0		
181.0	3.7	37.0		
188.0	4.8	40.0		
195.0	35.0	88.0		
202.5	60.0	380.0		
209.5	40.0	>500.0		
216.5	40.0	>500.0		
223.5	25.0	>500.0		
230.5	30.0	>500.0		
382.0	250.0	>500.0		
400.0	300.0	>500.0	>500.0	>500.0

Conditions:

1. 608D Generator 30% 1000 Hz Modulation
2. Radiometer on 3.5 MHz Channel
3. Level shown caused 40 mv increase in radiometer output.

Notes:

[1]This notation means the full output capability of the 608D Generator was used (~1.0v rms) but not measured.

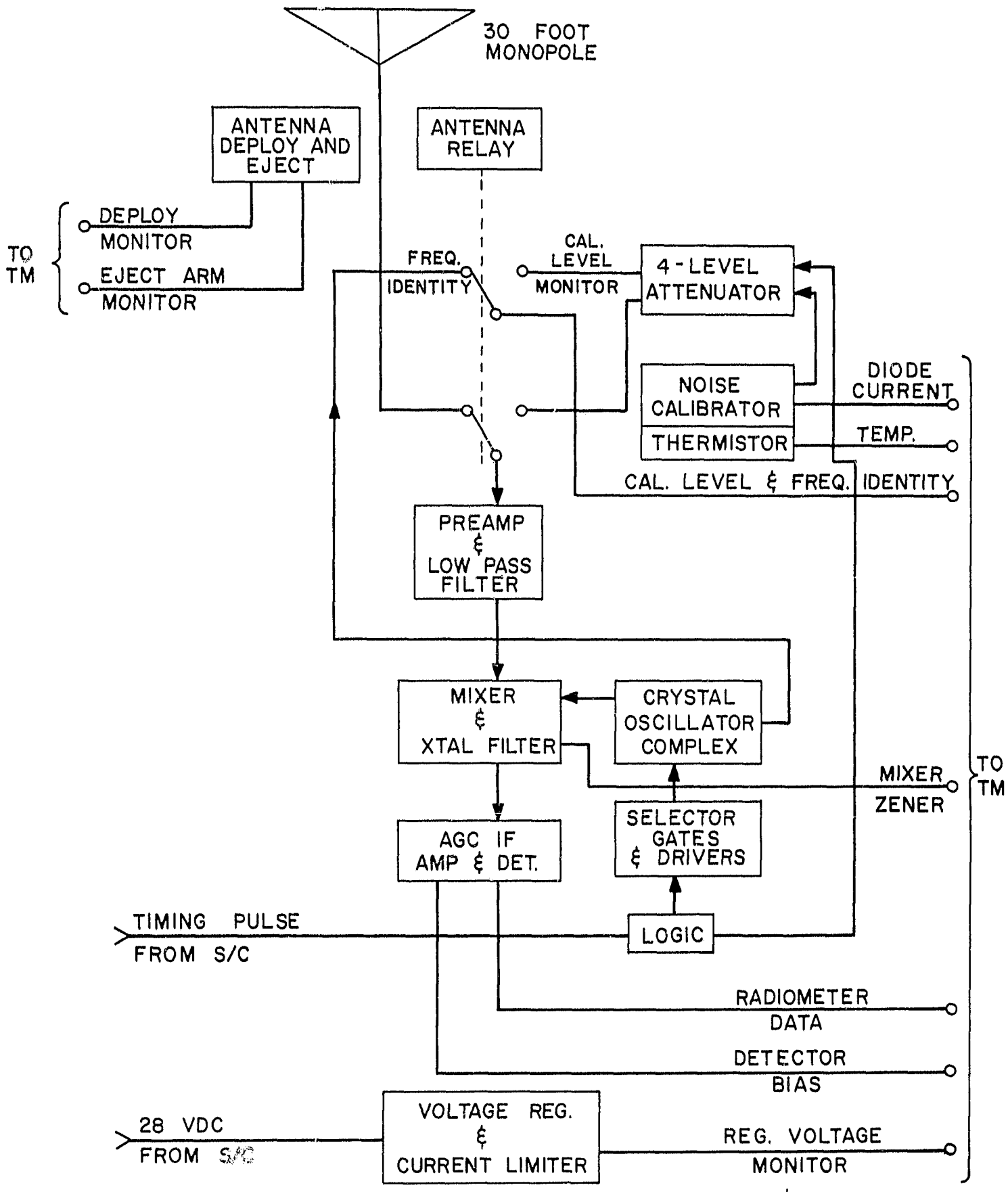

1. System Block Diagram

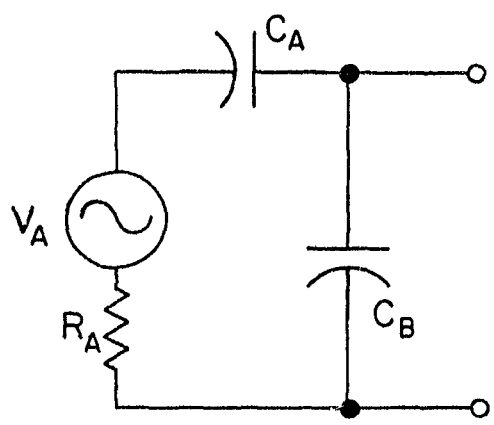

C_A = ANTENNA CAPACITANCE

R_A = RADIATION RESISTANCE

C_B = EQUIVALENT STRAY CAPACITANCE

$V_A^2 = 4 K T_A R_A \Delta f$

ANTENNA EQUIVALENT CIRCUIT

2. Antenna Equivalent Circuit

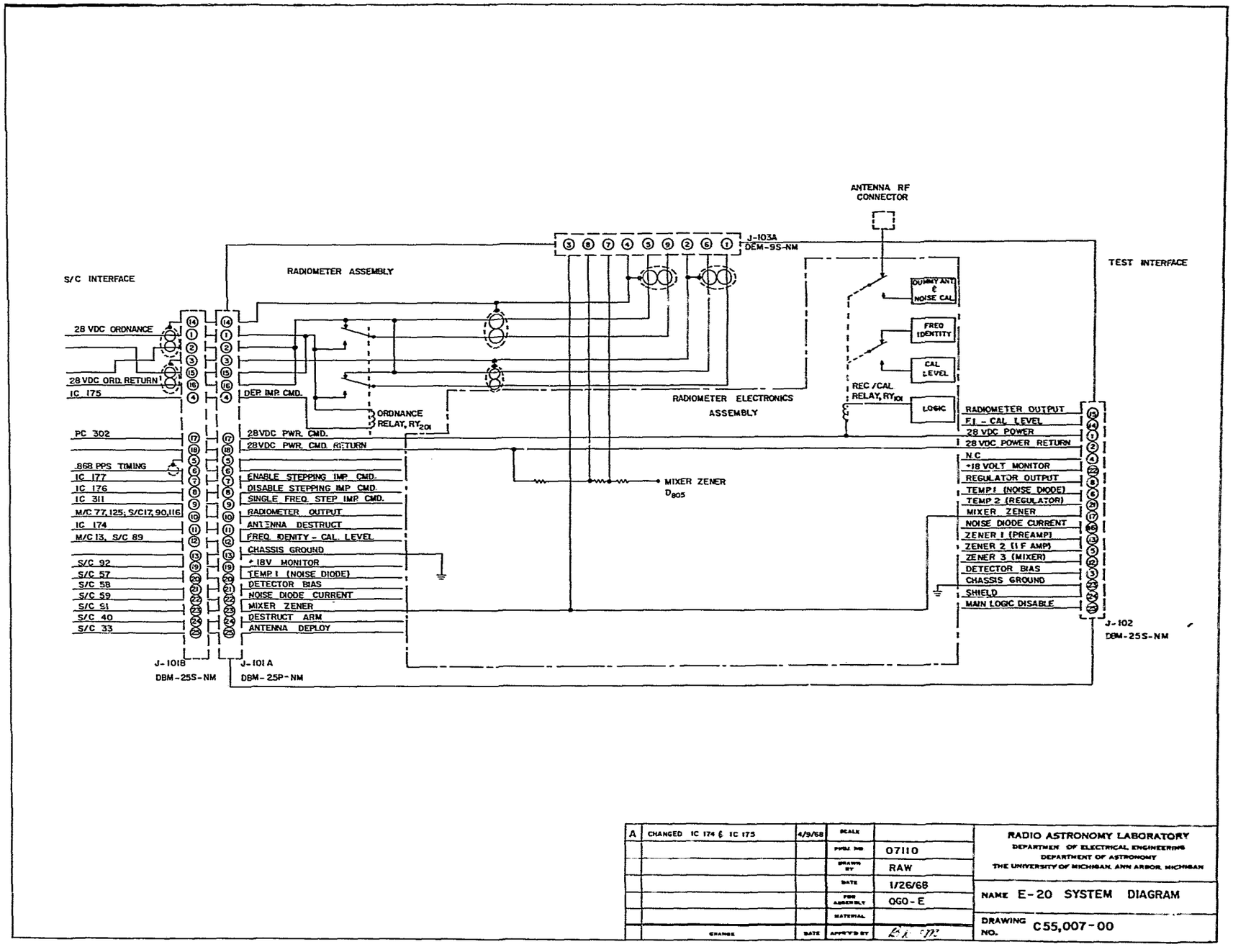

3. Radiometer Subassembly System Diagram

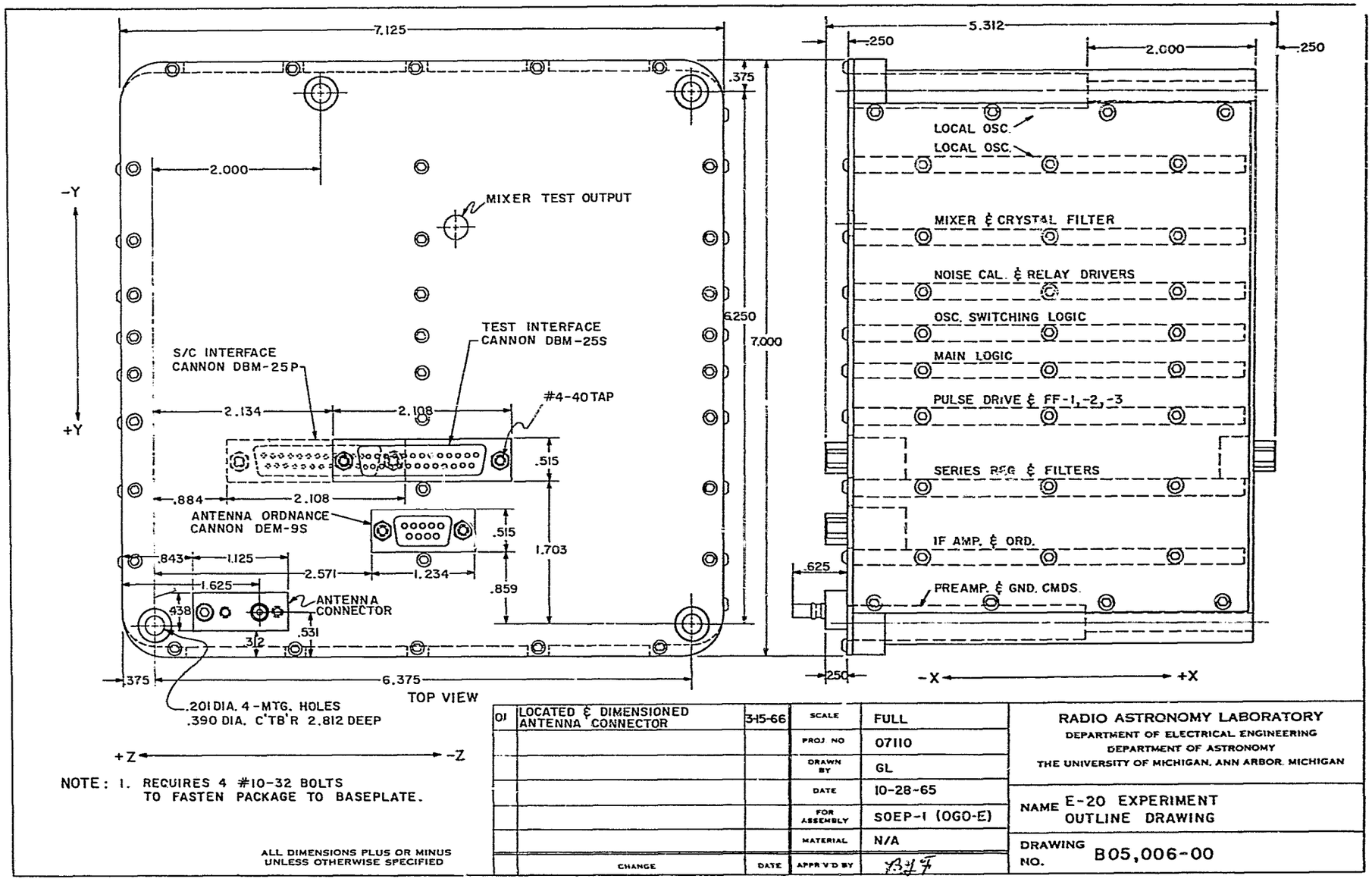

NOTE: 1. REQUIRES 4 #10-32 BOLTS TO FASTEN PACKAGE TO BASEPLATE.

ALL DIMENSIONS PLUS OR MINUS UNLESS OTHERWISE SPECIFIED

	CHANGE	DATE	APPR'D BY
01	LOCATED & DIMENSIONED ANTENNA CONNECTOR	3-15-66	BJF

SCALE	FULL
PROJ NO	07110
DRAWN BY	GL
DATE	10-28-65
FOR ASSEMBLY	SOEP-1 (OGO-E)
MATERIAL	N/A

RADIO ASTRONOMY LABORATORY
DEPARTMENT OF ELECTRICAL ENGINEERING
DEPARTMENT OF ASTRONOMY
THE UNIVERSITY OF MICHIGAN, ANN ARBOR, MICHIGAN

NAME E-20 EXPERIMENT OUTLINE DRAWING

DRAWING NO. B05,006-00

4. Radiometer Mechanical Layout

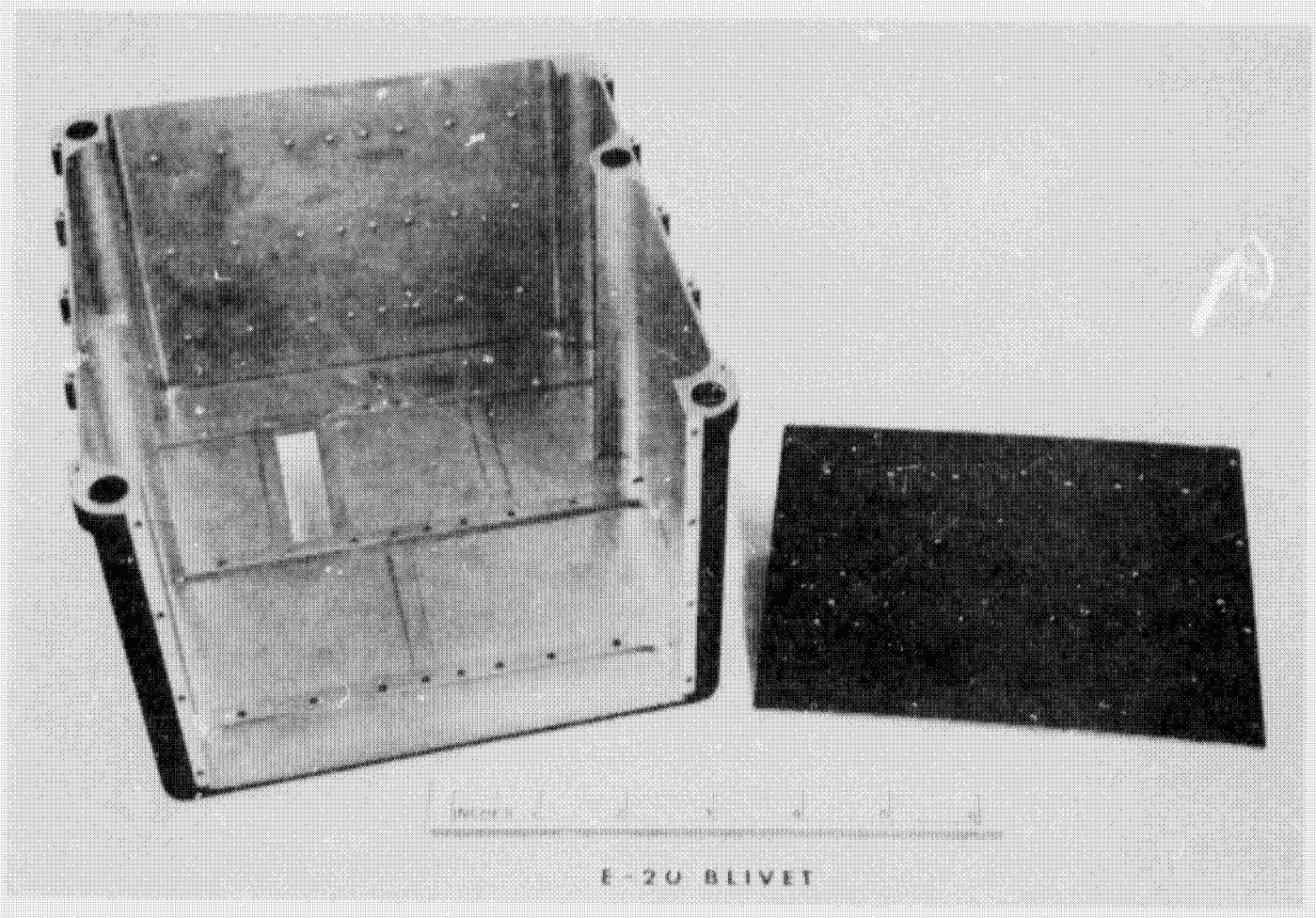

5. Radiometer Blivet

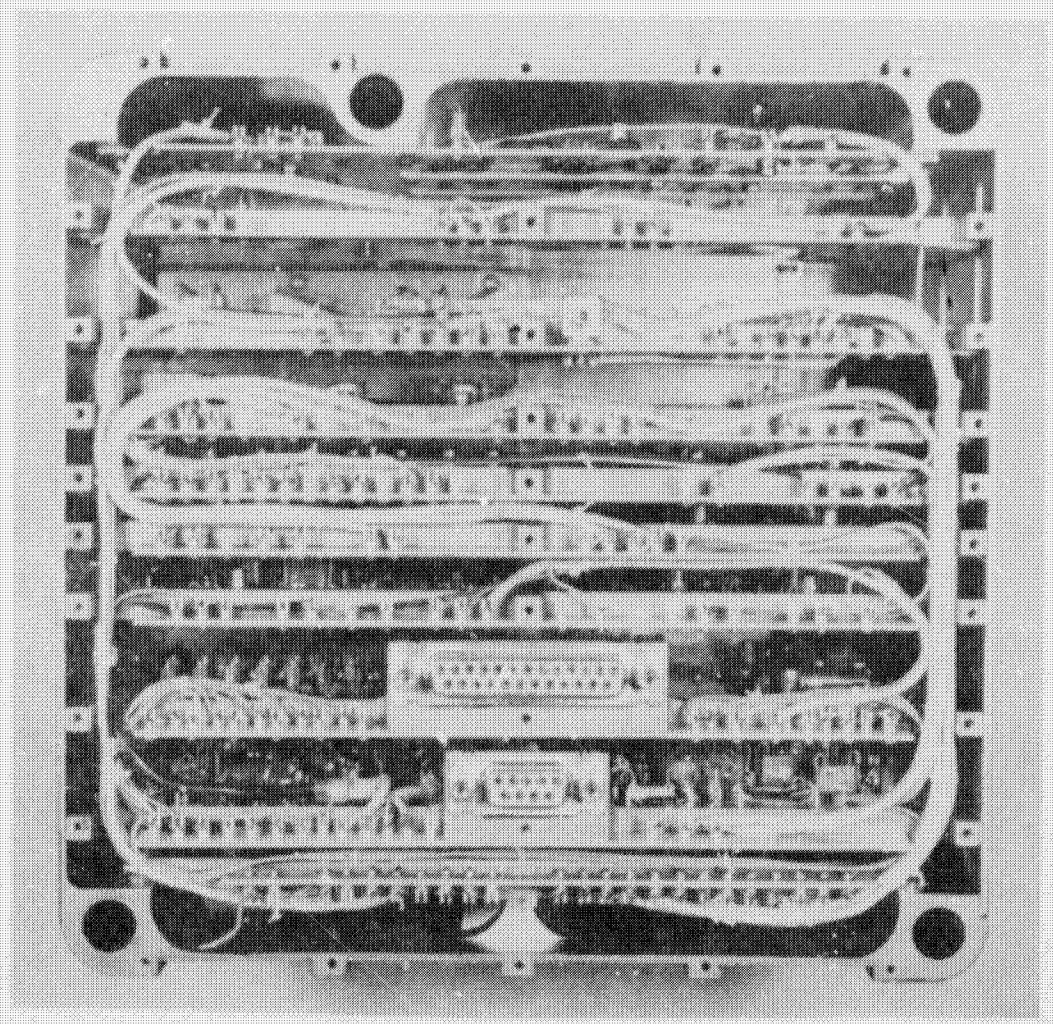

6. Assembled Radiometer Without Cover

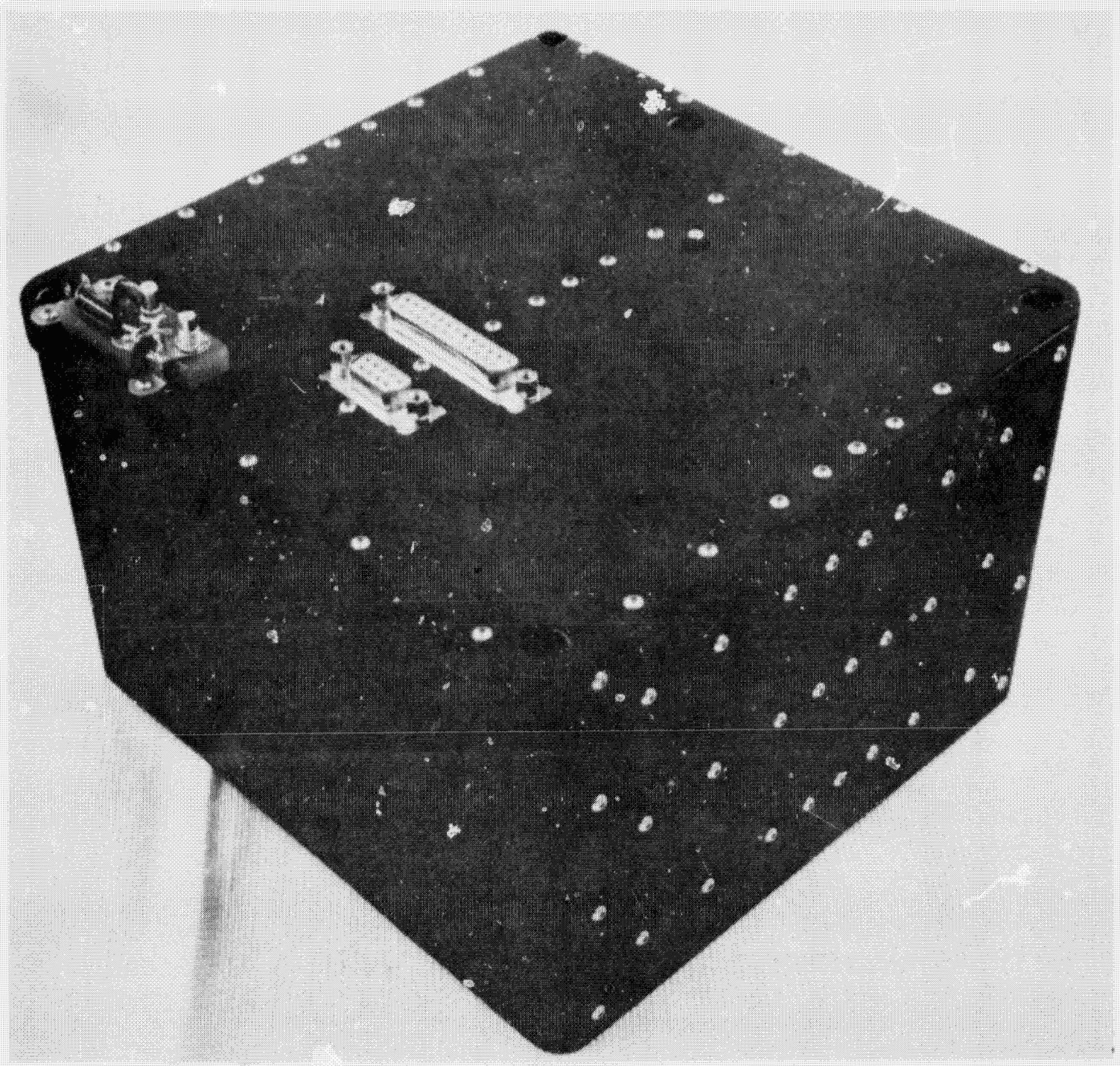

7. Assembled Radiometer

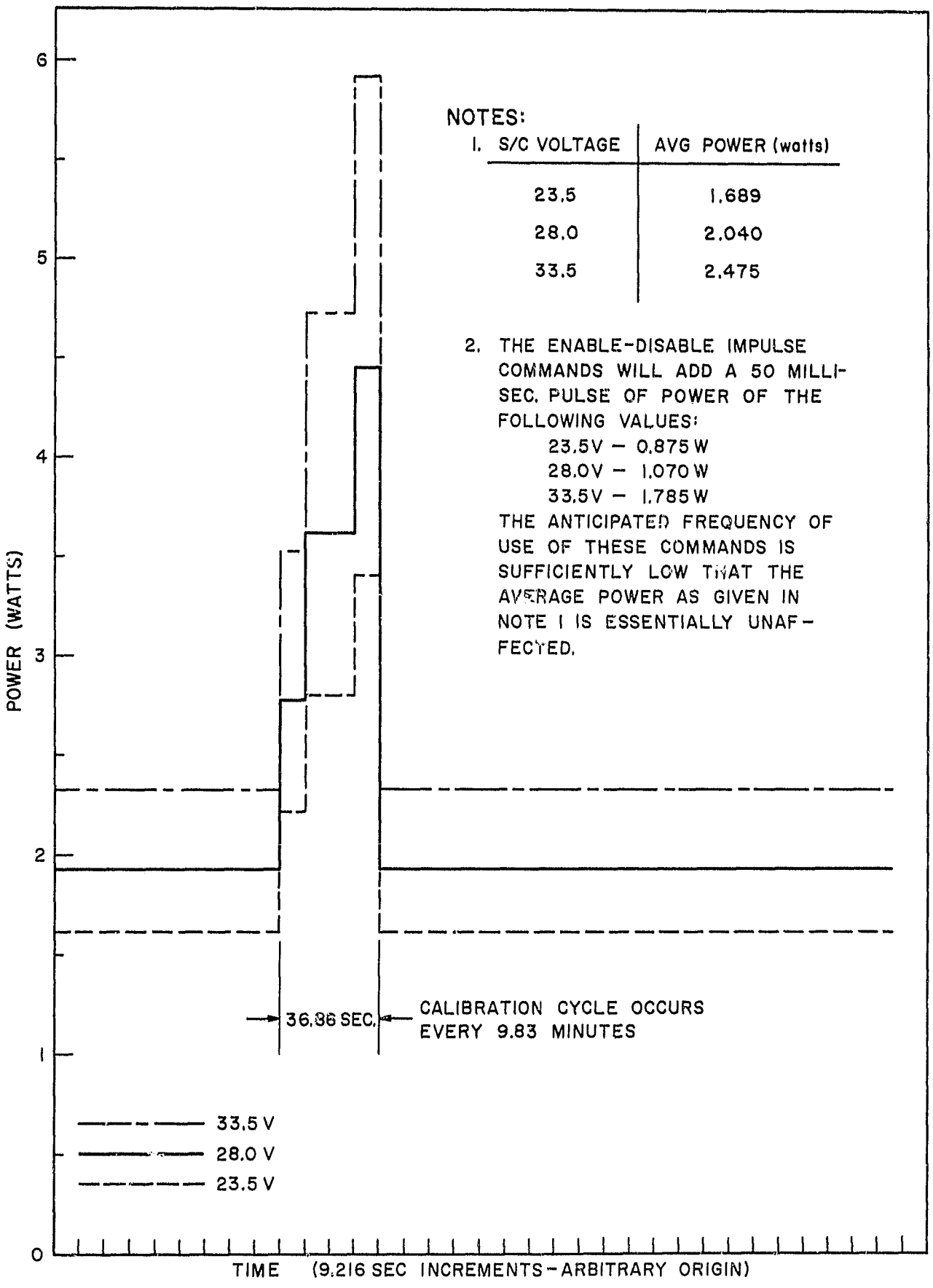

LOAD PROFILE FOR E-20 RADIOMETER ELECTRONICS

8. Power Profile

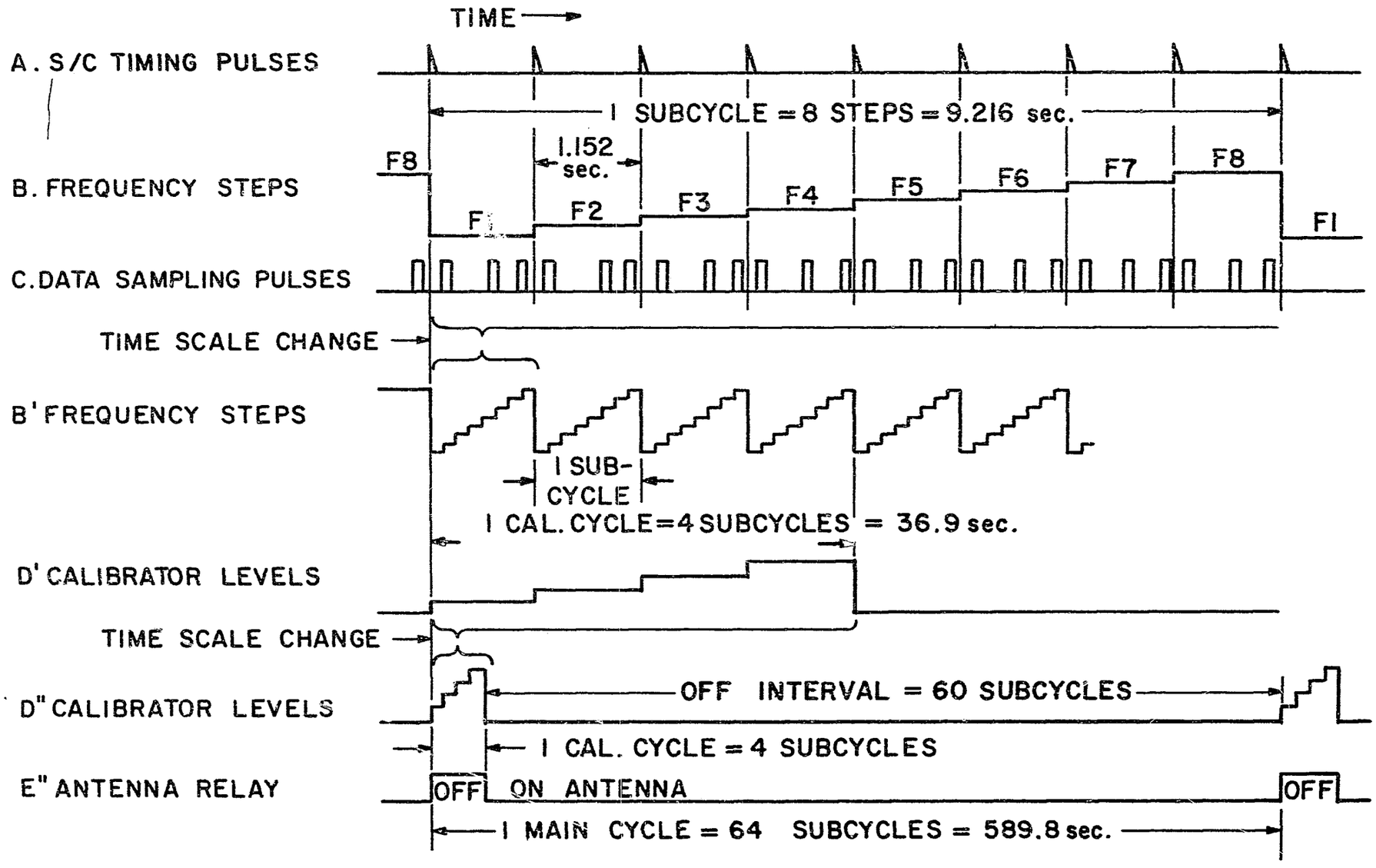

9. Timing Diagram

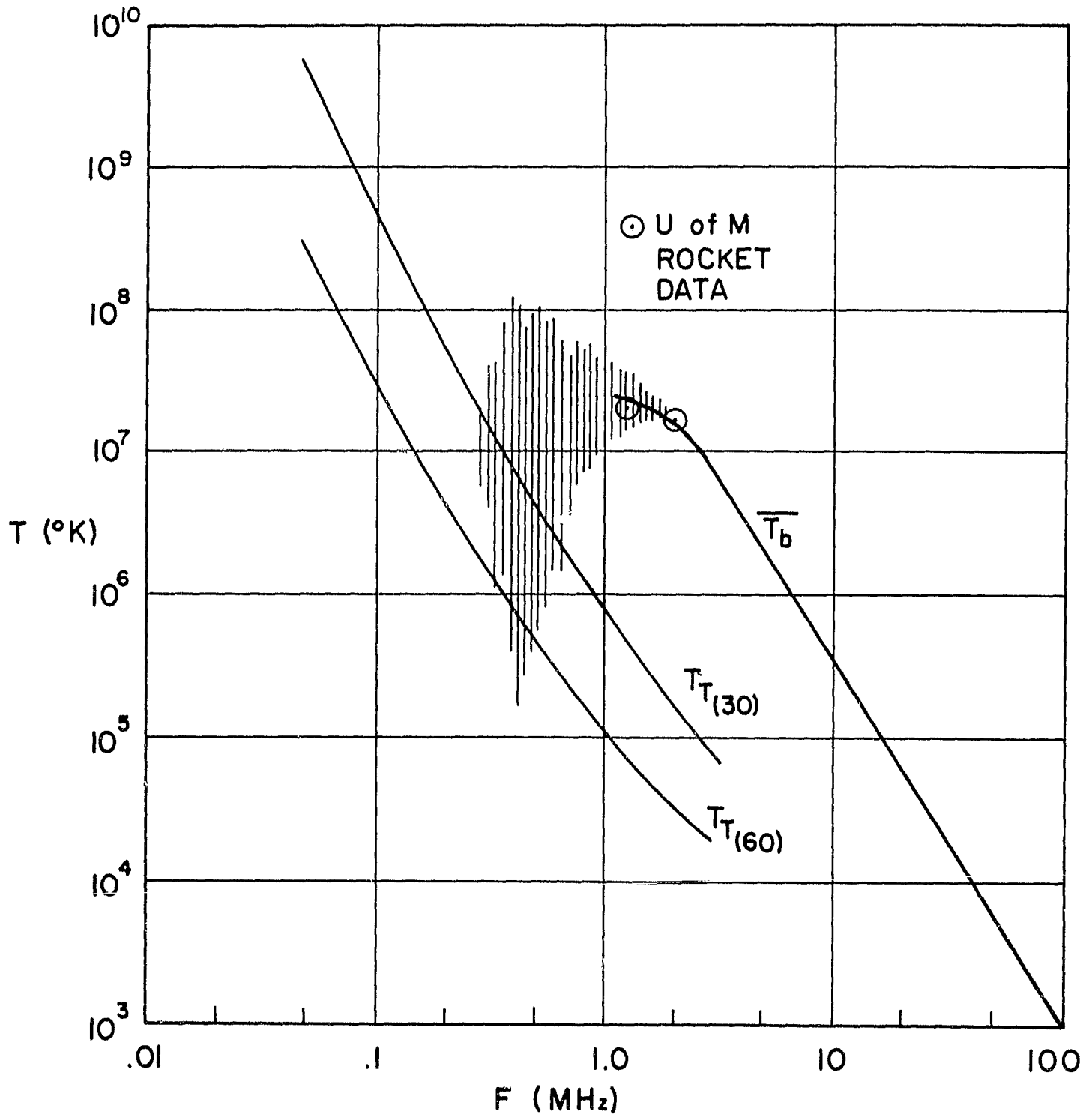

10. System Tangential Temperature

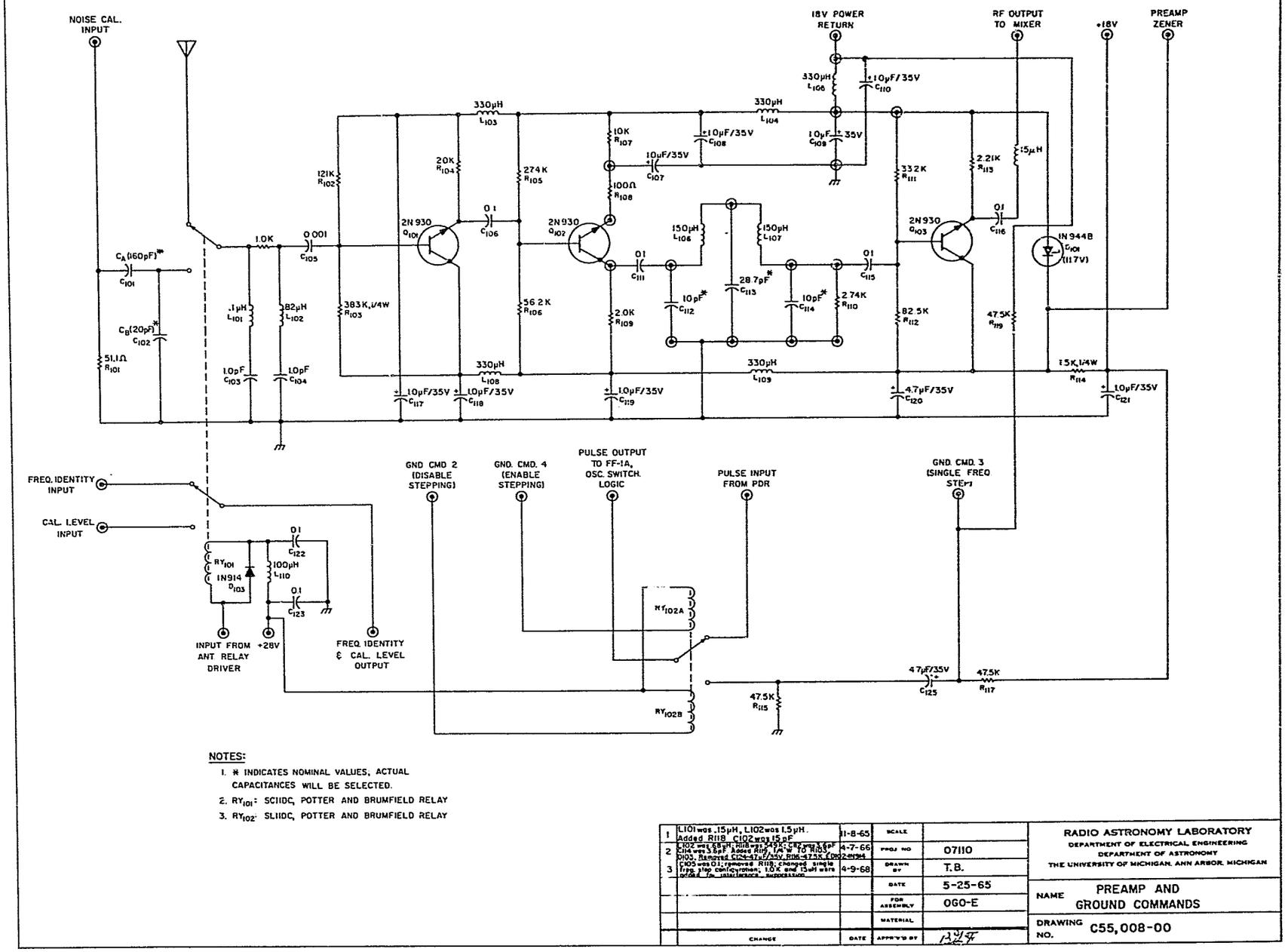

NOTES:

1. * INDICATES NOMINAL VALUES; ACTUAL CAPACITANCES WILL BE SELECTED.
2. RY_{101}: SCIIDC, POTTER AND BRUMFIELD RELAY
3. RY_{102}: SLIIDC, POTTER AND BRUMFIELD RELAY

	CHANGE	DATE
1	L101 was .15μH, L102 was 1.5μH. Added R118. C102 was 15pF	11-8-65
2	L102 was 1.8μH. R118 was 549K. CR2 was 3.6pF. C114 was 5.6pF. Added R119 1/4W to R103. D103, Removed. C124-47μF/35V, R116-47.5K. CR02-4V94	4-7-66
3	C105 was .01; removed R118, changed single stage step configuration; 1.0K and 15μH were added for interference suppression	4-9-68

SCALE	
PROJ NO	07110
DRAWN BY	T.B.
DATE	5-25-65
FOR ASSEMBLY	060-E
MATERIAL	
APPR'D BY	

RADIO ASTRONOMY LABORATORY
DEPARTMENT OF ELECTRICAL ENGINEERING
DEPARTMENT OF ASTRONOMY
THE UNIVERSITY OF MICHIGAN, ANN ARBOR, MICHIGAN

NAME: PREAMP AND GROUND COMMANDS

DRAWING NO. C55,008-00

11. Preamplifier and Ground Command Circuits

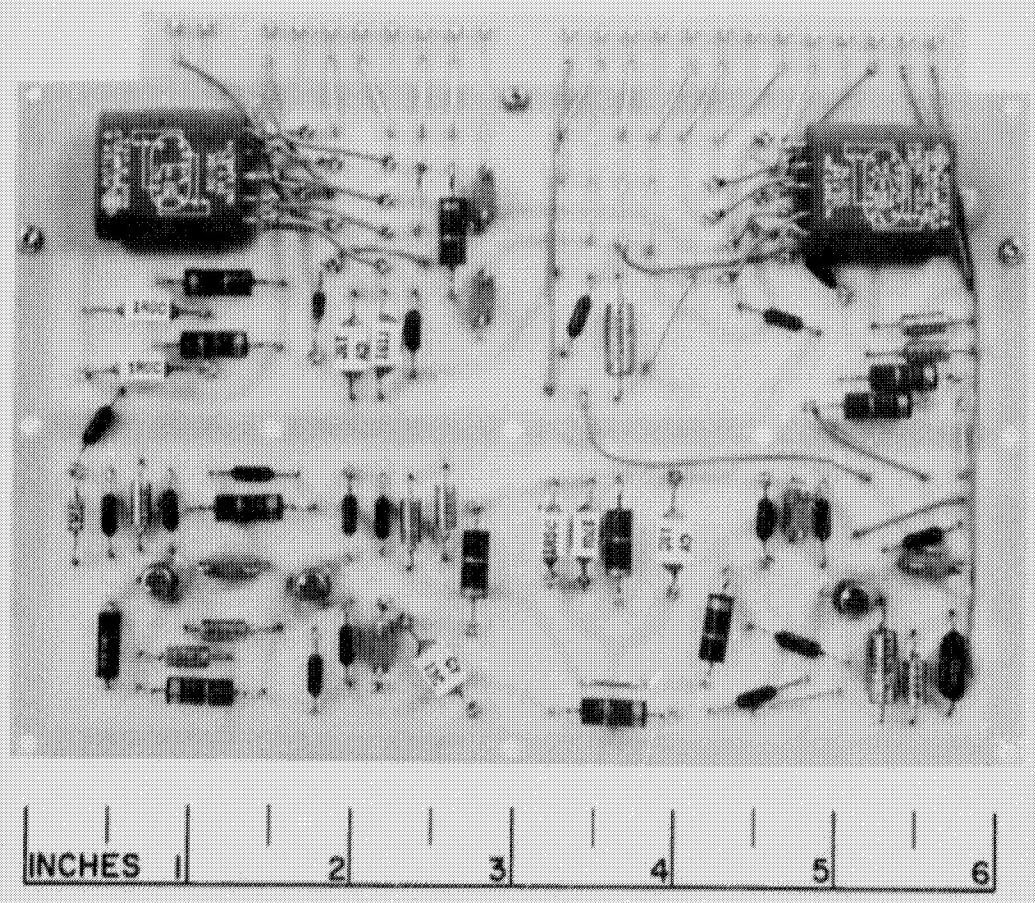

12. Preamplifier Board

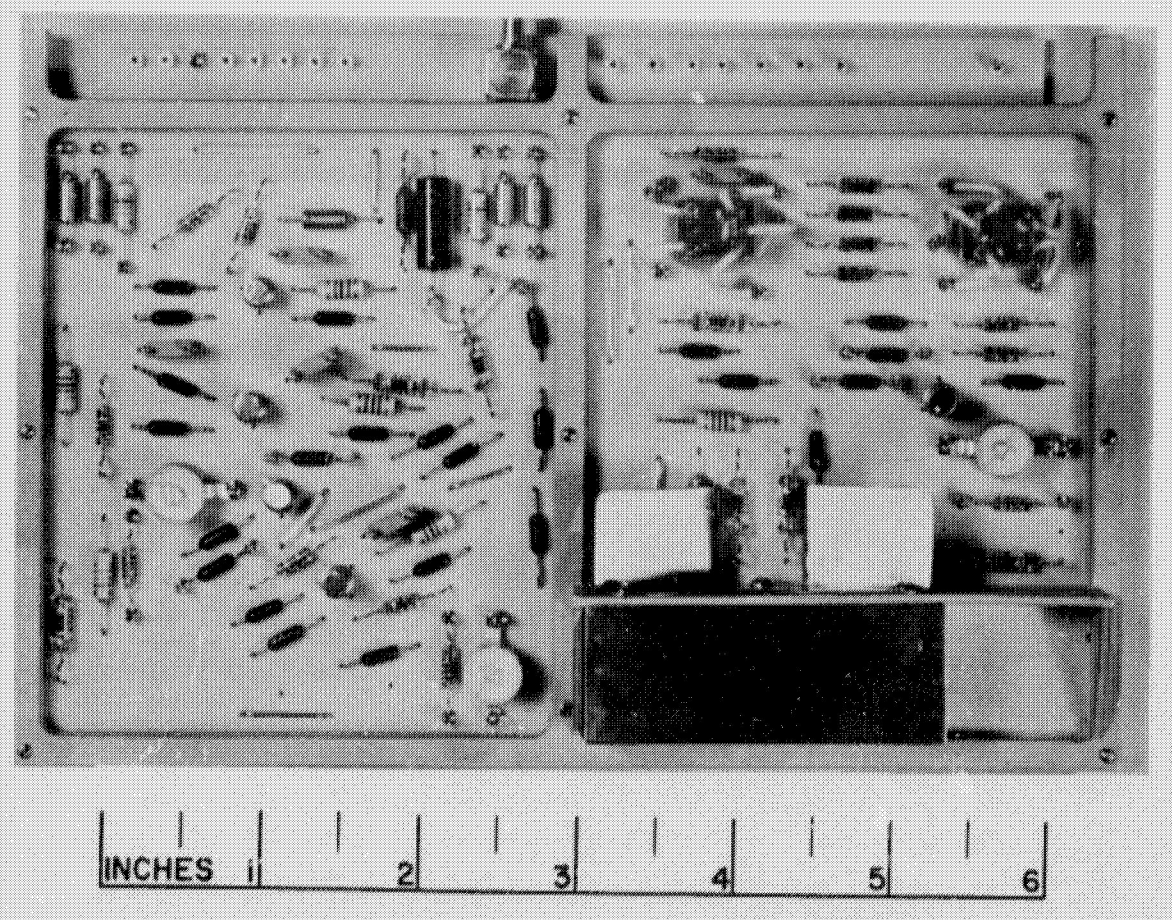

13. Mixer and Crystal Filter Board

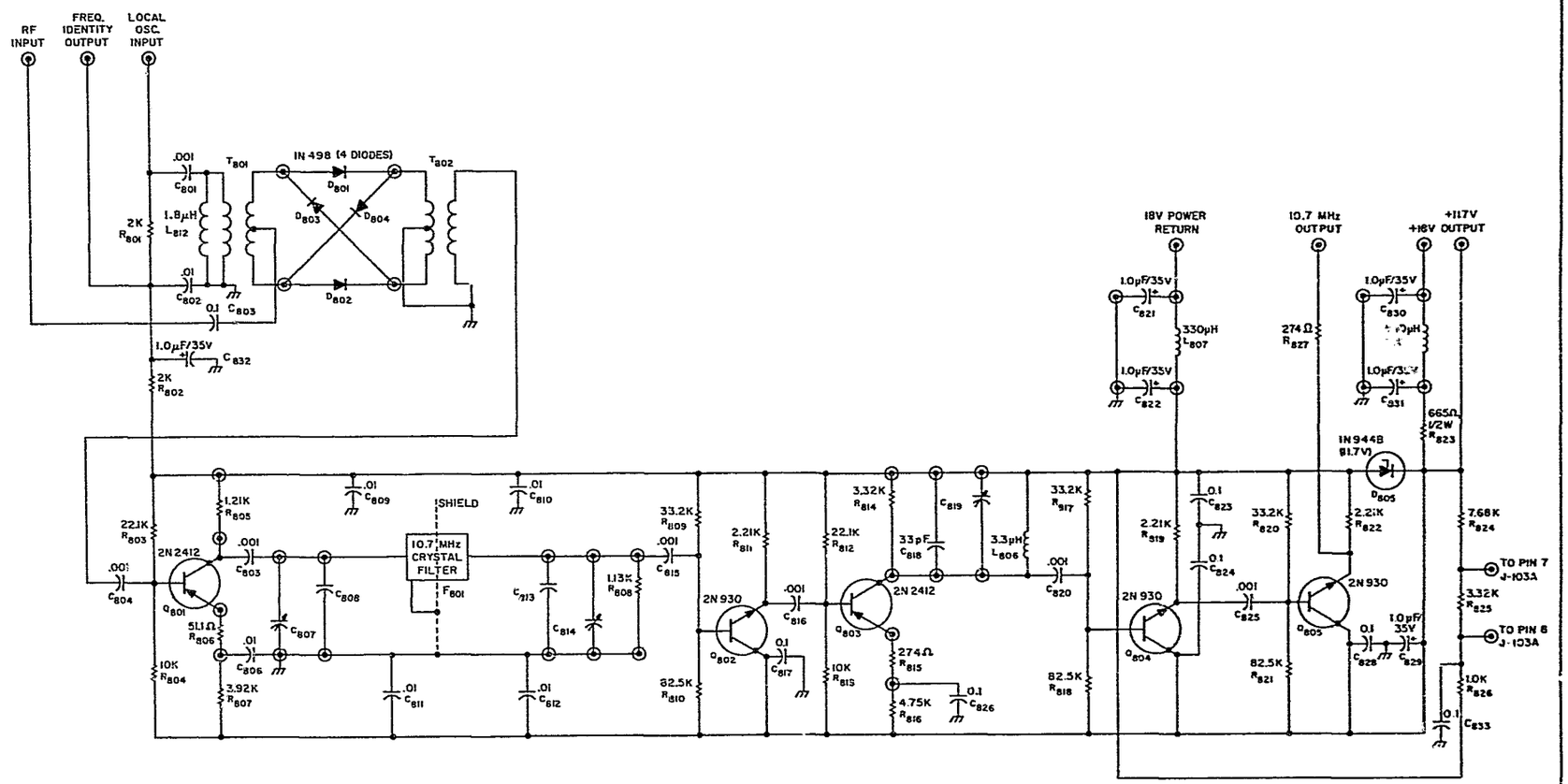

NOTES:

1. T_{801}, T_{802}: 01-878-03 ALADDIN TRANSFORMER
2. C_{807}, C_{814}, C_{819}: 5.5-18pf, 538-001-COPO-92P ERIE TRIMMERS
3. C_{808}, C_{813} : SELECTED CAPACITORS (NOMINAL VALUE-15pf)
4. D_{801}-D_{802} ; D_{803}-D_{804} ARE MATCHED PAIRS.
5. C_{818}: 301-N750 ERIE TEMPERATURE COMPENSATING CAPACITOR.

1	DELETED L801, & L804 3.3 μH. C808, & C813 were 33pf. ADDED NOTES	11-8-65	SCALE		RADIO ASTRONOMY LABORATORY DEPARTMENT OF ELECTRICAL ENGINEERING DEPARTMENT OF ASTRONOMY THE UNIVERSITY OF MICHIGAN, ANN ARBOR, MICHIGAN
2	Removed L802, L803, L805, L808, L809, & L810. 150 μH each. R803 was 2500Ω. C824 was .01. Removed C827 .001 10.7 MHz output. 10.7 MHz output was total output 10.7 MHz. Added C832 and 833, L812, and R827. Added note 4	4-13-6	PROJ NO.	07110	
			DRAWN BY	T.B.	
			DATE	4-28-65	
			FOR ASSEMBLY	060-E	NAME MIXER, CRYSTAL FILTER, AND DRIVERS
			MATERIAL		DRAWING NO. C55-005-00
	CHANGE	DATE	APPR'D BY	B.F.T.	

14. Mixer and Crystal Filter Circuits

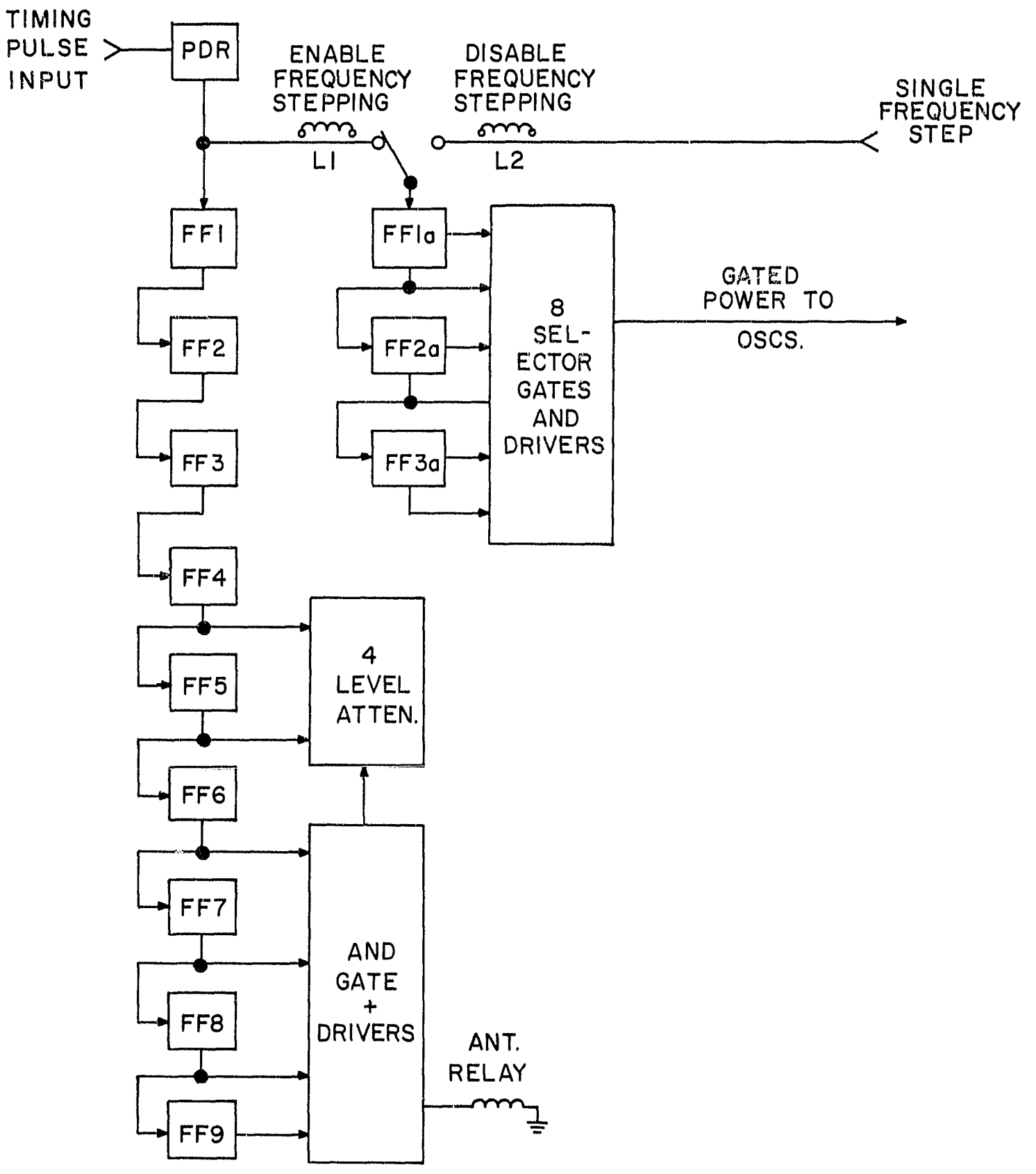

15. Logic Block Diagram

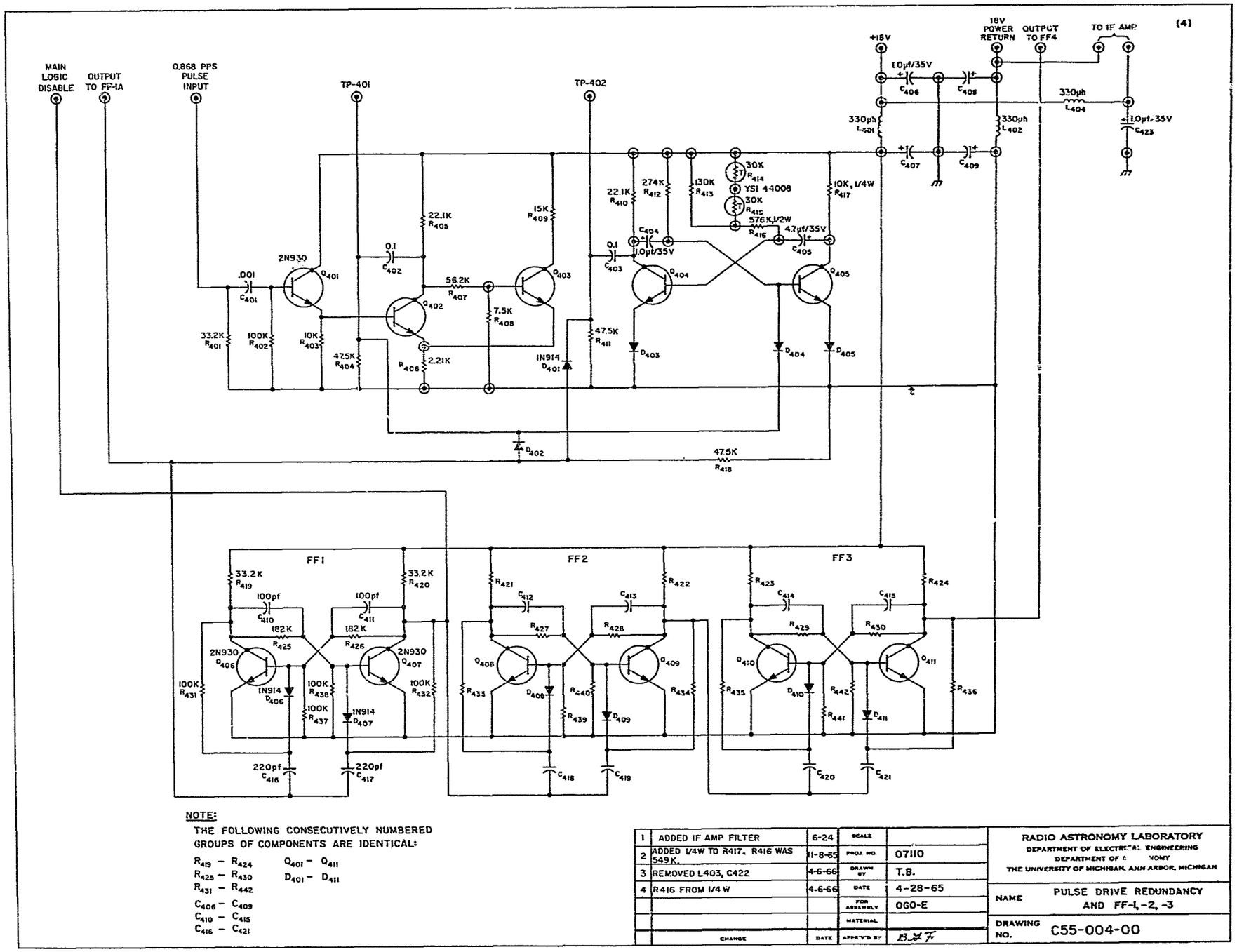

NOTE:

THE FOLLOWING CONSECUTIVELY NUMBERED GROUPS OF COMPONENTS ARE IDENTICAL:

$R_{419} - R_{424}$ $Q_{401} - Q_{411}$
$R_{425} - R_{430}$ $D_{401} - D_{411}$
$R_{431} - R_{442}$
$C_{406} - C_{409}$
$C_{410} - C_{415}$
$C_{416} - C_{421}$

1	ADDED IF AMP FILTER	6-24	SCALE		RADIO ASTRONOMY LABORATORY DEPARTMENT OF ELECTRICAL ENGINEERING DEPARTMENT OF ASTRONOMY THE UNIVERSITY OF MICHIGAN, ANN ARBOR, MICHIGAN
2	ADDED 1/4W TO R417, R416 WAS 549K.	11-8-65	PROJ. NO.	07110	
3	REMOVED L403, C422	4-6-66	DRAWN BY	T.B.	
4	R416 FROM 1/4 W	4-6-66	DATE	4-28-65	NAME: PULSE DRIVE REDUNDANCY AND FF-1,-2,-3
			FOR ASSEMBLY	060-E	
			MATERIAL		
	CHANGE	DATE	APPR'D BY	B.M.F	DRAWING NO. C55-004-00

16. Pulse Drive Redundancy and FF-1,-2,-3 Circuits

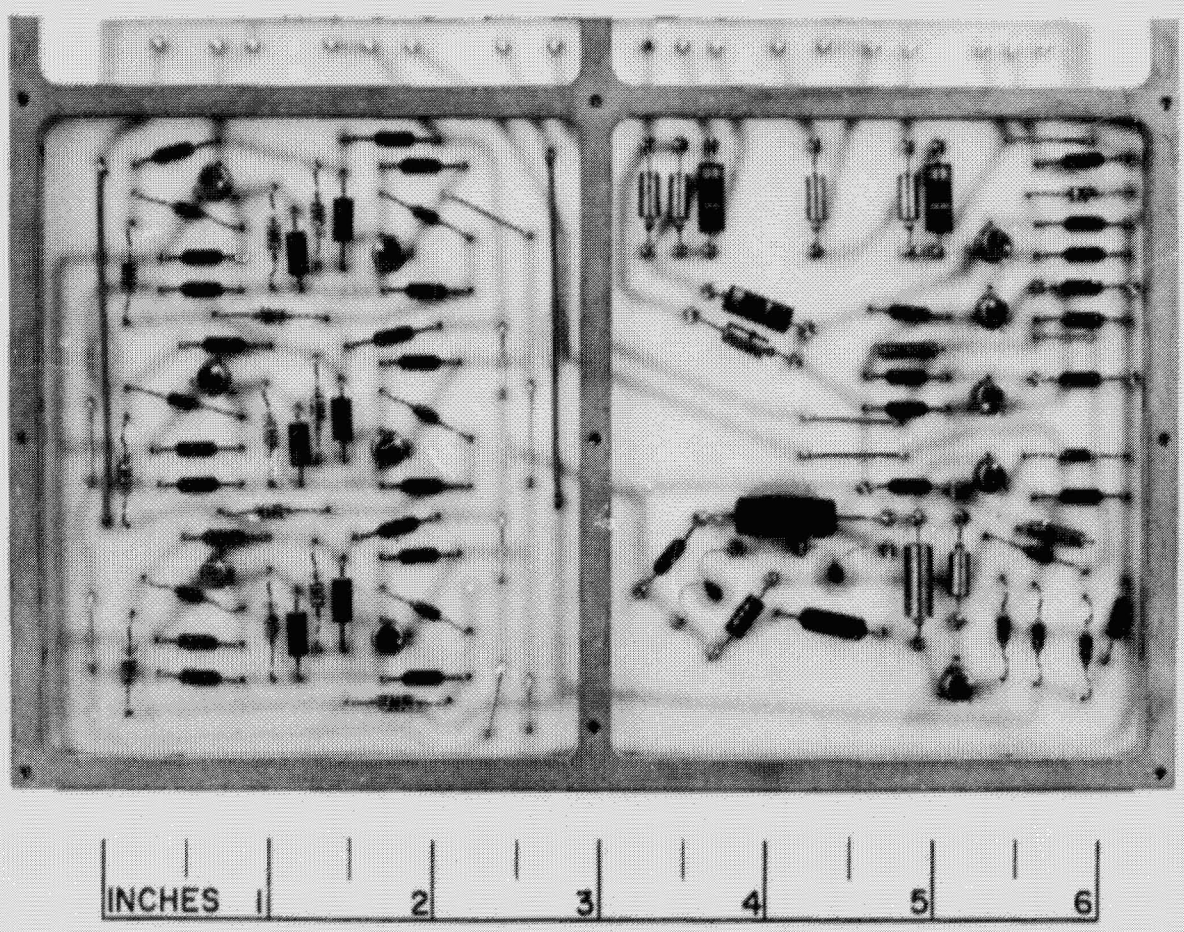

17. Pulse Drive and Logic Board

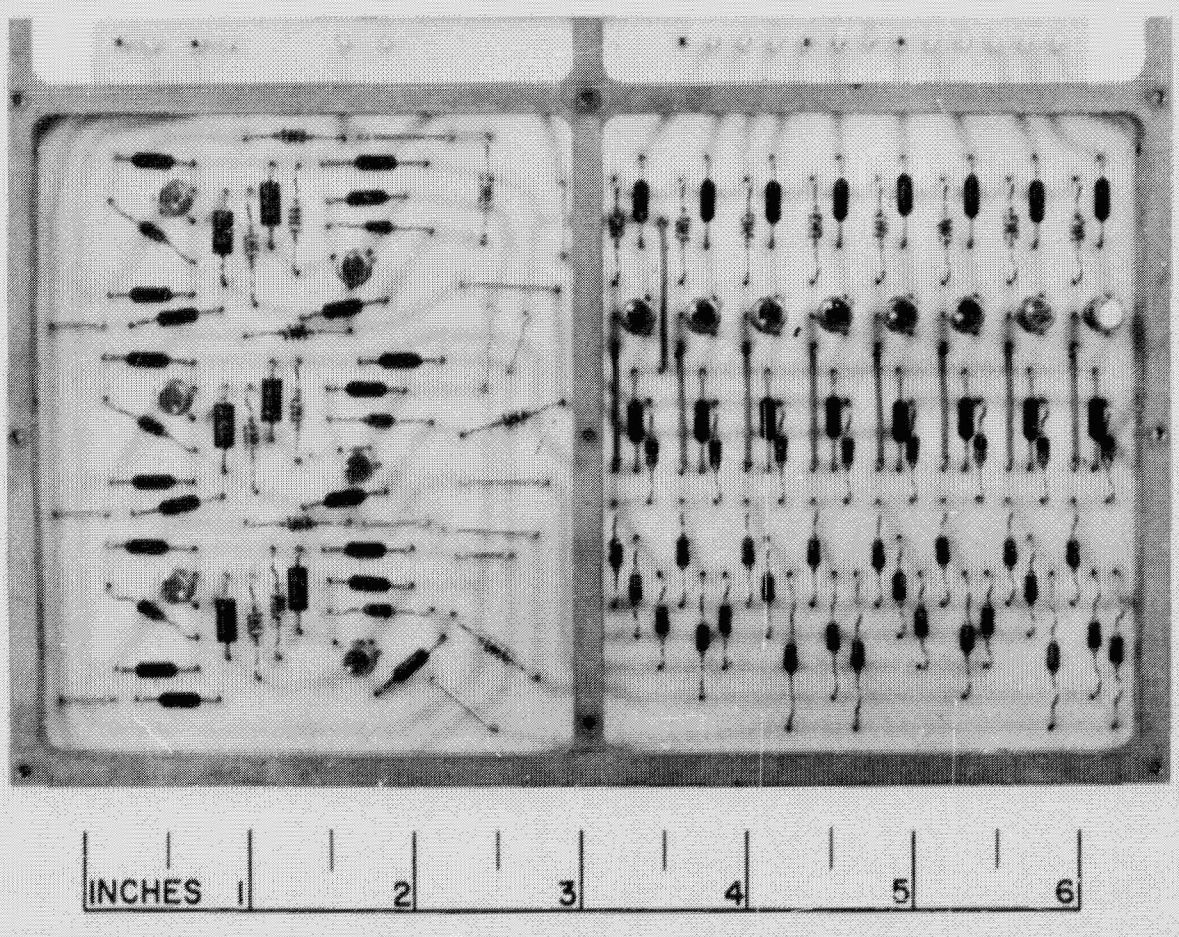

18. Oscillator Switching Logic Board

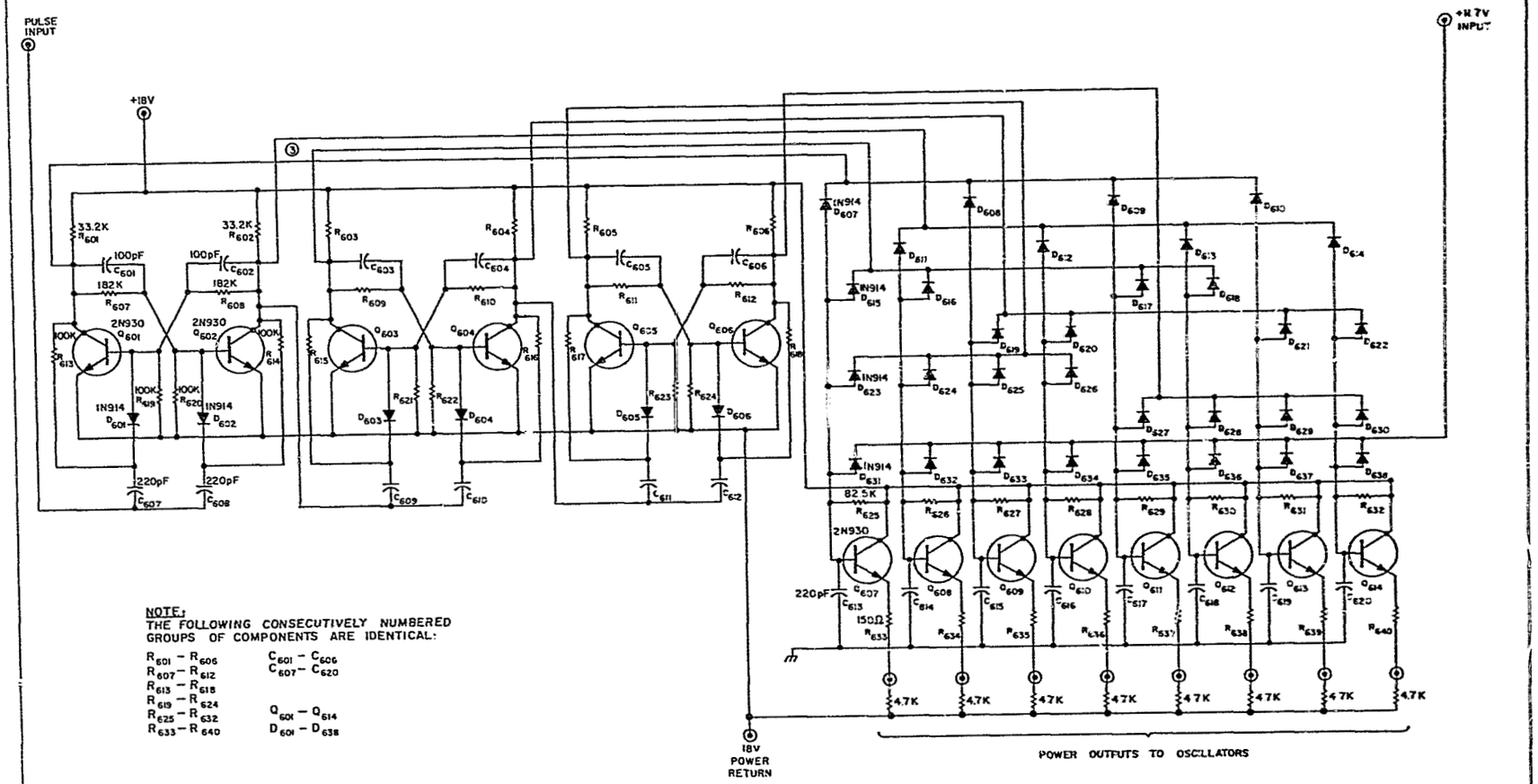

1	CORRECTED	7-30	SCALE	
2	R_{625}, ETC FROM 82K	4-6-66	PROJ NO	07110
3	CHANGED WIRING WHERE NOTED	4-6-66	DRAWN BY	GL
4	ADDED 47K RESISTORS	4-10-66	DATE	2-12-65
			FOR ASSEMBLY	060-E
			MATERIAL	
	CHANGE	DATE	APPR'D BY	RJF

RADIO ASTRONOMY LABORATORY
DEPARTMENT OF ELECTRICAL ENGINEERING
DEPARTMENT OF ASTRONOMY
THE UNIVERSITY OF MICHIGAN, ANN ARBOR, MICHIGAN

NAME OSCILLATOR SWITCHING LOGIC

DRAWING NO. C55,001-00

19. Oscillator Switching Logic Circuits

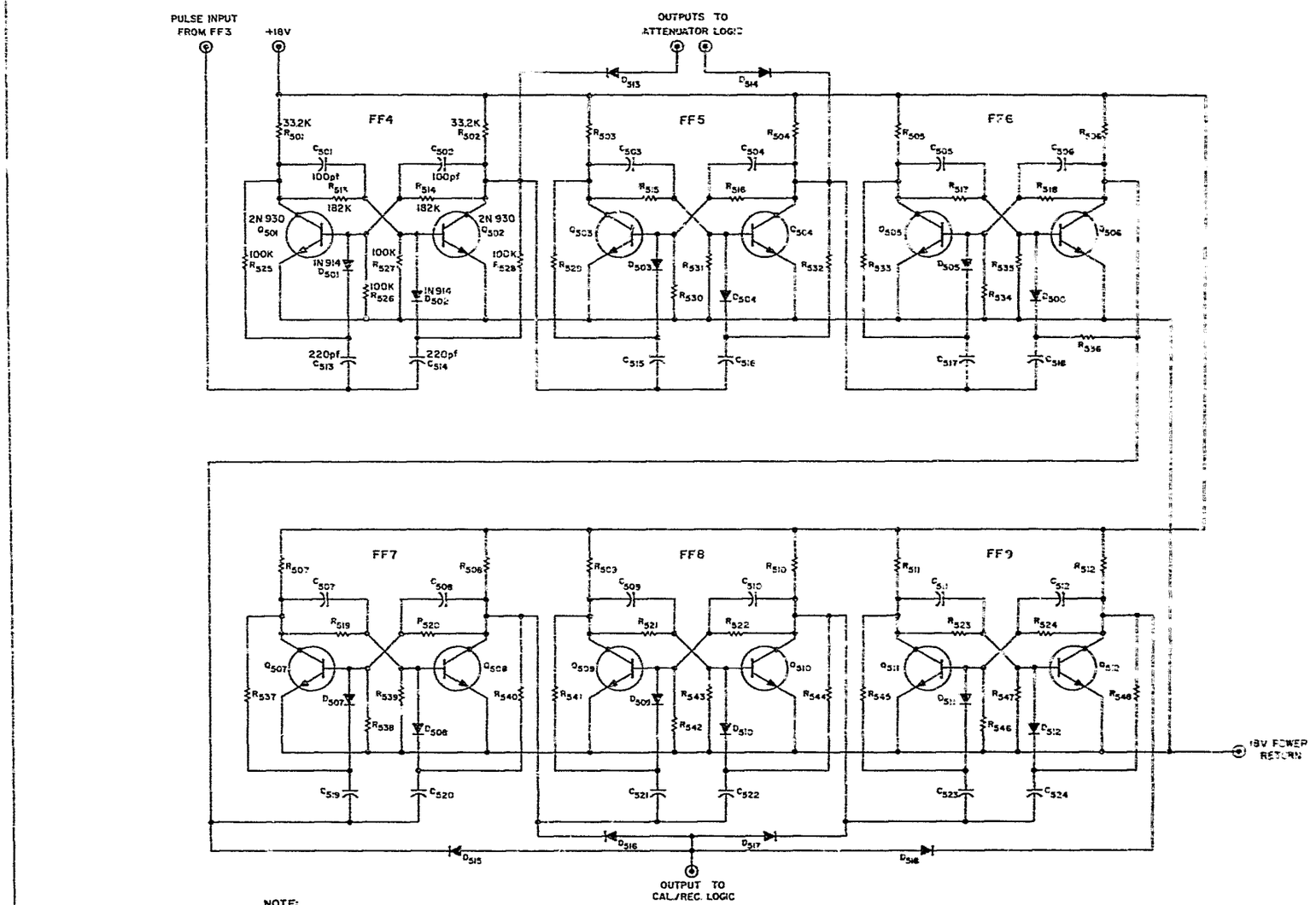

NOTE:

THE FOLLOWING CONSECUTIVELY NUMBERED GROUPS OF COMPONENTS ARE IDENTICAL:

$R_{501} - R_{512}$ $C_{501} - C_{512}$ $D_{501} - D_{518}$

$R_{513} - R_{524}$ $C_{513} - C_{524}$ $Q_{501} - Q_{512}$

$R_{525} - R_{548}$

		SCALE		RADIO ASTRONOMY LABORATORY DEPARTMENT OF ELECTRICAL ENGINEERING DEPARTMENT OF ASTRONOMY THE UNIVERSITY OF MICHIGAN, ANN ARBOR, MICHIGAN
		PROJ NO	07110	
		DRAWN BY	T.B.	
		DATE	5-3-65	
		FOR ASSEMBLY	GGO-E	NAME MAIN LOGIC
		MATERIAL		
	CHANGE	DATE	APPR'D BY A.E.F	DRAWING NO. C55,003-01

20. Main Logic Circuits

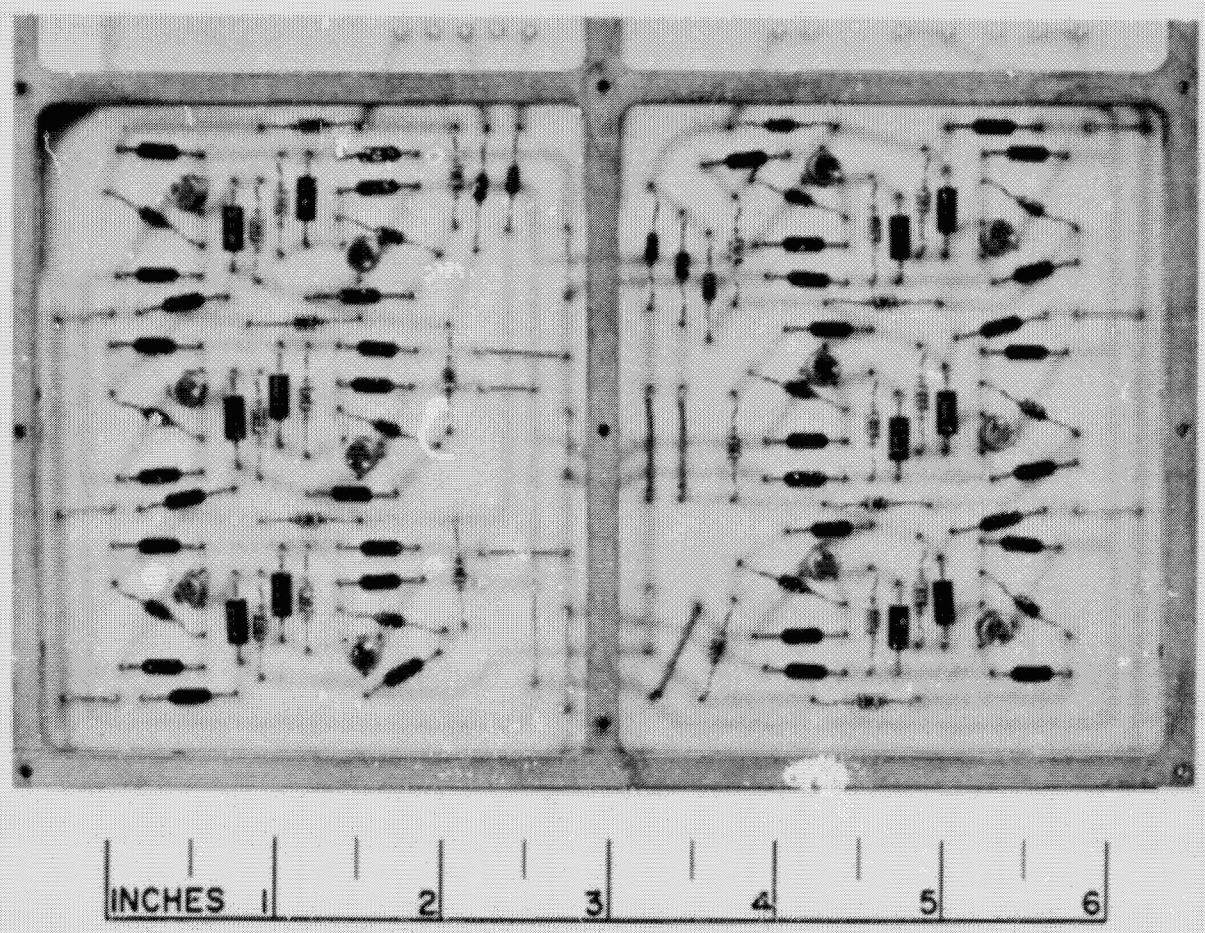

21. Main Logic Board

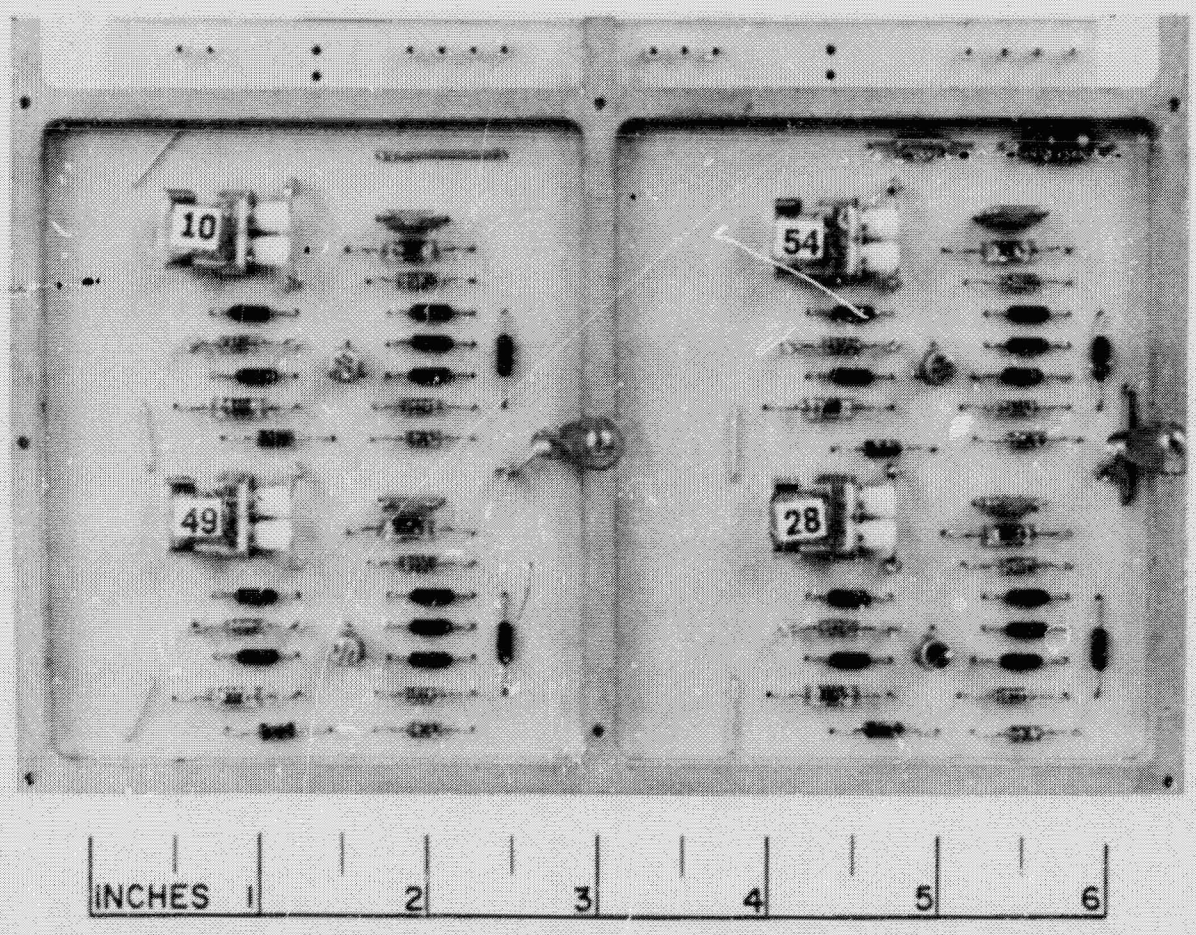

22. Local Oscillators 1-4 Board

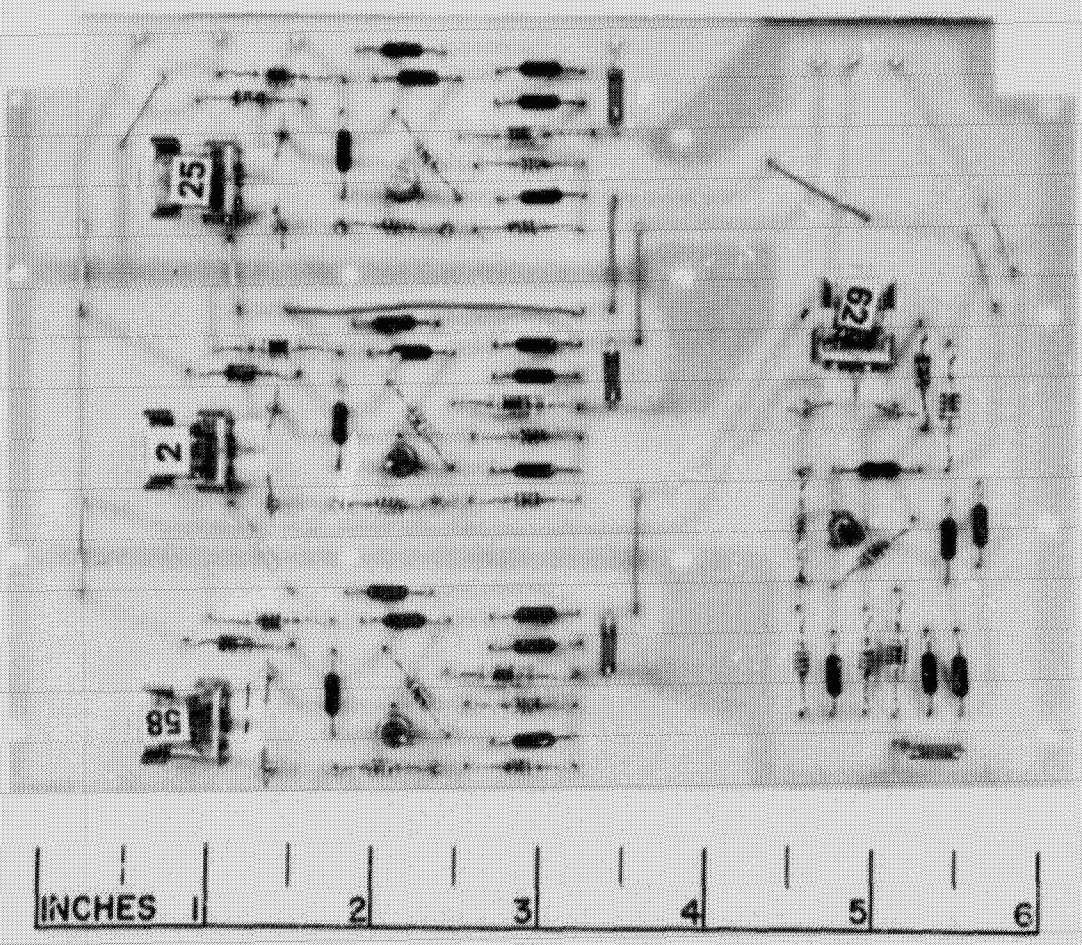

23. Local Oscillators 5-8 Board

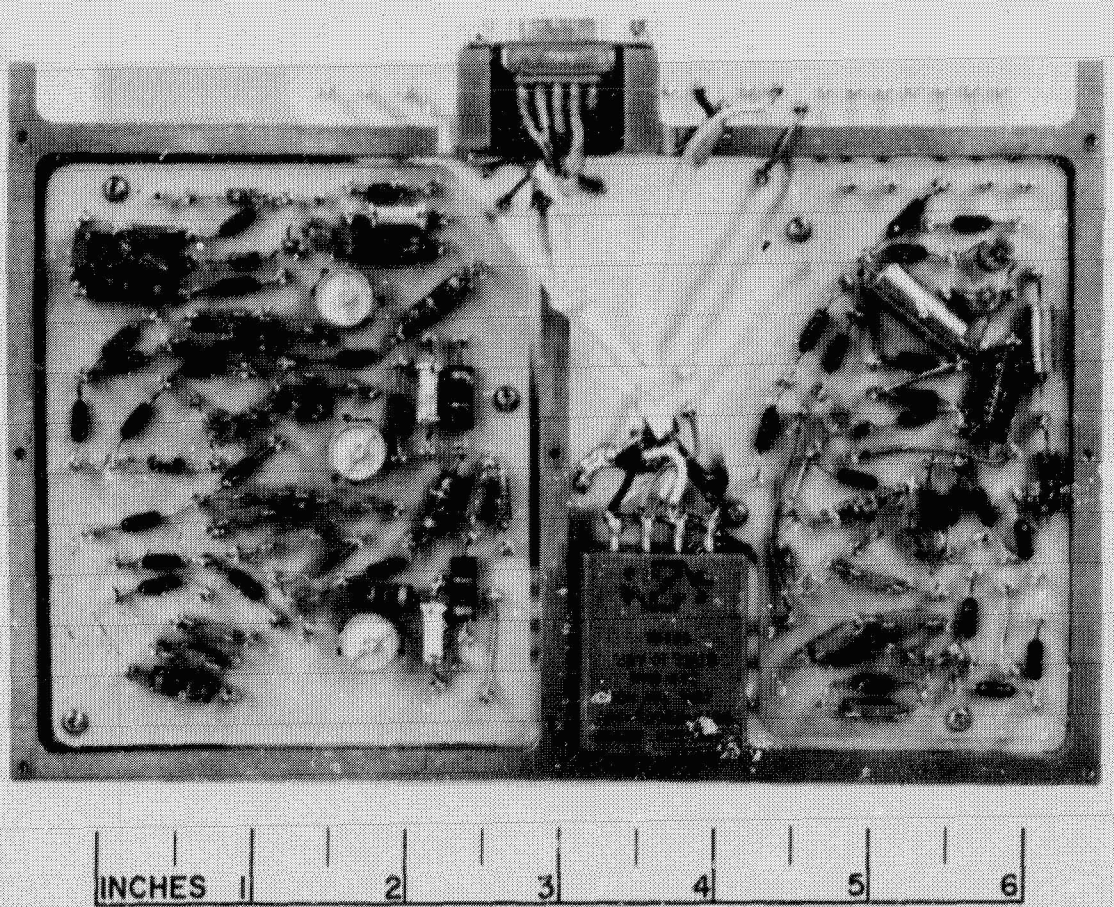

24. IF Amplifier and Detector Board

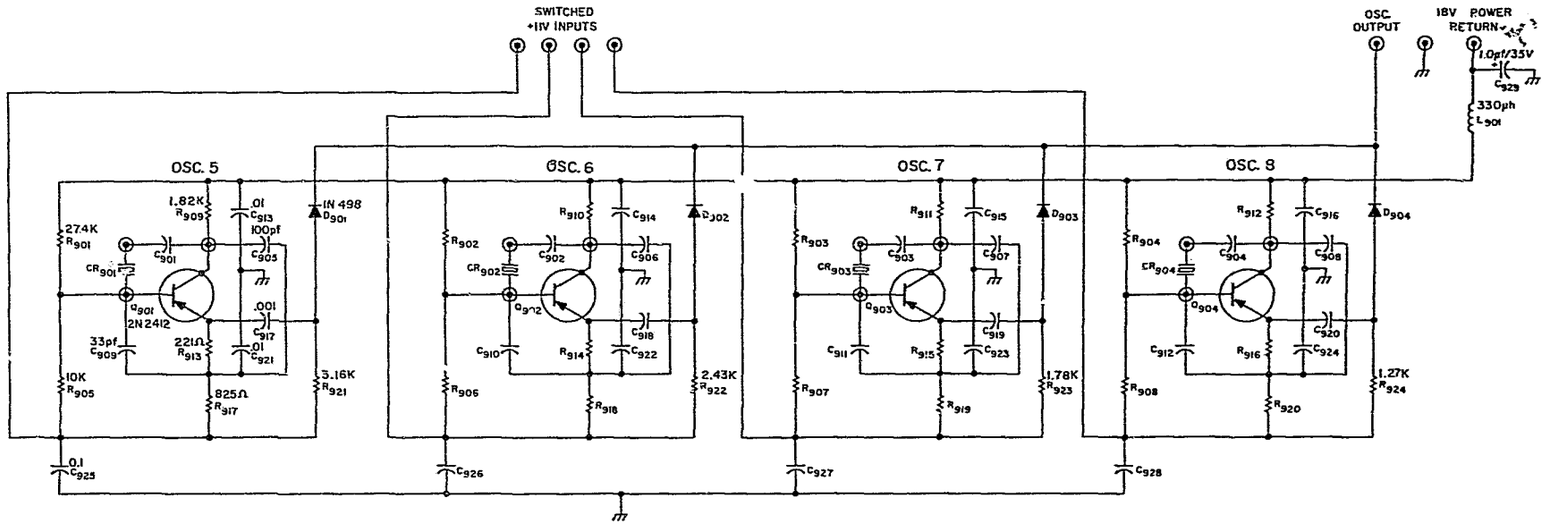

NOTES:

1. THE FOLLOWING CONSECUTIVELY NUMBERED GROUPS OF COMPONENTS ARE IDENTICAL:

$R_{901}-R_{904}$	$C_{905}-C_{908}$	$Q_{901}-Q_{904}$
$R_{905}-R_{908}$	$C_{909}-C_{912}$	
$R_{909}-R_{912}$	$C_{913}-C_{916}$	$D_{901}-D_{904}$
$R_{913}-R_{916}$	$C_{917}-C_{920}$	
$R_{917}-R_{920}$	$C_{921}-C_{924}$	
	$C_{925}-C_{928}$	

2. $C_{901}-C_{904}$, SELECTED CAPACITORS (FINAL SELECTED VALUE 47 pf)

3. CIRCUIT BOARDS 9 AND 10 ARE IDENTICAL WITH THE FOLLOWING EXCEPTIONS:
   - A. THE FILTER (L_{901} & C_{929}) OCCURS ON BOARD 9 ONLY AND IS USED ON BOTH BOARDS.
   - B. BOARD 10 CONTAINS OSCILLATORS 1-4
   - C. COMPONENT NUMBERS ARE IN 1000 SERIES.
   - D. R_{1021} – 9.76K
     R_{1022} – 7.15 K
     R_{1023} – 5.49K
     R_{1024} – 4.12K
   - E. R_{1009} – 1.5K

	CHANGE	DATE	APPR'D BY
1	OSC. 5 was1, 6 was2, 7 was3, 8 was4. R909 was 2.74K, R921 was 3.75K, R922 was 7.15K, R923 was 1.40K, R924 was 4.12K	4-6-66	
1	NOTE 3B: J-4 was 5-8; 3D: R1021 was 3.83K, R1022 was 2.45K, R1023 was 1.78K, R1024 was 1.27K. Added to note 3E - R1009 1.5K	4-6-66	

SCALE	
PROJ. NO.	07110
DRAWN BY	T.B.
DATE	5-7-65
FOR ASSEMBLY	060-E
MATERIAL	
APPR'D BY	BHF

RADIO ASTRONOMY LABORATORY
DEPARTMENT OF ELECTRICAL ENGINEERING
DEPARTMENT OF ASTRONOMY
THE UNIVERSITY OF MICHIGAN, ANN ARBOR, MICHIGAN

NAME LOCAL OSCILLATORS

DRAWING NO. C55, 002-01

25. Local Oscillator Circuits

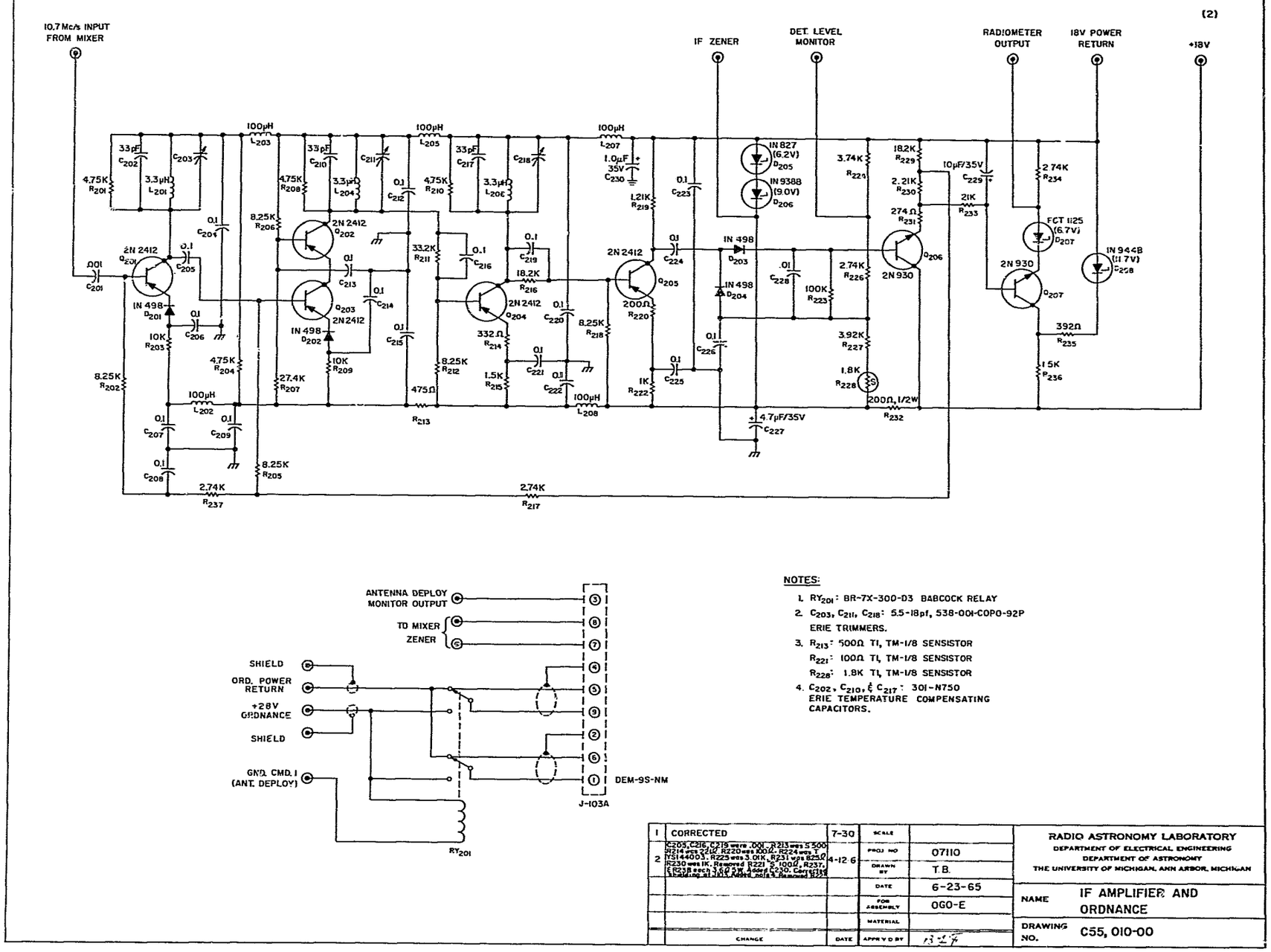

NOTES:

1. RY_{201}: BR-7X-300-03 BABCOCK RELAY
2. C_{203}, C_{211}, C_{218}: 5.5-18pf, 538-001-COPO-92P ERIE TRIMMERS.
3. R_{213}: 500Ω TI, TM-1/8 SENSISTOR
   R_{221}: 100Ω TI, TM-1/8 SENSISTOR
   R_{228}: 1.8K TI, TM-1/8 SENSISTOR
4. C_{202}, C_{210}, & C_{217}: 301-N750 ERIE TEMPERATURE COMPENSATING CAPACITORS.

1	CORRECTED	7-30	SCALE		RADIO ASTRONOMY LABORATORY DEPARTMENT OF ELECTRICAL ENGINEERING DEPARTMENT OF ASTRONOMY THE UNIVERSITY OF MICHIGAN, ANN ARBOR, MICHIGAN
2	C203, C216, C219 were .001, R213 was S 500, R214 was 2.2UF, R220 was 300Ω, R224 was T YS144003, R225 was 3.01K, R231 was 825Ω, R230 was 1K, Removed R221 S 100Ω, R237, E R238 each 3.6Ω 2W, Added C230, Corrected	4-12 6	PROJ NO	07110	
			DRAWN BY	T.B.	
			DATE	6-23-65	NAME IF AMPLIFIER AND ORDNANCE
			FOR ASSEMBLY	060-E	
			MATERIAL		DRAWING NO. C55, 010-00
	CHANGE	DATE	APPR'D BY		

26. IF Amplifier and Detector Circuits

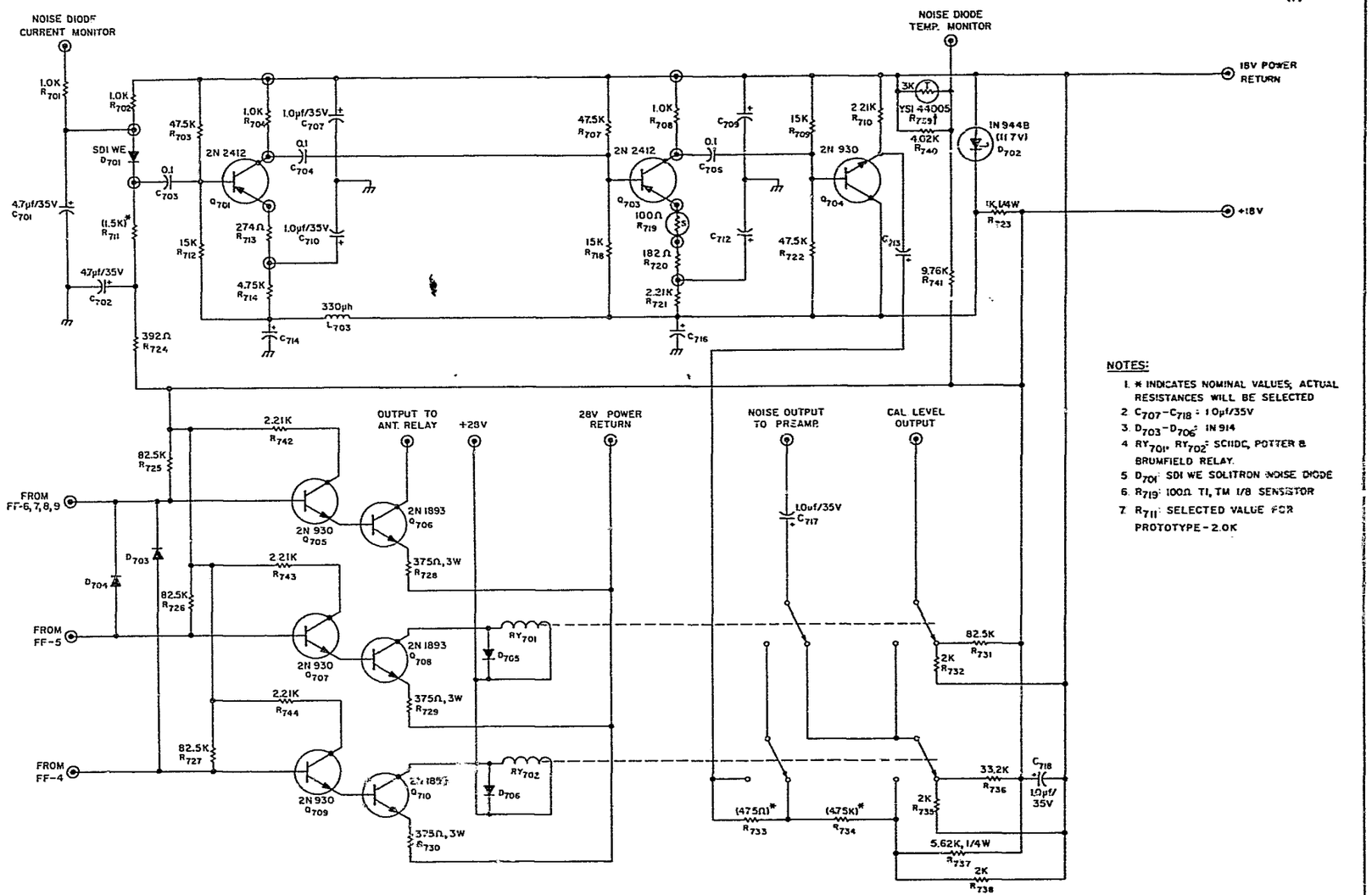

NOTES:

1. * INDICATES NOMINAL VALUES, ACTUAL RESISTANCES WILL BE SELECTED
2. C_{707}–C_{718} : 1.0µf/35V
3. D_{703}–D_{706}: IN 914
4. RY_{701}, RY_{702}: SCHDC, POTTER & BRUMFIELD RELAY.
5. D_{701}: SDI WE SOLITRON NOISE DIODE
6. R_{719}: 100Ω TI, TM 1/8 SENSISTOR
7. R_{711}: SELECTED VALUE FOR PROTOTYPE – 2.0K

	CHANGE	DATE		
1	CHANGED FROM BOARD 3 TO 7	6-22	SCALE	
2	REMOVED MAN. CONT. STAKES	7-30	PROJ NO.	07110
3	ADDED D705 & D706	8-8-65	DRAWN BY	T.B.
4	REMOVED L701, 702, 704; Q702; R705, 706, 715, 716, 717; C705, 708, 714, 715	4-12-66	DATE	4-30-65
5	ADDED R742, 743, 744 R737 CHANGED TO 1/4 W	4-12-66	FOR ASSEMBLY	060-E
			MATERIAL	
			APPR'D BY	B.L.F.

RADIO ASTRONOMY LABORATORY
DEPARTMENT OF ELECTRICAL ENGINEERING
DEPARTMENT OF ASTRONOMY
THE UNIVERSITY OF MICHIGAN, ANN ARBOR MICHIGAN

NAME: NOISE CALIBRATOR, RELAYS AND RELAY DRIVERS

DRAWING NO. C55-006-00

27. Noise Calibrator and Relay Driver Circuits

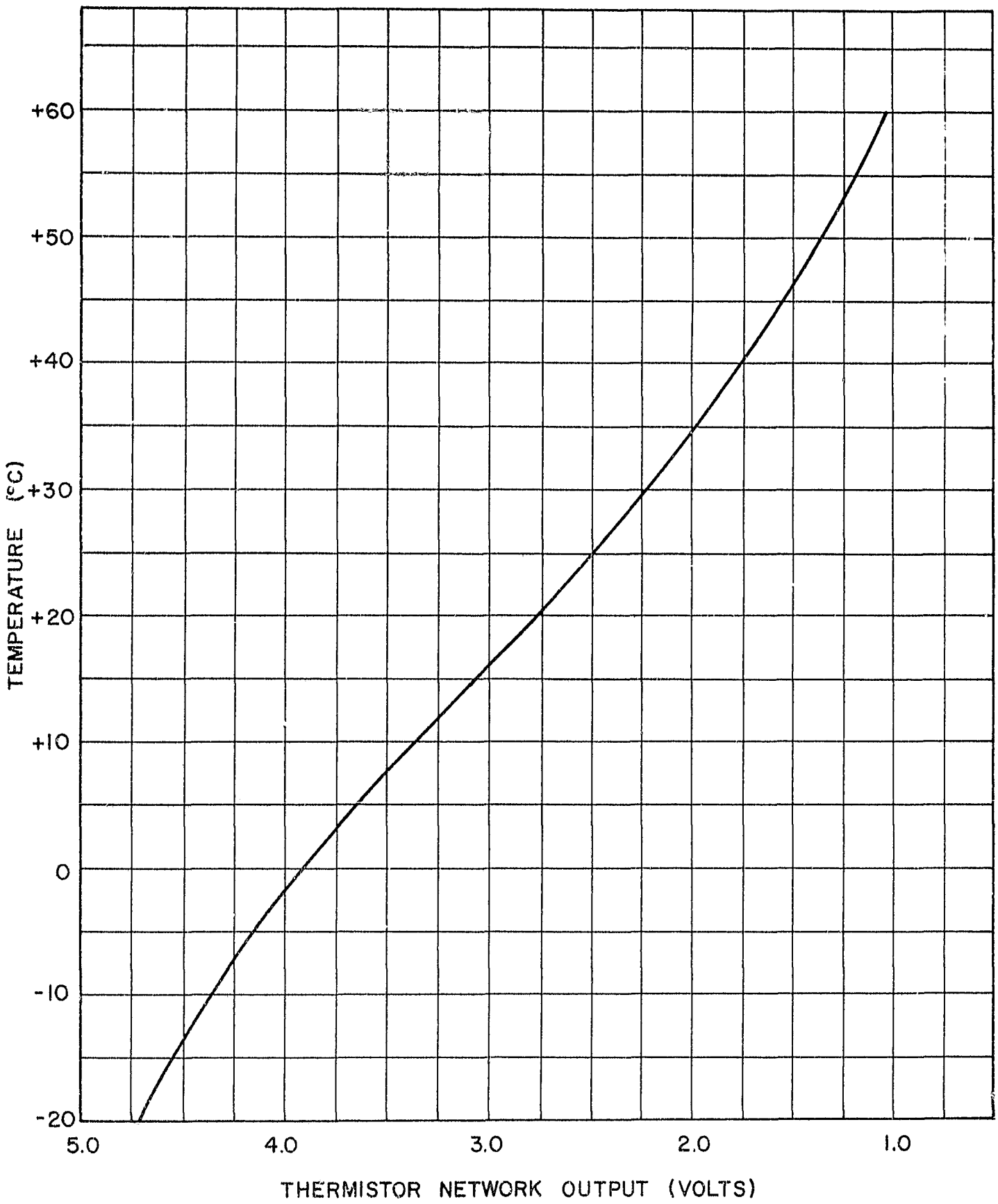

28. Temperature Sensor Calibration

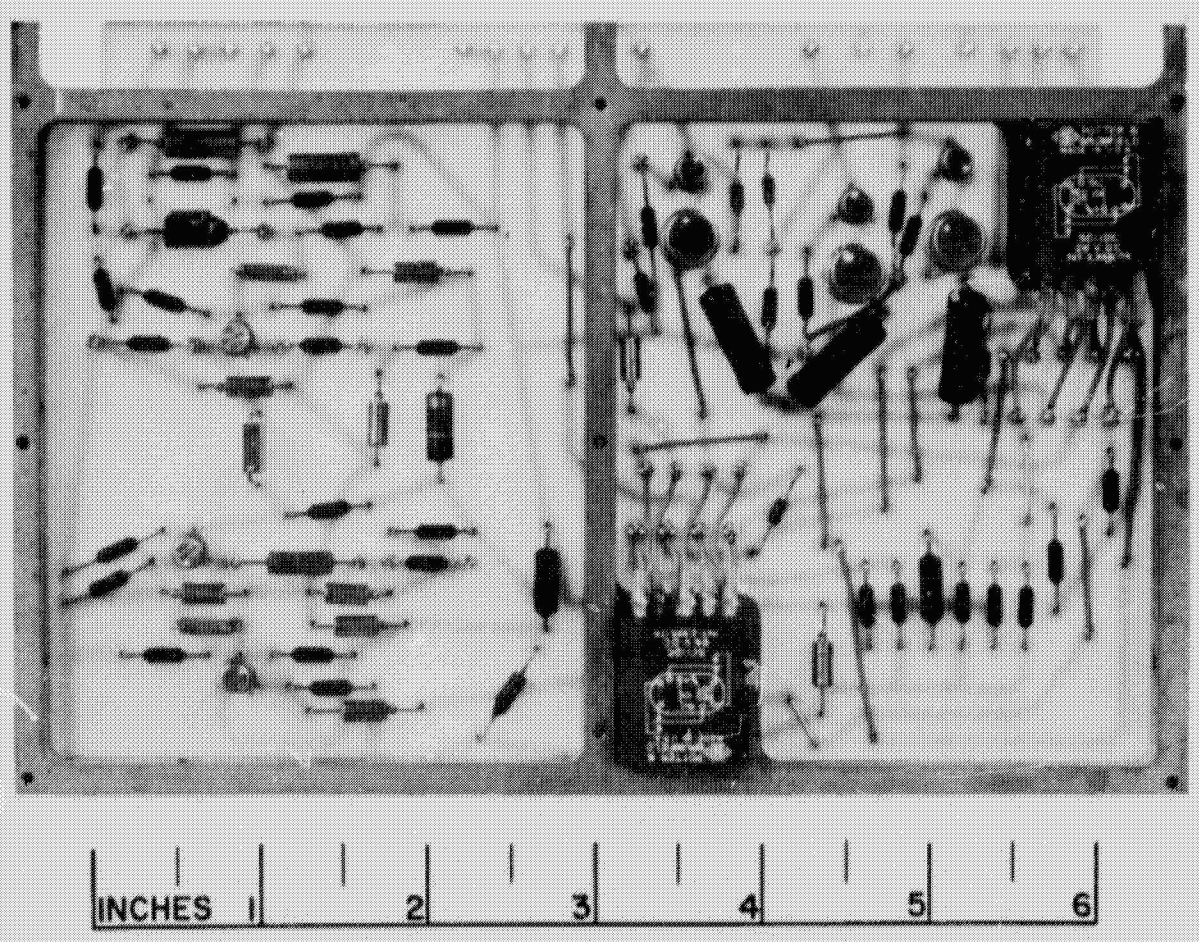

29. Noise Calibrator and Relay Drivers Board

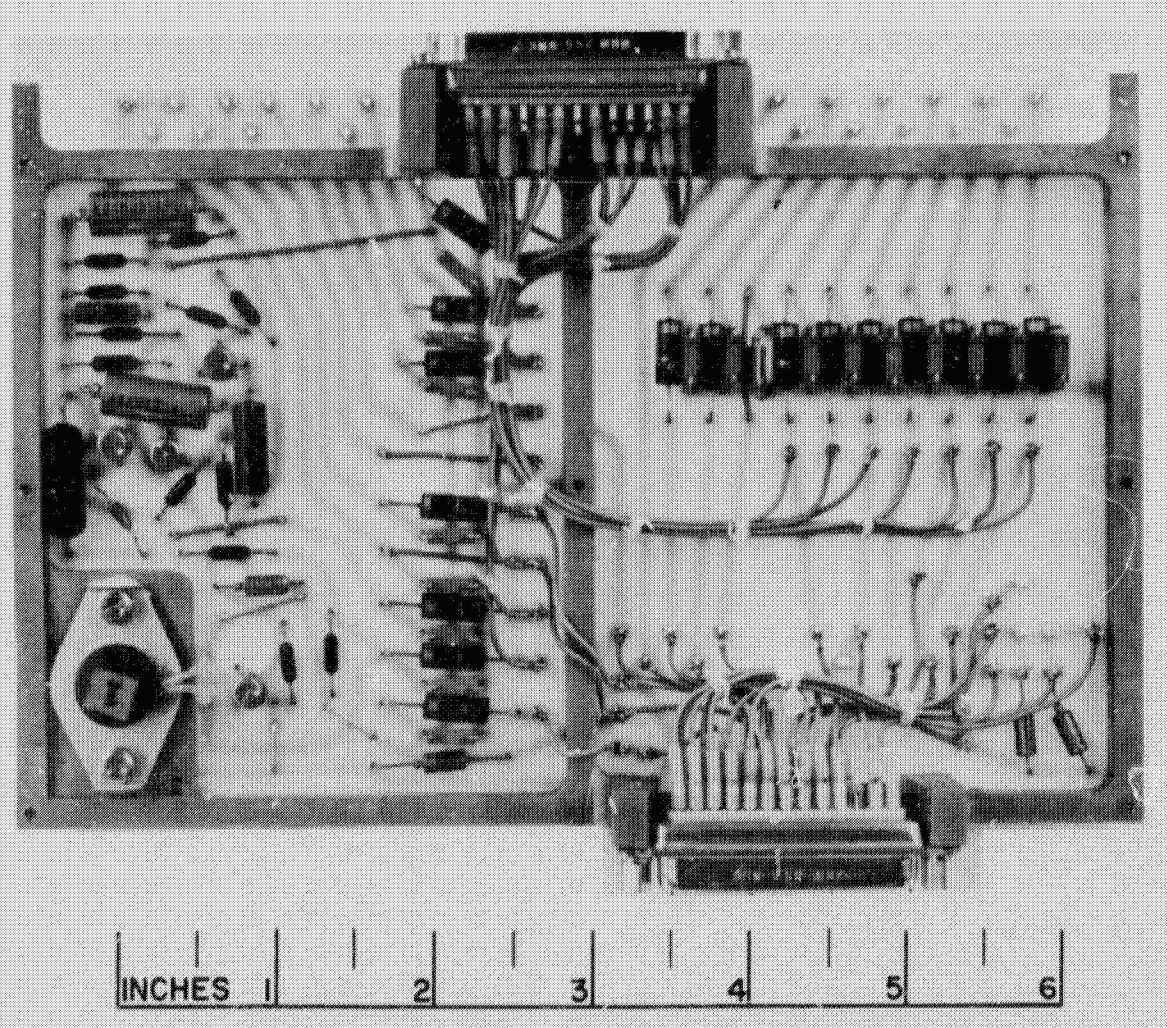

30. Series Regulator and Line Filters Board

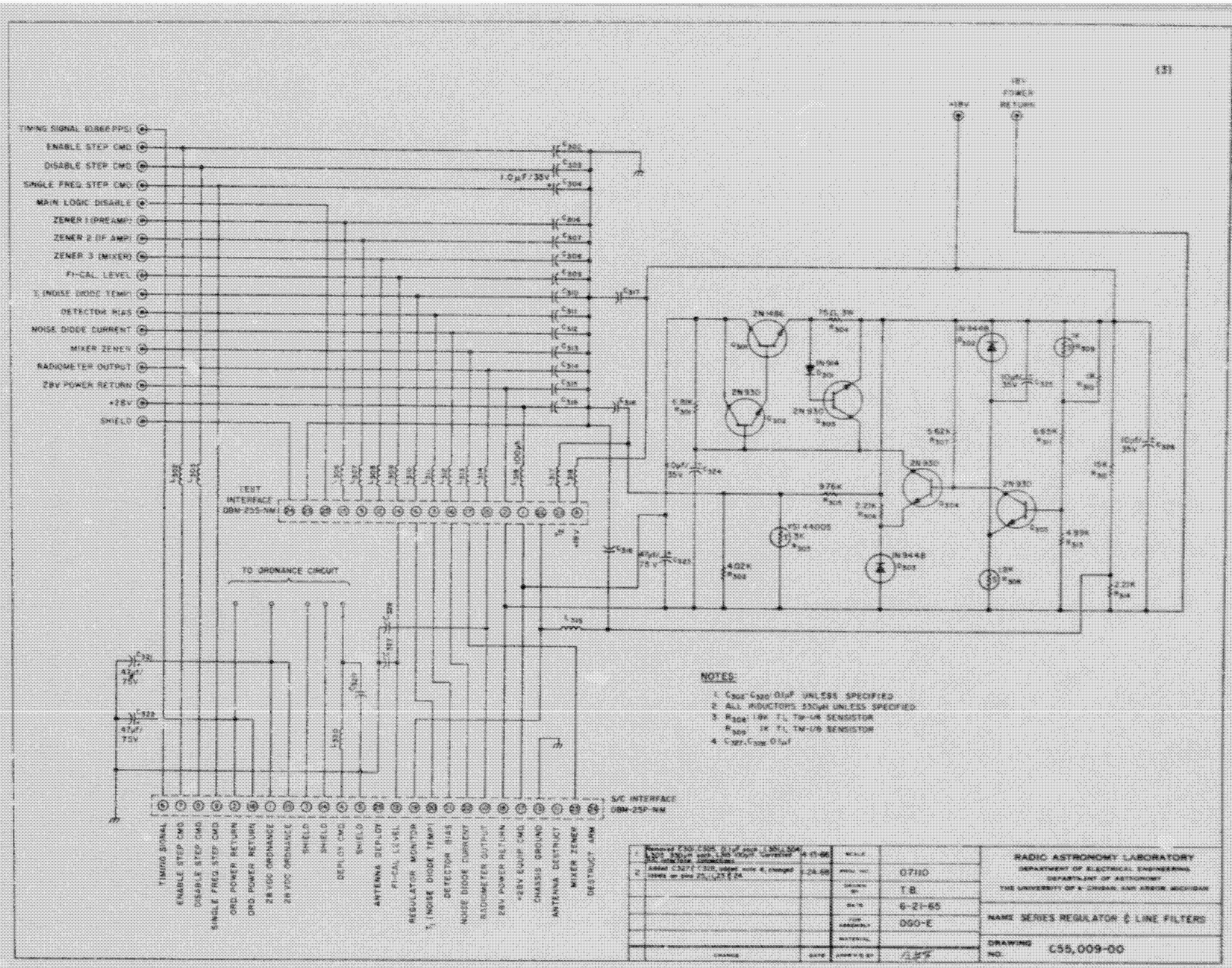

31. Series Regulator and Line Filter Circuits

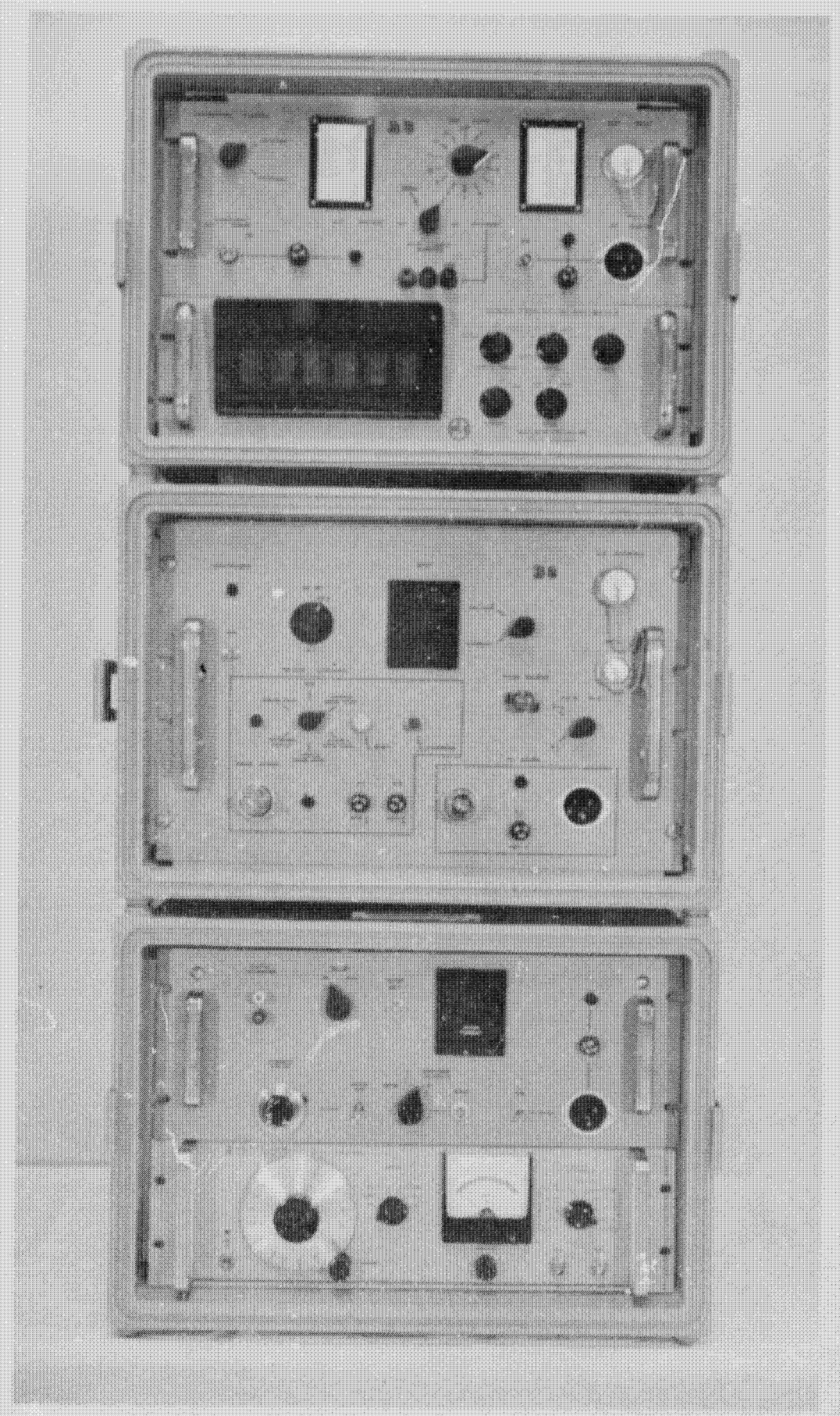

32. Ground Support Equipment

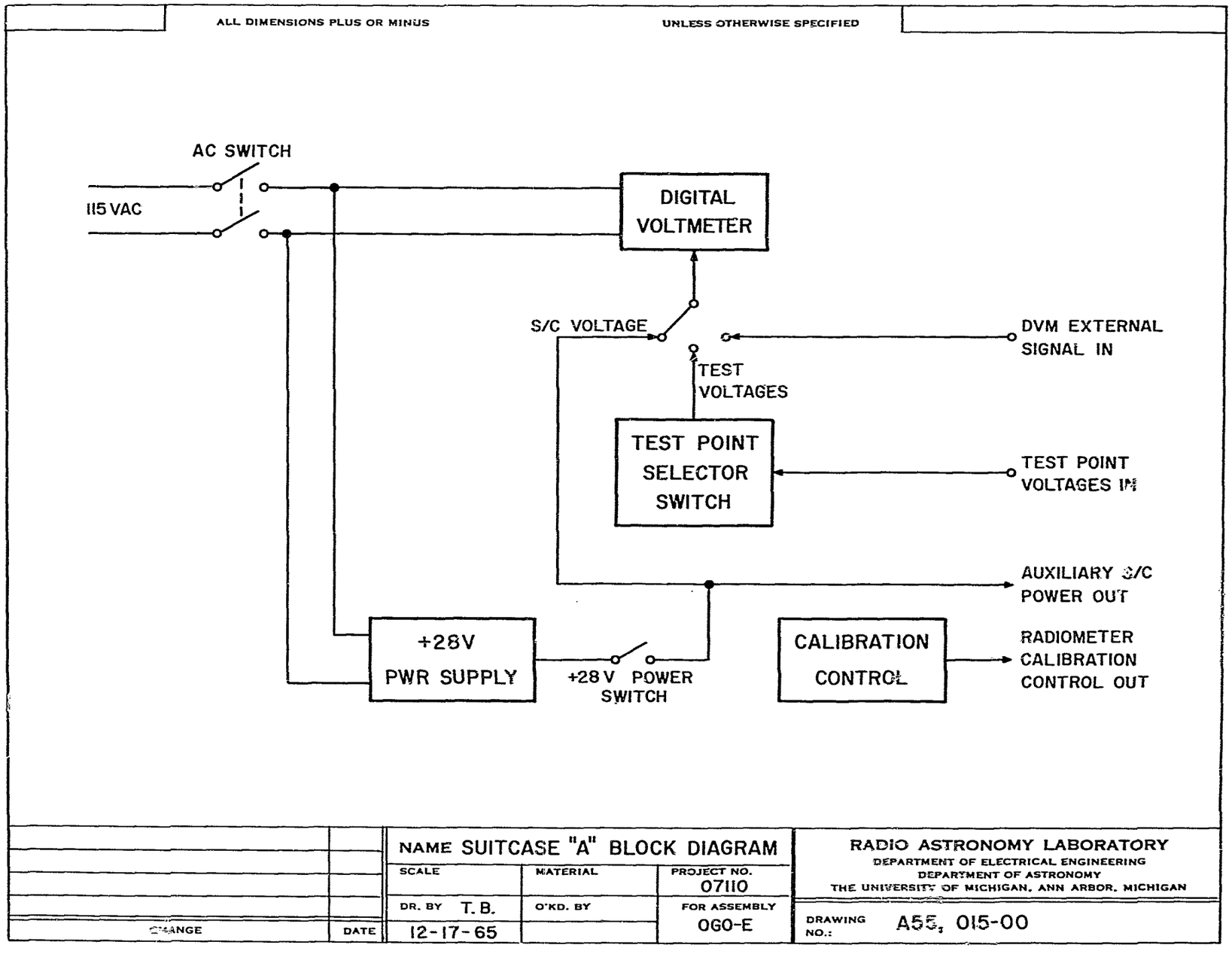

33. Suitcase A Block Diagram

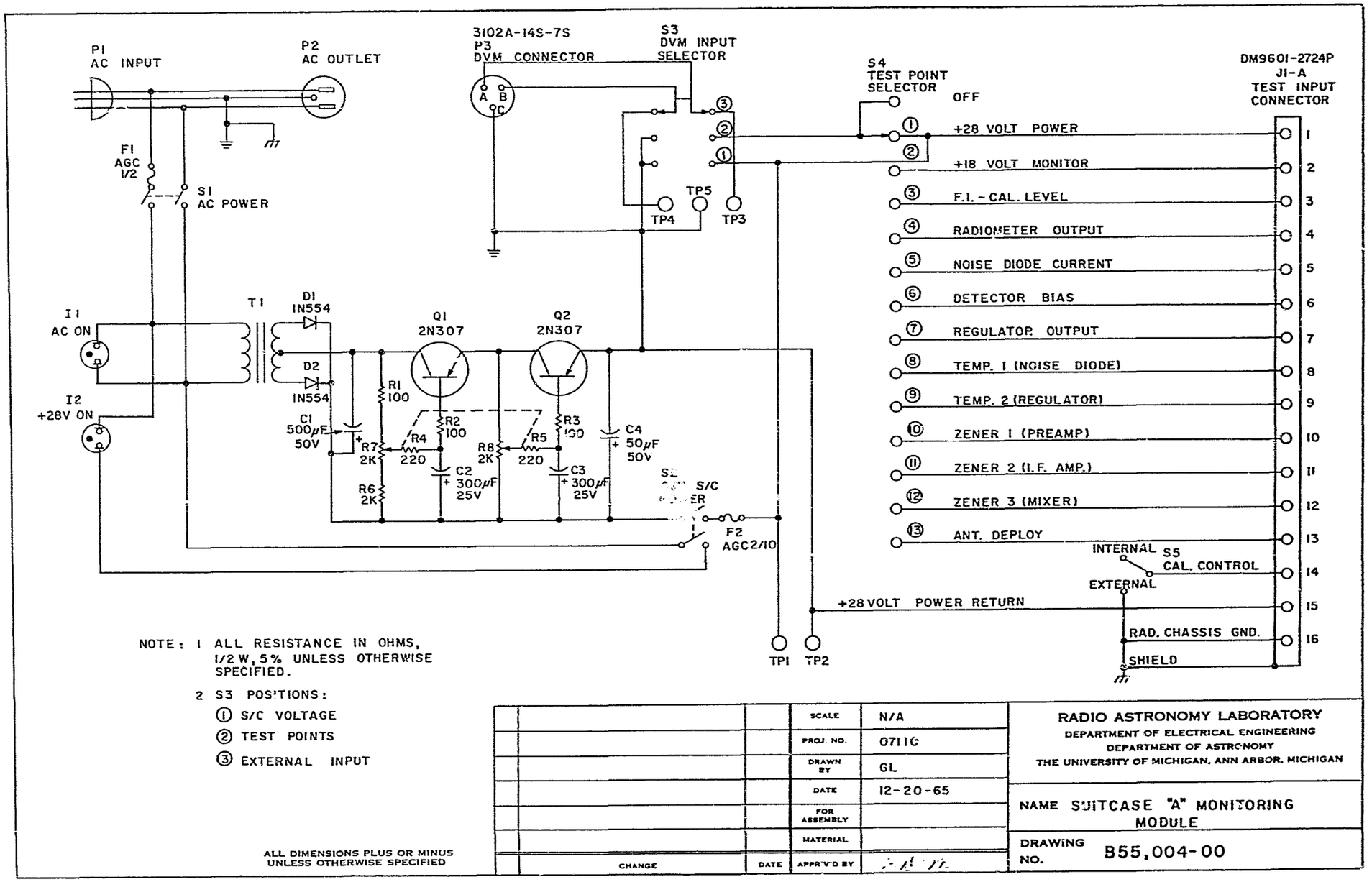

NOTE: 1 ALL RESISTANCE IN OHMS, 1/2 W, 5% UNLESS OTHERWISE SPECIFIED.

2 S3 POSITIONS:

① S/C VOLTAGE

② TEST POINTS

③ EXTERNAL INPUT

ALL DIMENSIONS PLUS OR MINUS UNLESS OTHERWISE SPECIFIED

CHANGE	DATE	APPR'D BY

SCALE	N/A
PROJ. NO.	G7116
DRAWN BY	GL
DATE	12-20-65
FOR ASSEMBLY	
MATERIAL	

RADIO ASTRONOMY LABORATORY
DEPARTMENT OF ELECTRICAL ENGINEERING
DEPARTMENT OF ASTRONOMY
THE UNIVERSITY OF MICHIGAN, ANN ARBOR, MICHIGAN

NAME SUITCASE "A" MONITORING MODULE

DRAWING NO. B55,004-00

34. Suitcase A Circuit Diagram

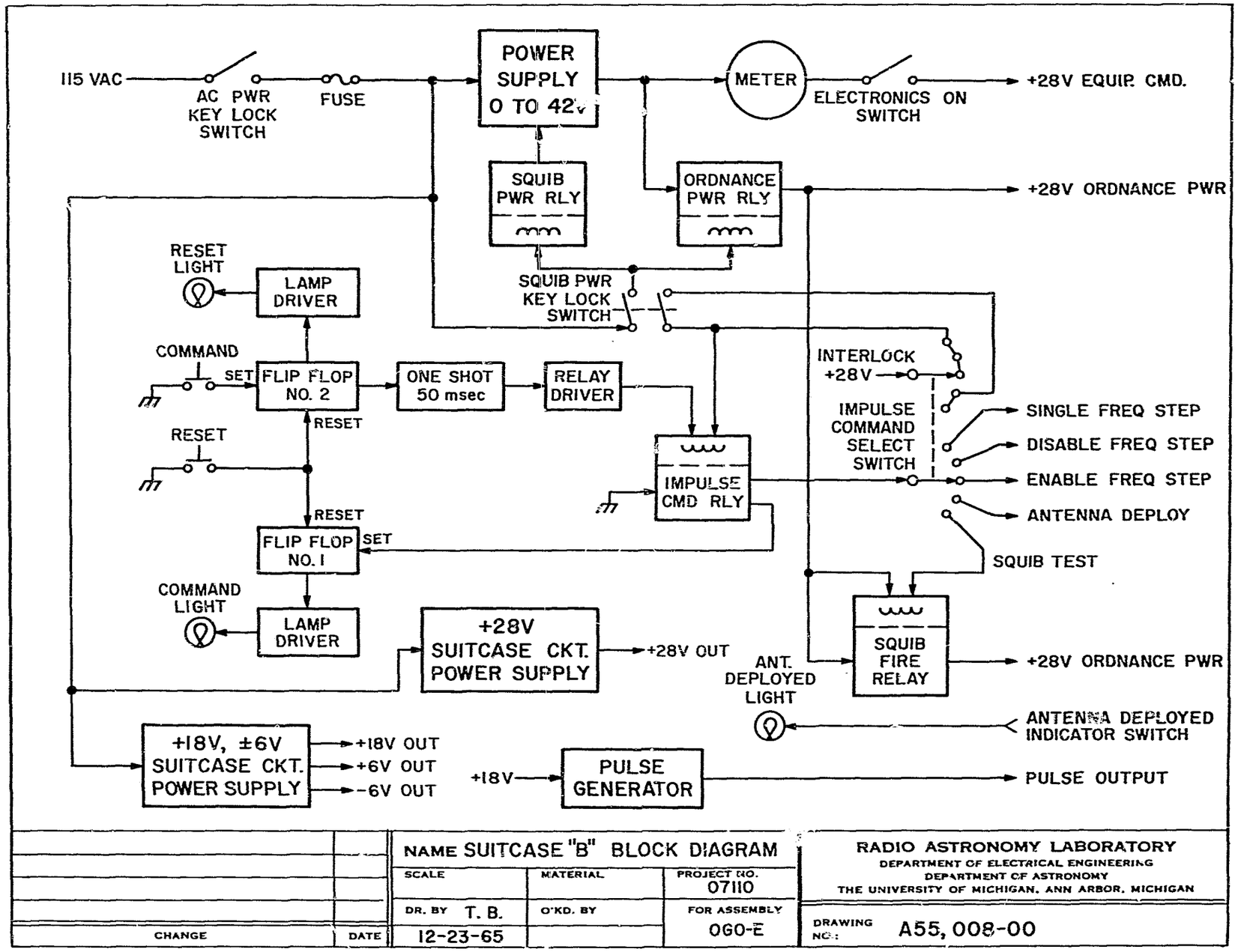

35. Suitcase B Block Diagram

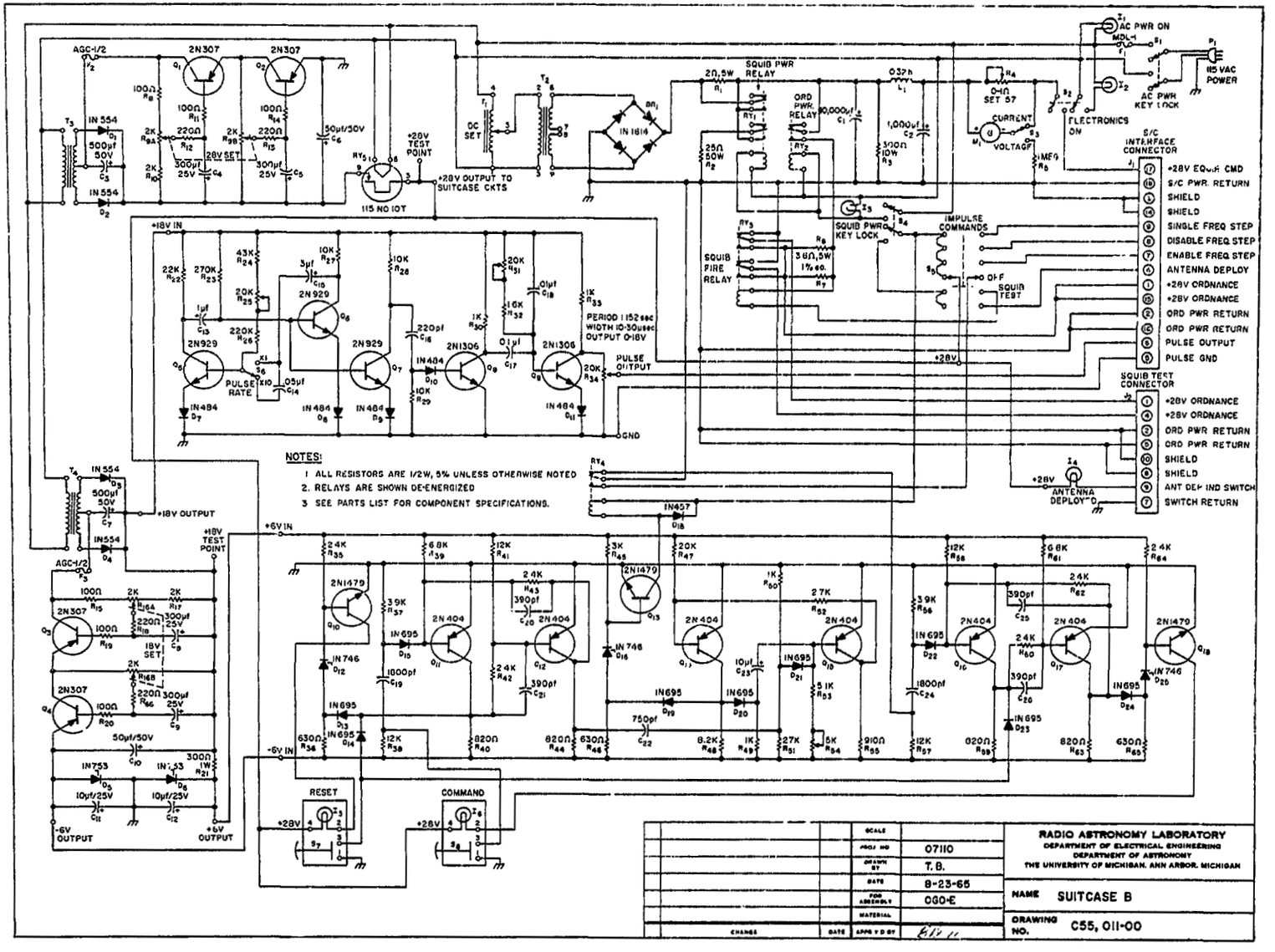

36. Suitcase B Circuit Diagram

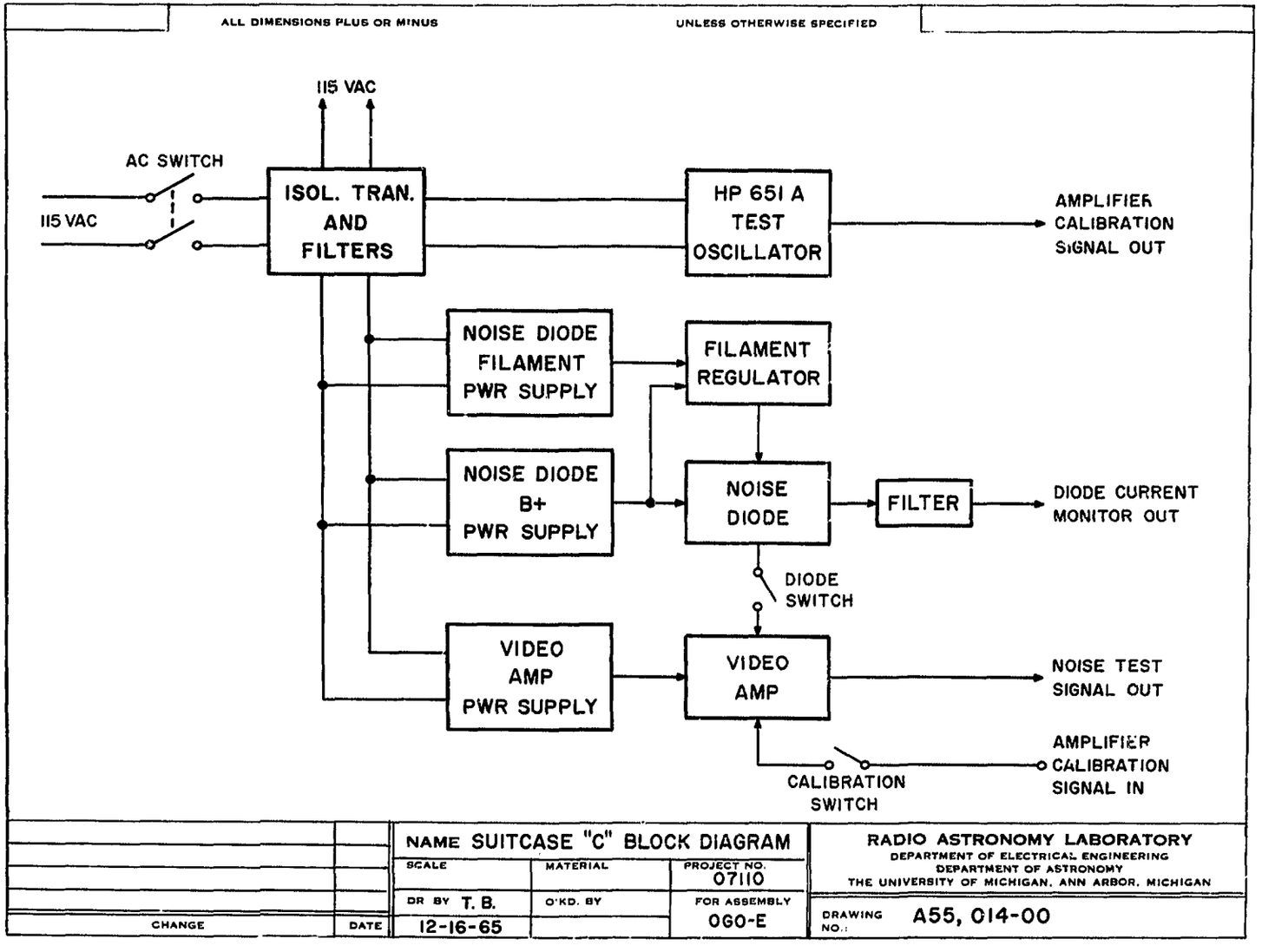

37. Suitcase C Block Diagram

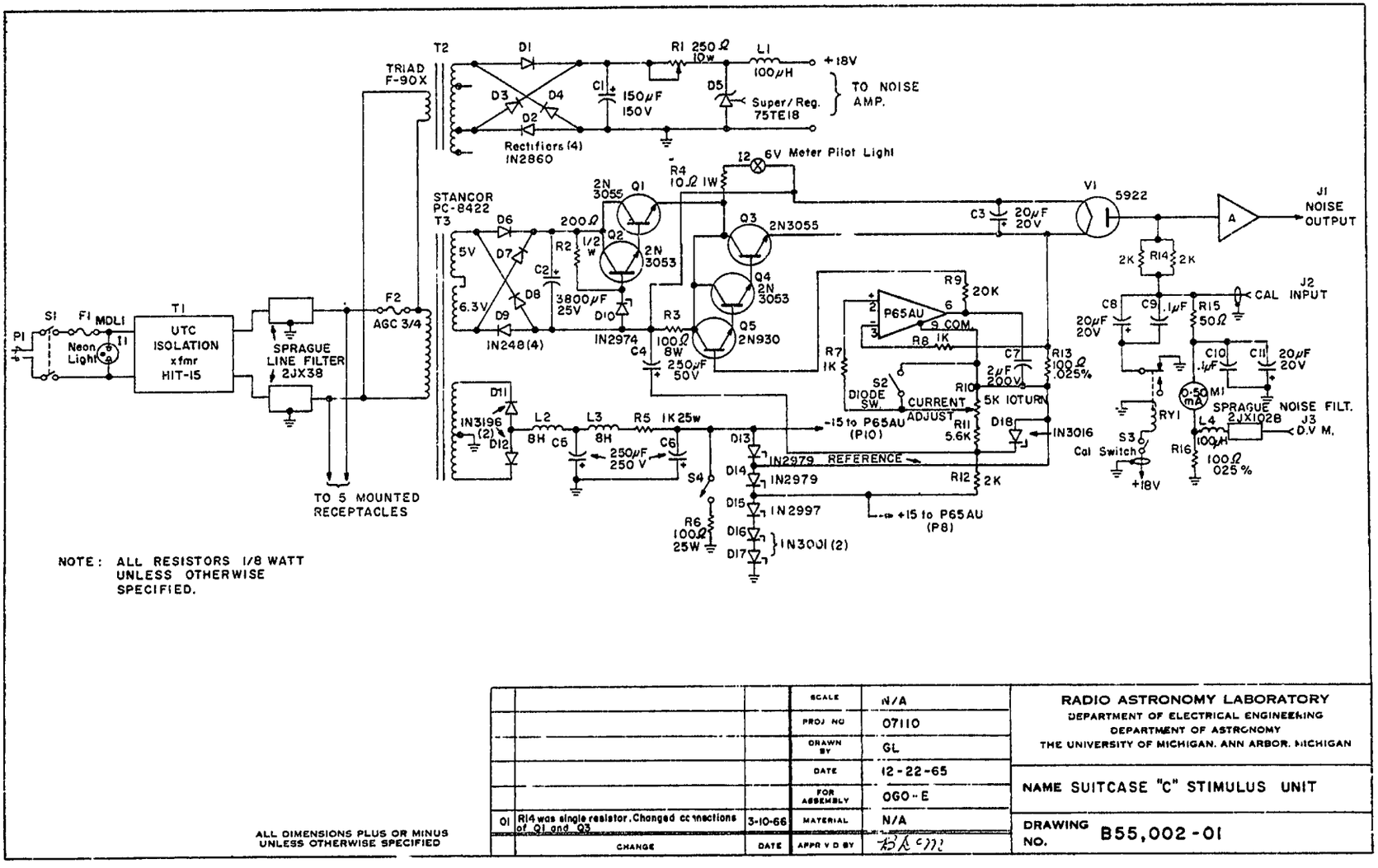

NOTE: ALL RESISTORS 1/8 WATT UNLESS OTHERWISE SPECIFIED.

ALL DIMENSIONS PLUS OR MINUS UNLESS OTHERWISE SPECIFIED

			SCALE	N/A
			PROJ NO	07110
			DRAWN BY	GL
			DATE	12-22-65
			FOR ASSEMBLY	060-E
01	R14 was single resistor. Changed connections of Q1 and Q3	3-10-66	MATERIAL	N/A
	CHANGE	DATE	APPR'D BY	

RADIO ASTRONOMY LABORATORY
DEPARTMENT OF ELECTRICAL ENGINEERING
DEPARTMENT OF ASTRONOMY
THE UNIVERSITY OF MICHIGAN, ANN ARBOR, MICHIGAN

NAME SUITCASE "C" STIMULUS UNIT

DRAWING NO. B55,002-01

38. **Suitcase C Circuit Diagram**

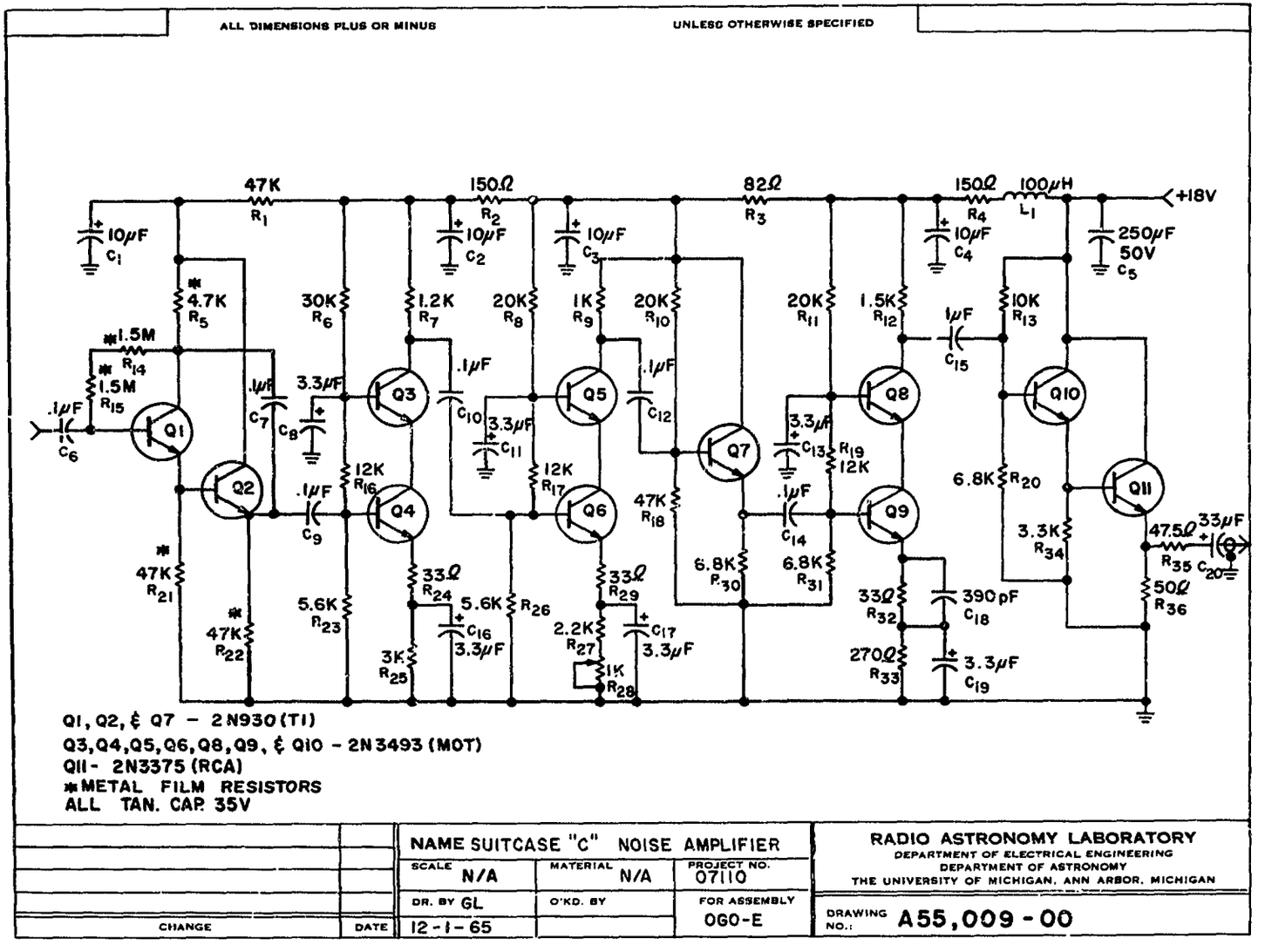

39. Suitcase C Noise Amplifier

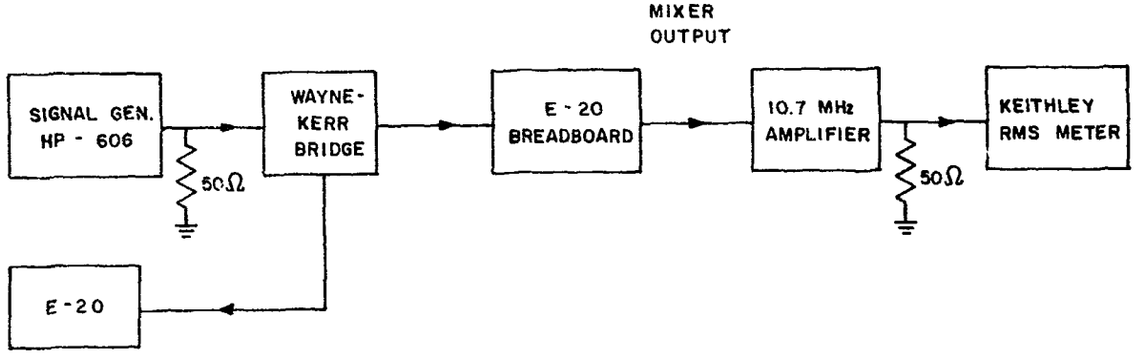

40. Input Impedance Measurement Setup

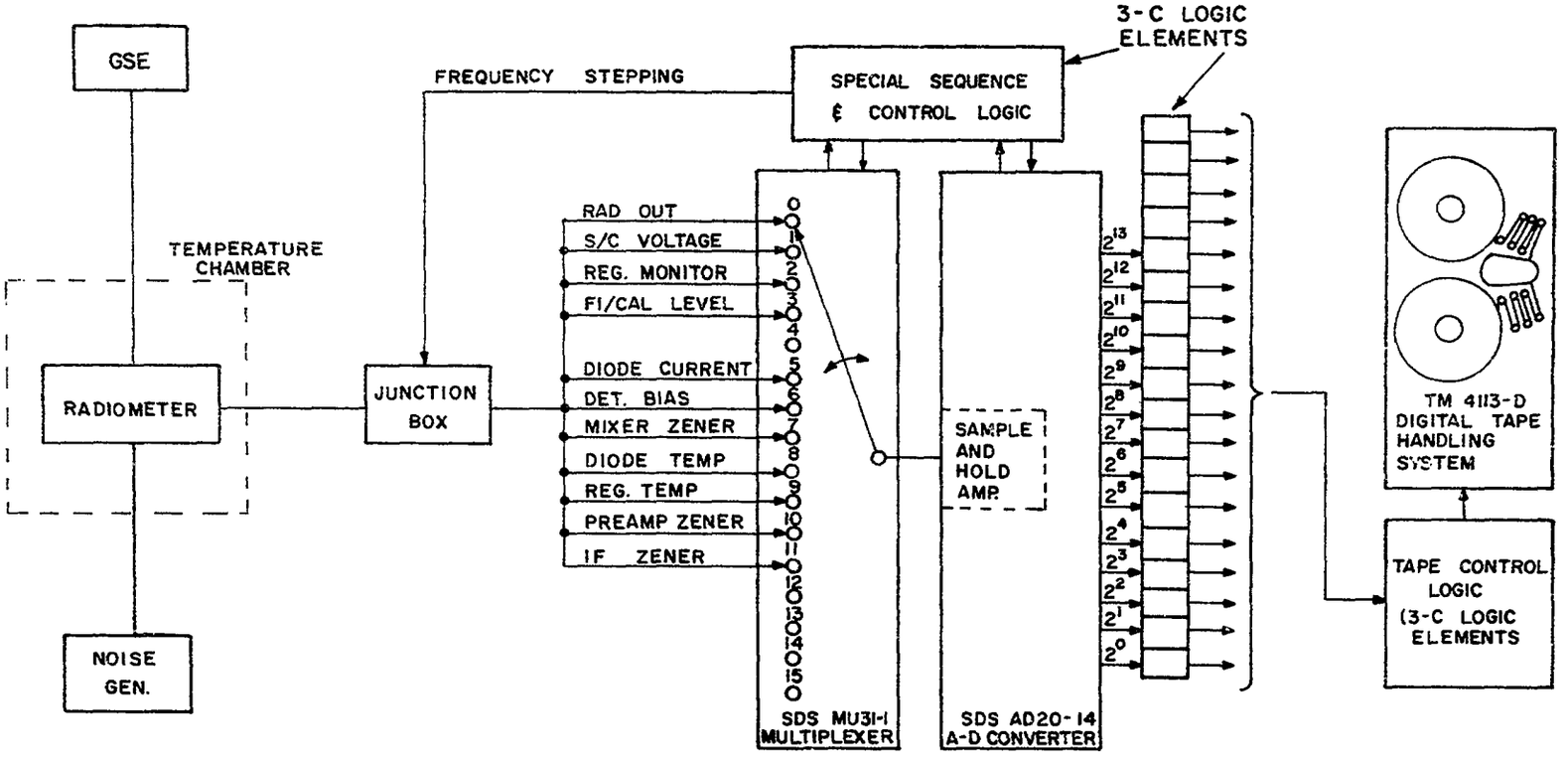

41. Calibration Setup Block Diagram

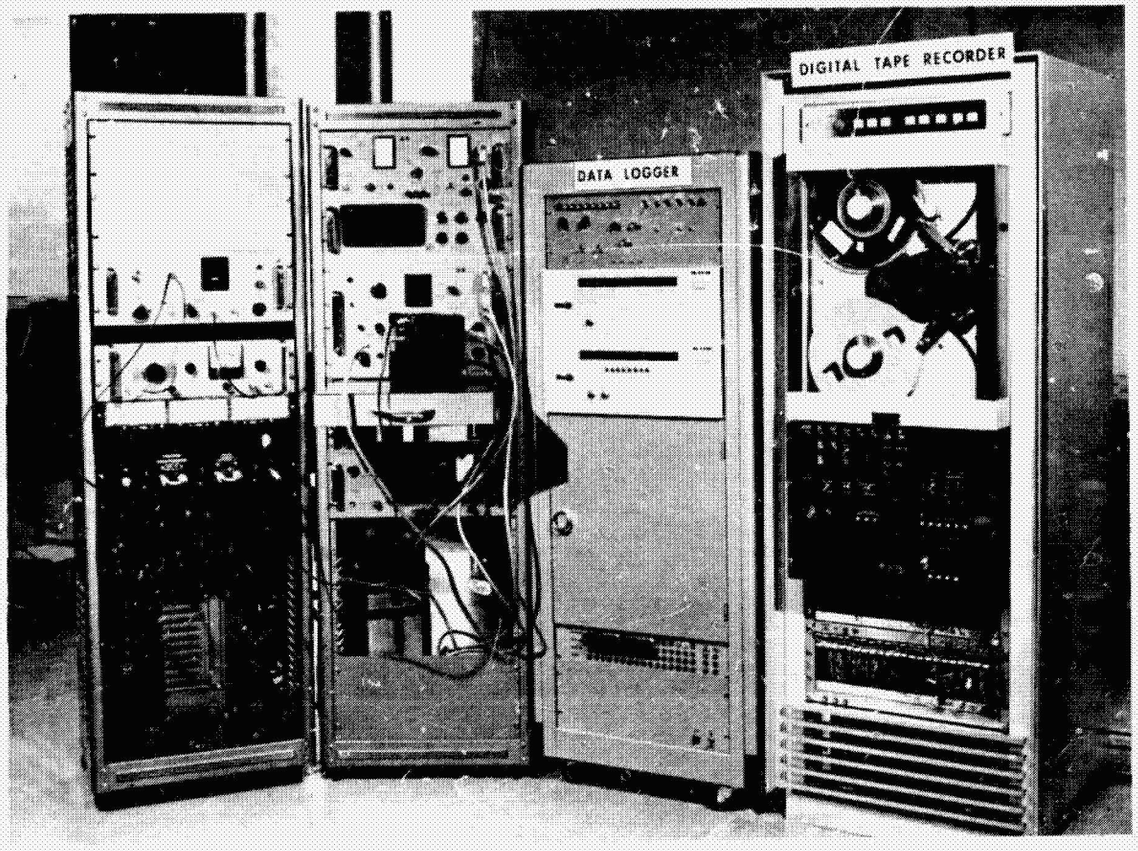

42. Data Logger Facility

9G9-E CALIBRATION DATA

SEPT. 14, 1967

INPUT TAPE NUMBER 2826 - FU-2 CALIBRATION

TEMP = -20 DEGREES C

FILE NO = 1

	FREQ [KH]	REC	RAD OTPT	SPPLY VOLT	REG MON	FID/ CALID	DIODE CURR	DETR BIAS	ANT DEPLY	DIODE TEMP	REG TEMP	PAMP ZENER	IFAMP ZENER
CAL 1, 23.5V	50	4	.9307	23.4783	2.3485	.5190	2.6892	4.8901	3.9951	4.7252	4.7189	11.3213	15.0931
	100	5	.4755	23.4440	2.3445	.5156	2.6855	4.8647	3.9742	4.7205	4.7165	11.2728	15.0369
	200	6	.3289	23.4359	2.3475	.5189	2.6870	4.8658	3.9808	4.7238	4.7195	11.2662	15.0413
	350	7	.4012	23.4638	2.3439	.5170	2.6847	4.8625	3.9808	4.7202	4.7173	11.2706	15.0292
	600	8	.2301	23.5745	2.3490	.5185	2.6857	4.8658	3.9852	4.7236	4.7189	11.2948	15.0248
	900	9	.1545	23.5549	2.3443	.5173	2.6841	4.8625	3.9841	4.7227	4.7169	11.2970	15.0501
	1800	10	.1951	23.5582	2.3463	.5176	2.6849	4.8592	3.9907	4.7236	4.7175	11.2684	15.0501
	3500	11	.1817	23.5386	2.3461	.5175	2.6846	4.8691	3.9907	4.7229	4.7181	11.2640	15.0457
25.5V	50	12	.9586	25.5406	2.3479	.5198	2.6880	4.8691	3.9830	4.7246	4.7193	11.2750	15.0567
	100	13	.4952	25.5129	2.3484	.5190	2.6878	4.8779	3.9929	4.7242	4.7183	11.2970	15.0391
	200	14	.3303	25.4933	2.3460	.5183	2.6877	4.8636	3.9830	4.7236	4.7165	11.2970	15.0479
	350	15	.3995	25.5047	2.3460	.5189	2.6872	4.8625	3.9808	4.7248	4.7165	11.2860	15.0259
	600	16	.2292	25.4884	2.3465	.5183	2.6854	4.8724	3.9885	4.7229	4.7154	11.2662	15.0501
	900	17	.1505	25.4982	2.3479	.5184	2.6866	4.8724	3.9863	4.7244	4.7162	11.2860	15.0501
	1800	18	.1588	25.4802	2.3447	.5174	2.6847	4.8570	3.9797	4.7219	4.7131	11.2882	15.0303
	3500	19	.1770	25.5406	2.3472	.5186	2.6862	4.8713	3.9841	4.7229	4.7145	11.2640	15.0479
28.0V	50	20	.9334	28.1196	2.3474	.5218	2.6892	4.8713	3.9863	4.7291	4.7101	11.3069	15.0523
	100	21	.4851	28.0153	2.3492	.5215	2.6890	4.8625	3.9830	4.7260	4.7049	11.3488	15.0325
	200	22	.3316	28.0039	2.3461	.5186	2.6876	4.8669	3.9841	4.7258	4.7043	11.2816	15.0259
	350	23	.4038	27.9229	2.3465	.5193	2.6885	4.8669	3.9874	4.7252	4.7043	11.2838	15.0314
	600	24	.2301	27.8295	2.3467	.5185	2.6879	4.8702	3.9863	4.7248	4.7038	11.3014	15.0391
	900	25	.1651	27.8686	2.3468	.5171	2.6866	4.8570	3.9764	4.7236	4.6999	11.2463	15.0093
	1800	26	.1686	27.8392	2.3467	.5175	2.6875	4.8669	3.9819	4.7244	4.7015	11.2882	15.0501
	3500	27	.1816	27.8539	2.3479	.5177	2.6870	4.8603	3.9830	4.7217	4.6991	11.2640	15.0226
31.0V	50	28	.9452	30.9547	2.3474	.5202	2.6911	4.8647	3.9775	4.7275	4.6983	11.2706	15.0325
	100	29	.4870	30.9400	2.3471	.5198	2.6901	4.8680	3.9830	4.7260	4.6943	11.2794	15.0281
	200	30	.3310	30.9074	2.3503	.5192	2.6903	4.8658	3.9819	4.7268	4.6947	11.3058	15.0281
	350	31	.4025	30.8944	2.3475	.5182	2.6896	4.8636	3.9830	4.7273	4.6920	11.3400	15.0435
	600	32	.2304	30.9253	2.3478	.5189	2.6889	4.8746	3.9885	4.7254	4.6941	11.2794	15.0479
	900	33	.1546	30.8895	2.3469	.5182	2.6876	4.8680	3.9874	4.7252	4.6897	11.2618	15.0182
	1800	34	.1735	30.8927	2.3475	.5192	2.6888	4.8680	3.9830	4.7248	4.6859	11.2750	15.0325
	3500	35	.1831	30.9172	2.3473	.5192	2.6878	4.8614	3.9918	4.7244	4.6856	11.2750	15.0226
33.5V	50	36	.9448	33.2534	2.3486	.5184	2.6906	4.8636	3.9797	4.7266	4.6813	11.2816	15.0336
	100	37	.4732	33.2615	2.3473	.5184	2.6908	4.8702	3.9841	4.7264	4.6788	11.3014	15.0071
	200	38	.3307	33.2566	2.3486	.5194	2.6913	4.8702	3.9841	4.7269	4.6788	11.2618	15.0303
	350	39	.4023	33.2745	2.3466	.5202	2.6902	4.8691	3.9808	4.7256	4.6739	11.2750	15.0336
	600	40	.2306	33.3055	2.3497	.5208	2.6918	4.8757	4.0018	4.7277	4.6767	11.3036	15.0501
	900	41	.1606	33.2371	2.3460	.5174	2.6880	4.8504	3.9742	4.7250	4.6714	11.2684	15.0259
	1800	42	.1692	33.2452	2.3492	.5218	2.6910	4.8702	3.9863	4.7256	4.6705	11.3058	15.0270
	3500	43	.1821	33.2582	2.3497	.5219	2.6907	4.8691	3.9885	4.7272	4.6718	11.2684	15.0501
CAL 2, 23.5V	50	44	1.2397	23.4995	2.3538	.5250	2.6899	4.9088	4.0216	4.7289	4.6918	11.3378	15.0810
	100	45	1.0755	23.5419	2.3515	.5211	2.6876	4.8945	4.0128	4.7265	4.6887	11.3102	15.0722
	200	46	.9331	23.5663	2.3514	.5205	2.6870	4.8768	3.9885	4.7248	4.6916	11.3334	15.0655
	350	47	.8325	23.5076	2.3506	.5199	2.6857	4.8779	3.9929	4.7256	4.6895	11.2838	15.0435
	600	48	.8778	23.5223	2.3521	.5221	2.6868	4.8890	4.0040	4.7248	4.6921	11.2992	15.0567
	900	49	.8581	23.5093	2.3520	.5220	2.6869	4.8846	4.0073	4.7248	4.6922	11.2794	15.0523
	1800	50	.7582	23.4734	2.3520	.5229	2.6870	4.8846	4.0029	4.7248	4.6929	11.3246	15.0744

43. Calibration Digital Printout

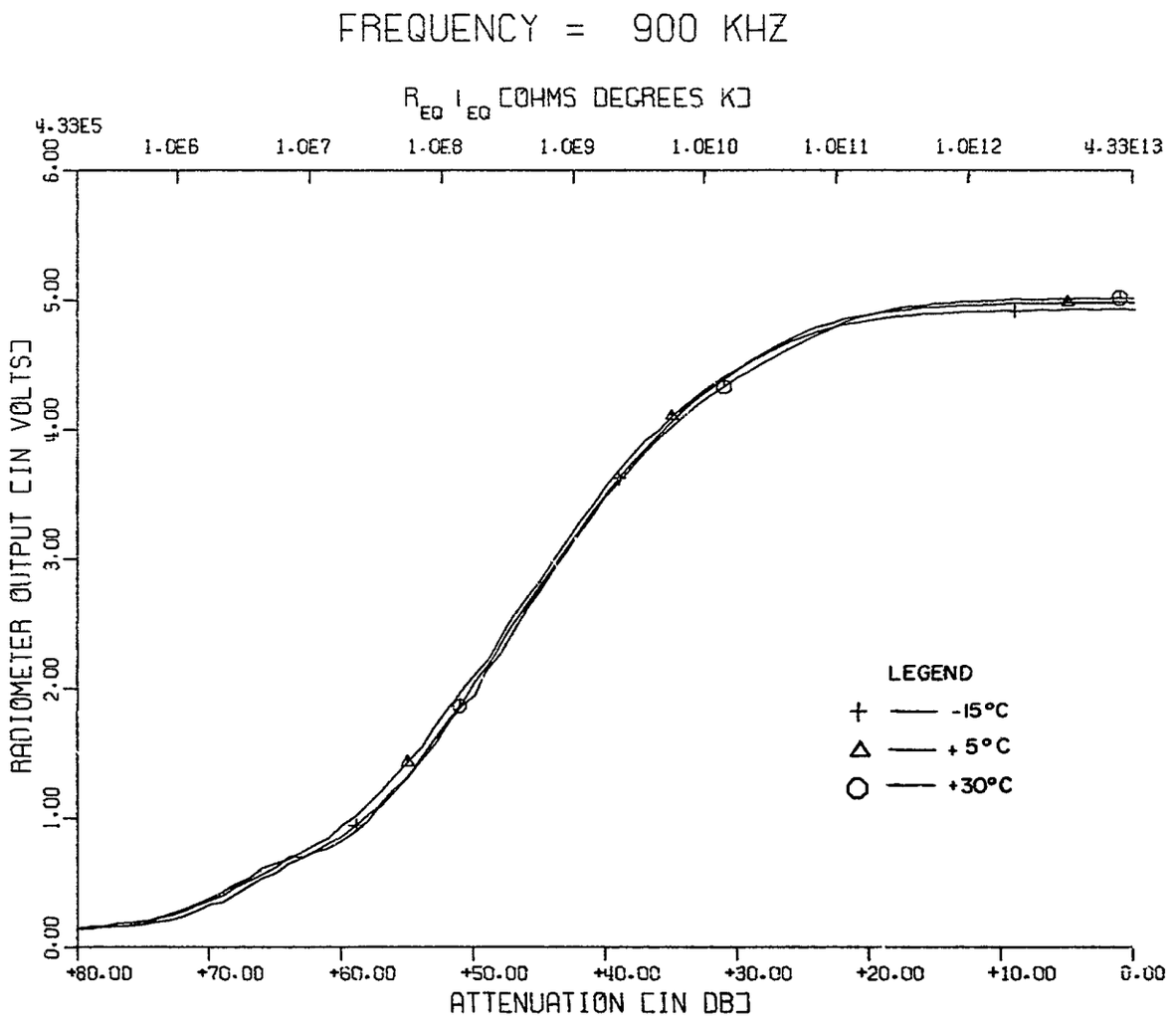

44. Calibration Response Plot

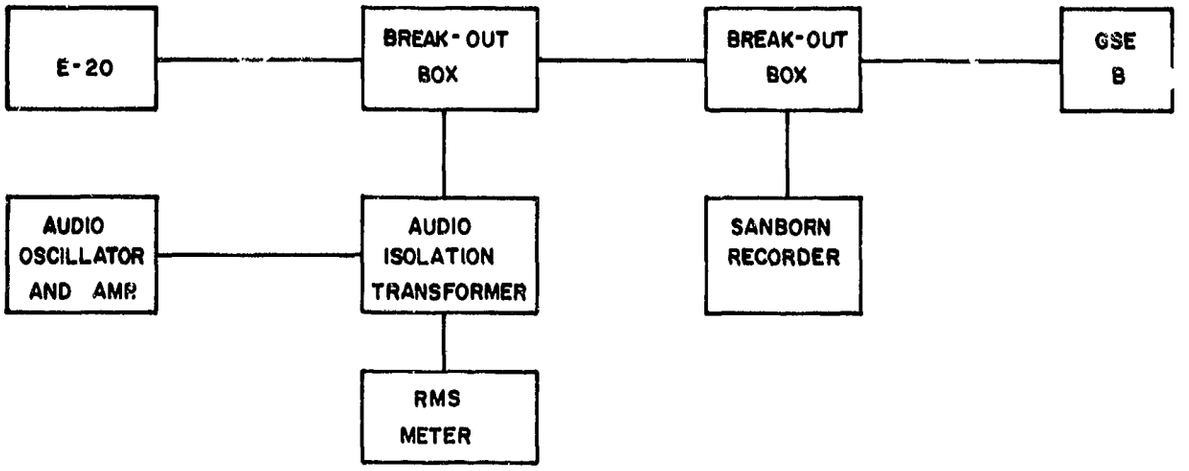

45. Audio Frequency Conducted Interference Test Setup

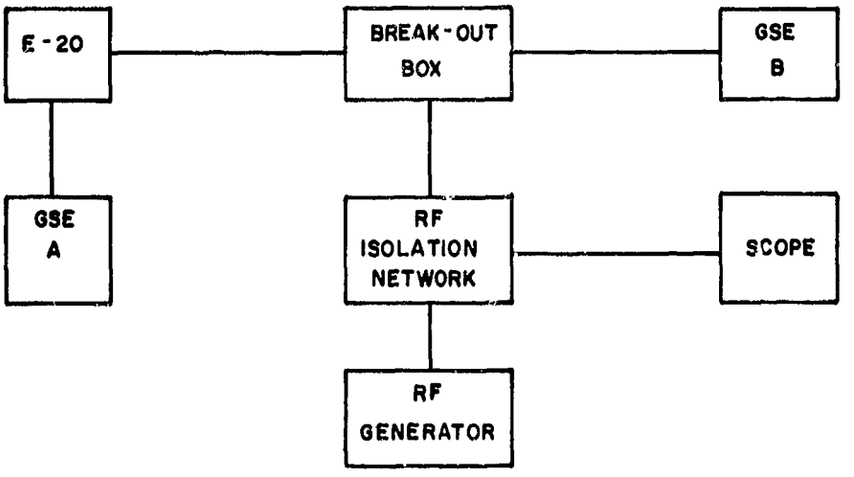

46. Radio Frequency Conducted Interference Test Setup

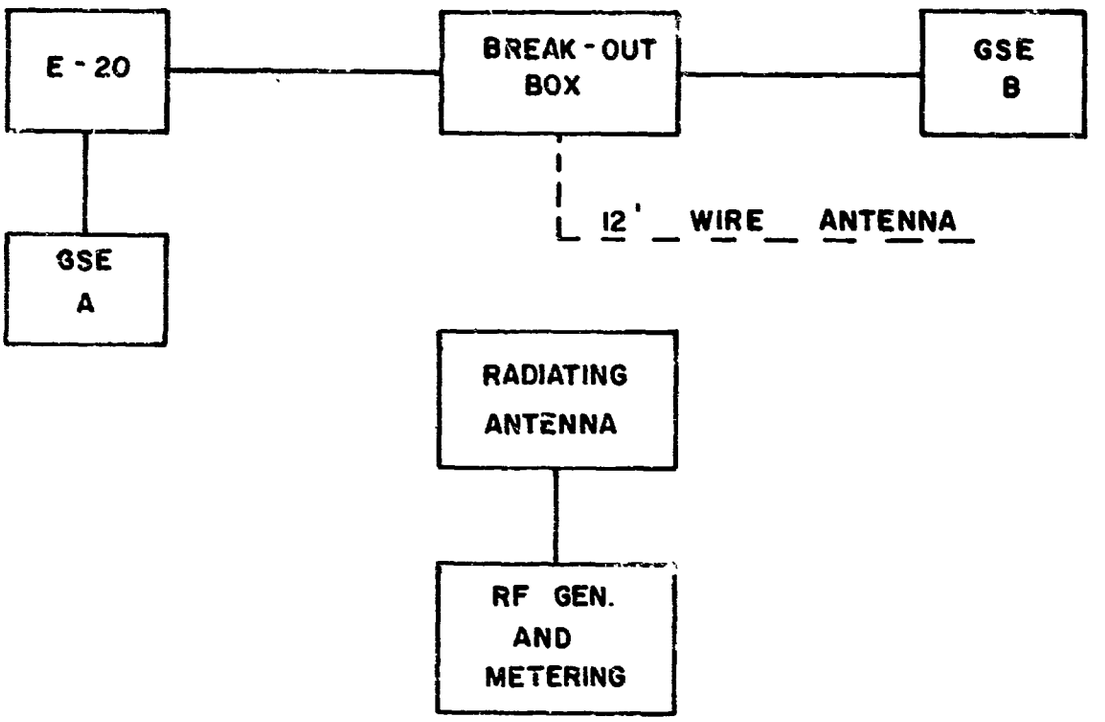

47. Radio Frequency Radiated In terference Test Setup

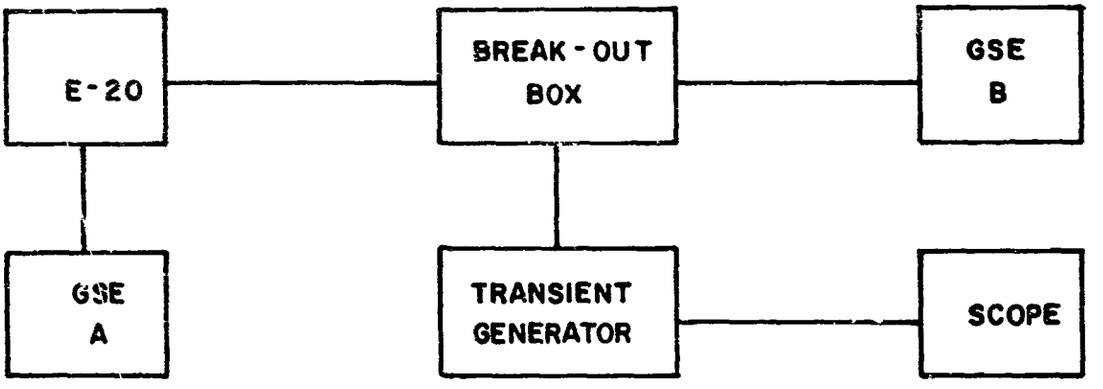

48. Transient Conducted Interference Test Setup

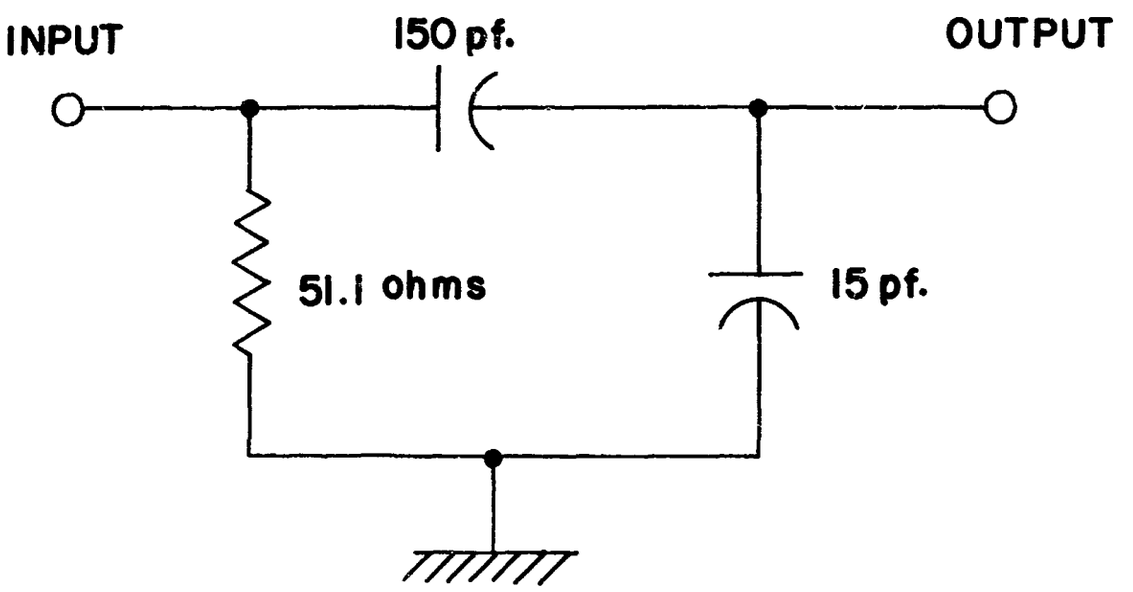

49. Radiometer Input Termination

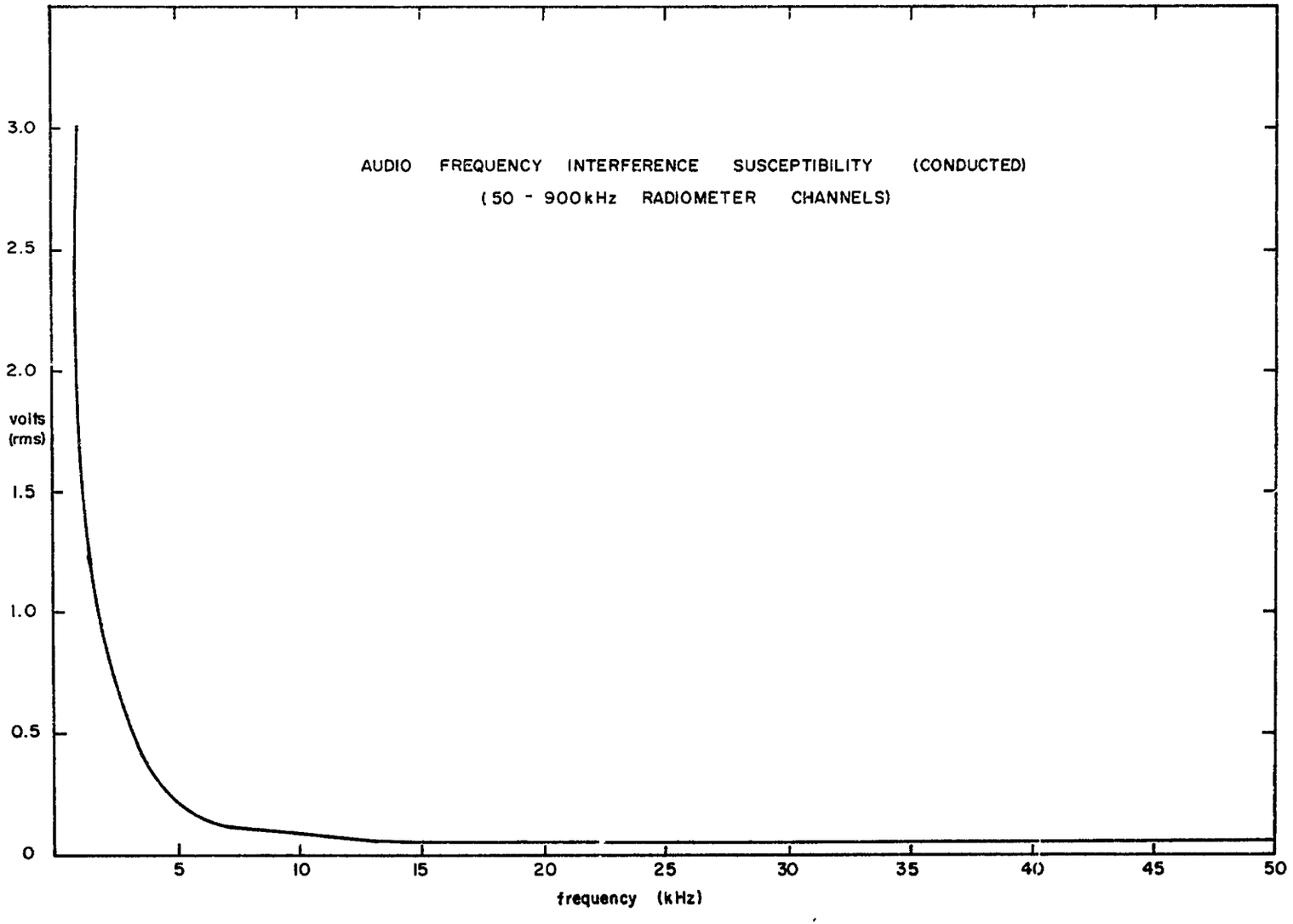

50. **AF Conducted Interference Susceptibility (50 - 900 kHz)**

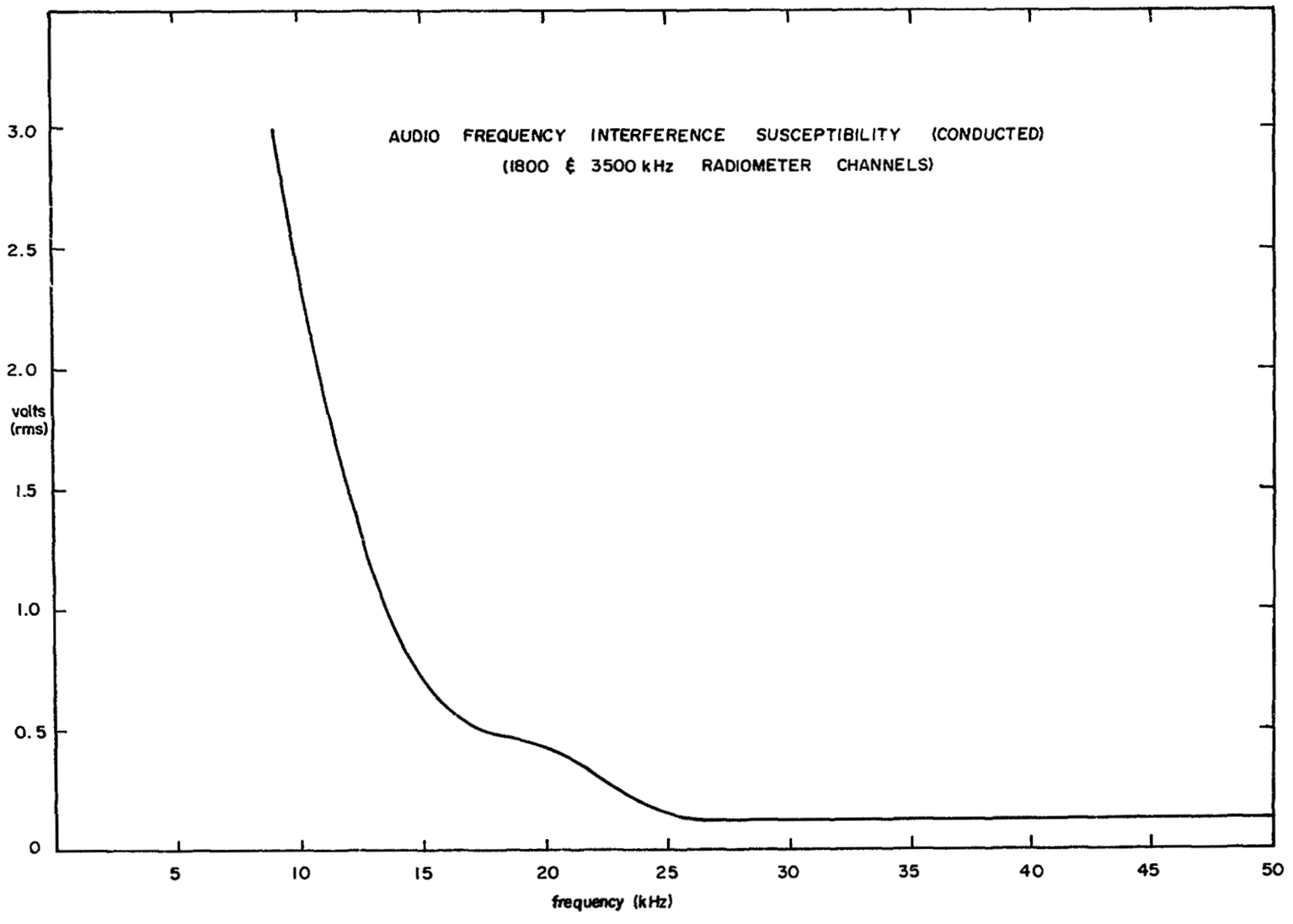

51. AF Conducted Interference Susceptibility (1.8 and 3.5 MHz)

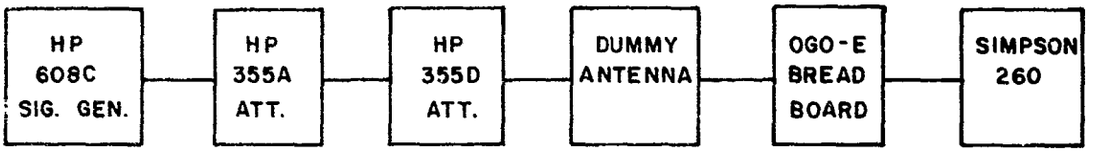

52. RFI Susceptibility Measurement Setup

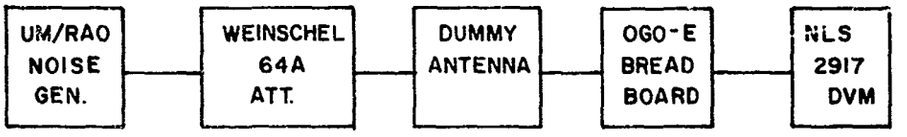

53. Radiometer Sensitivity Measurement Setup